JIMMA UNIVERSITY

SCHOOL OF GRADUATE STUDIES

JIMMA INSTITUTE OF TECHNOLOGY

FACULTY OF CIVIL AND ENVIRONMENTAL ENGINEERING

HYDROLOGY AND HYDRAULIC ENGINEERING CHAIR

MASTERS OF SCIENCE PROGRAM IN HYDRAULIC ENGINEERING

FLOOD INUNDATION MAPPING AND HAZARD ASSESSMENT:A CASE OF WERA RIVER FLOOD PLAIN OF BOYO CATCHMENT, ETHIOPIA

By:

Tamirat Samuel

A Thesis Submitted to School of Graduate Studies of Jimma University in Partial Fulfillment of the Requirements for the Degree of Masters of Science Program in Hydraulic Engineering

October, 2021 G.C

Jimma, Ethiopia

JIMMA UNIVERSITY

SCHOOL OF GRADUATE STUDIES

JIMMA INSTITUTE OF TECHNOLOGY

FACULTY OF CIVIL AND ENVIRONMENTAL ENGINEERING

HYDROLOGY AND HYDRAULIC ENGINEERING CHAIR

MASTERS OF SCIENCE PROGRAM IN HYDRAULIC ENGINEERING

FLOOD INUNDATION MAPPING AND HAZARD ASSESSMENT:A CASE OF WERA RIVER FLOOD PLAIN OF BOYO CATCHMENT, ETHIOPIA

By

Tamirat Samuel (MSc.)

A Thesis Submitted to School of Graduate Studies of Jimma University in Partial Fulfillment of the Requirements for the Degree of Masters of Science Program in Hydraulic Engineering.

Advisors:

Dr. Tamene Adunga (Associated Professor)

Mr. Tedale Shefaraw (MSc.)

DECLARATION

I, Tamirat Samuel Ushe declare that this research work done under the title as **Flood Inundation Mapping and Hazard Assessment: A Case of Wera River Flood Plain of Boyo Catchment, Ethiopia** is my own work and which has not been presented by me to any other university for similar or any other degree award receiving.

Tamirat Samuel Ushe	_____	_____
Name	Signature	Date

As a university research advisor, we certify that we have read and evaluate this thesis entitled as Flood Inundation Mapping and Hazard Assessment: A Case of Wera River Flood Plain of Boyo Catchment, Ethiopia is submitted by Tamirat Samuel Ushe under our supervisor-ship and guidance.

Dr. Tamene Adunga	_____	____/____/2021 G.C
Main advisor	Signature	Date
Mr. Tedale Shefaraw	_____	____/____/2021 G.C
Co-advisor	Signature	Date
Mr. Walabuma	_____	____/____/2021 G.C
Internal Examiner	Signature	Date

APPROVAL PAGE

We certify that the thesis entitled “Flood Inundation Mapping and Hazard Assessment: A Case of Wera River Flood Plain of Boyo Catchment, Ethiopia” is the work of Tamirat Samuel and we here by recommend for the examination by Jimma Institute of Technology in partial fulfillment of the requirements for degree of Masters of Science in Hydraulic Engineering.

Dr. Tamene Adunga (Associated Professor)

---------- ----------

Main Advisor Signature Date

Mr. Tedale Shefaraw (MSc.) ---------- ----------

Co-Advisor Signature Date

As a member of Board of Examiners of the MSc. Thesis open Defense Examination, we certify that we have read, evaluated the Thesis prepared by Tamirat Samuel and examined the candidate. We recommended that the Thesis could be accepted as fulfilling the Thesis requirements for the Degree of Masters of Science in Hydraulic Engineering.

---------- ---------- ----------

External examiner Signature Date

---------- ---------- ----------

Internal examiner Signature Date

---------- ---------- ----------

Chairperson Signature Date

ACKNOWLEDGEMENT

First and for Most I am to give great thanks to the Almighty God for giving me the strength to go on and finish writing this thesis research work. Next, I would like to express my appreciation and thanks to Ethiopian Road Authority for providing such a chance to continue my study at Jimma University Institute of Technology and for their Cooperative work that made this research possible through financing.

In addition, also JIT, HHEC is one of the specials what I want to say thanks for its coordination of the program and accepting me as per criteria for entrance. Also, I would like to express my gratefulness to My Main Advisor. Dr. Tamene Adugna (Associate Professor).

Secondly, I want to thank my Co. Advisor Mr. Tadele Shiferaw Geresu (MSc.) for his best comment, kindly advise, and suggestions those have a great contribution to this work. Another party I want to give my deepest gratitude to is MoWIE for their willingness to give all necessary raw data for this research. Lastly, I would like to thank all my best friends for their continued support and encouragement. Finally, I thank my loving family who always supports and wishes me a fruitful future.

ABSTRACT

Floods are one of the most common hazards in the world and cause loss of lives, livelihood, and property destruction. The objective of this research is to carry out flood inundation mapping and hazard assessment in the Wera River flood plain of Boyo catchment. The flooded areas along the Wera River flood plain of Boyo catchment have been mapped based on using the HEC-RAS (5.0.7) model, GIS (10.4.1) for spatial data processing, and HEC-GeoRAS (10.3) for interfacing between HEC-RAS and GIS. From this study peak floods was estimated statistical frequency analysis was carried out by log persons three distribution function based on the procedure frequency analysis for 5, 10, 25, 50, 100, 200, 500 years return periods were 61.03, 159.82, 239.71, 344.84, 421.22, 493.50, 560.96, 642.16m3/s for Alaba kulito ,55.18, 147.42, 218.82, 307.52, 368.01, 422.07, 469.61, 522.93m3/s for Wera and 12.23, 24.82, 37.74, 61.27, 85.57, 117.23, 158.30, 231.46m3/s for Batena respectively for respective return period, inundation map in study area was delineated for 5, 10, 25, 50,100, 200, and 500 years return period were 112.31,112.97, 113.56, 113.85, 114.25, 114.43, 114.73 and 114.77 Km² respectively. Flood hazard maps were prepared by reclassifying the depth grid and its area bounding polygon. Also, the area inundated at very severe, severe, high, moderate, and low flood hazards around 90%, 2%, 2% 2.33%, and 4%, respectively for all return periods. Due to the topographic setup, most of the tributaries of Lake Boyo start their courses from relatively higher elevations, so heavy floods during the rainy season at very flatlands of the area, especially flood plains in shashogo Woreda which is susceptible to flooding every year during the rainy season. Consequence waters remain stagnant for about one to two weeks over the flood plain of the Woreda. A flood hazard map was developed, to reduce economic and environmental losses, crop failure, loose life, and property study area. This study results recommended that Government and other concerned bodies should make a motivation program policy for planting endemic vegetation on flooded areas and change those flooded areas into green areas.

Keywords: Boyo Catchment, Flood Frequency, Flood Hazard Map, Flood Inundation Map, GIS, HEC-GeoRAS, HEC-RAS

Table of Contents

LIST OF TABLES

LIST OF FIGURES

ACRONNOMY AND ABBREVIATION

DEM	Digital Elevation Model
DG	Depth Grid
DHM	Department of Hydrology and Meteorology
DMC	Double Mass Curve
DPPA	Disaster Prevention and Preparedness Agency
DTM	Digital Train Model
ENMA	Ethiopian National Metrologic Agency
ERA	Ethiopian Rod Authority
ERVLB	Ethiopian Rift Valley Lakes Basin
ESRI	Environmental Systems Research Institute
Geo-RAS	Geometrical River Analysis
GIS	Geographic Information System
GPS	Geographic Positioning System
GUI	Graphical User Interface
HEC-RAS	Hydraulic Engineering Center-River Analysis System
HHEC	Hydrology and Hydraulic Engineering Chair
IPCC	Intergovernmental Panel on Climate Change
IWRM	Integrated Water Resources Management
LULCC	Land Use Land Cover Condition
MoWIE	Ministry of Water, Irrigation and Electricity
MLM	Methods of Maximum Likelihood
MOM	Method of Moment
PWM	Probability of Weight method
SNNPRS	Southern Nations Nationality & People Regional State
TIN	Triangulated Irregular Network
USACE	US Army Corps of Engineers
USWRC	United State Water Resources Council

1. INTRODUCTION

1.1 Background of the Study

A flood is defined as a large, sudden flow of water, particularly a body of water, rising, swelling, and overflowing over the land surface as a result of excessive rainfall, snowmelt, land subsidence, groundwater rising, and dam collapses. Flooding can take many forms, including coastal flooding, river floods, flash flooding, urban flooding, and snowmelt flooding (Jeyaseanln, 2003).

Flood control refers to the actions made to mitigate the negative effects of a flood that results in the loss of lives and property. Flooding is one of the worst natural disasters in terms of economic damages around the world. Flood plain maps that are accurate and up to date can be extremely useful in preventing significant social and economic losses as a result of floods. These new floodplain maps also help to protect people and property. During an emergency, public safety groups can establish warning and evacuation priority by identifying flood-prone properties early. Flooding is produced by high river stages, which can be caused by a variety of factors including excessive discharges, water backing up, and a rise in bed levels. An ever-increasing amount of human interference is taking place in the highlands (Asadi A., 2013).

Unexpected floods can be caused by either naturally occurring or human-caused problems on the planet. High and long-lasting precipitation, as well as catastrophic occurrences like earthquakes and tsunamis, can be natural causes. The breakdown of water retention structures such as dams or levees are examples of man-made causes. Information on flooding characteristics and how they propagate is needed for management and control of flood effects and related concerns. Hydraulic models that can mimic flood episodes, depths, levels, velocity, and timing over a dispersed model domain and over time can provide this information. Models of hydraulics can be used to overcome such issues. HEC-RAS/HEC-GeoRAS is a strong model that can model flooding characteristics if sufficient high-quality input data is available (Ohimain, E. I., 2014).

Other elements that generate unexpected floods in the river system or Man-made roots are human activities. The spatial and temporal distribution of hazards can be influenced by unplanned rapid settlement development, uncontrolled building construction in general, and substantial land-use changes (Elias, 2015).

Flooding is a major concern in Ethiopia throughout the long rainy season, which lasts from June to September. During this time, river runoff increases, causing river banks to overflow or rupture, inundating downstream plane lands. Floods are weather-related natural disasters in Ethiopia, and there are two types of river floods: flash floods and river floods. When heavy rains fall in surrounding high-land areas, flash floods occur in low-lying places (NDRMC, 2018).

These hydrological models, which use a variety of techniques, are being used for a variety of water resource development projects. The method of peak discharge estimation chosen is determined by the data requirements and data availability. Because of their ability to handle the geographical variance of the watershed's hydrological and physiographic inputs, GIS-based hydrological model systems are gradually becoming key hydrological modeling tools. Several models that are either embedded in the GIS environment or have the ability to import the produced GIS-derived spatial and temporal variables. The US Army Corps of Engineers' HEC-RAS (the Hydrologic Engineering Center's River Analysis System) is one of them. The application accurately replicates steady and erratic flow (USACE, 2016).

The availability of data with the requisite geographical and temporal resolution is critical in hydraulic flood simulation. One type of data utilized as an input in hydraulic flood modeling is topographic data. The principal source of topography data for portraying floodplain and river topography in clear raster format was the Digital Elevation Model (DEM) and/or its derivation Triangular Irregular Network (TIN).

The availability and quality of geometric data for river cross-sections, on the other hand, was a serious constraint. A high-resolution DEM is required for such availability of basic data sources. Despite the fact that there is still a gap in finding this high-resolution DEM to reflect the topography of the study region, the 30m-by-30m DEM is chosen to best describe the topography of the study area (Ohimain, E. I., 2014).

1.2 Statements of Problem

Flooding is the most common catastrophic natural phenomenon on the planet, affecting both rural and urban areas, as well as developed and developing countries (Santosa, 2002). However, in developing nations such as Ethiopia, where need forces the poor to occupy the most susceptible locations, the degree of vulnerability to natural catastrophes, particularly flooding, is great. With economic growth and the accumulation of property in flood-prone areas, industrialized countries' vulnerability to floods grows (WMO, 2009).

According to the report, nearly 70% of all global disasters are caused by hydro-meteorological occurrences, particularly flooding, which is the world's second-leading natural disaster in terms of fatalities. Thousands of people are forced from their homes each year, and millions of people are killed by floods. Flooding has caused more deaths in Africa in recent decades as a result of population settlement patterns than as a result of climate change. Floods displaced 2.5 million people in Africa in 2009 and more than a million in 2007, according to the report. Furthermore, from 1950 to 2009, the number of individuals killed in African floods grew by a factor of ten, with over 15,000 people dying between 2000 and 2009. On the other hand, throughout the same time period, habitation in flood-prone areas rose by a factor of ten, and the frequency and severity of floods in most African countries increased significantly (Sinafikish, 2013).

In Ethiopia, flooding is mostly caused by the country's terrain, which includes highland mountains and lowland plains, as well as natural drainage networks established by the major river basins. The geography of the lake in this Boyo catchments is varied, ranging from relatively flat to dissected plateaus. Such relief kinds are evenly dispersed across Shashogo Woreda, with a very flat portion of the entire territory. Because of this physical configuration, most of the Boyo catchment's tributaries begin their journeys from comparatively higher altitudes and catchment areas. Every year during the rainy season, the very flatlands in the area Boyo catchments, particularly floodplains in Shashogo Woreda, are prone to flooding and flood waters in the Shashogo Woreda's flood plain remain stagnant for one to two weeks. A Farmers living in and around the Boyo catchement have endured crop failures and expulsion from the living region of the Boyo catchment as a result of the quick emergence of flood.

The purpose of this thesis work was to generate flood inundation mapping and hazard assessments for the study area in order to avoid economic and environmental losses, crop failure, loss of life, and property.

1.3 Objectives of the study

1.3.1 General objective

The main objective of this research is mapping flood inundation and hazard assessment of Wera river flood plain, Boyo catchment, Ethiopia.

1.3.2 Specific Objectives

1. To Peak discharges estimation for different return periods.
2. To Simulation of flood water surface profile.
3. To Developing a flood inundation map and hazard assessment for the Wera River flood Plian Boyo catchment.

1.4 Research Questions

1. What is the magnitude of peak discharges for different return period of the Wera river flood plain,Boyo catchment? .
2. What is the level of flood water surface profile extracted from the output of HEC-RAS Model?
3. How many area of catchiment is inundated and What is level of hazard in each return and how it is mapped?

1.5 Significance of the Study

One of the most essential aspects of the study was the facilitation of mapping flood hazard regions in order to prevent economic and environmental losses, as well as the loss of life and property in the studied area.

This research has raised awareness among Hydrologists and Engineers about how to develop cost-effective sub-river hydraulic structures. Finally, the government and non-governmental organizations (NGOs) may use the findings of this study to teach the community critical lessons about floods, as well as to contribute to stronger flood control actions based on research findings.

1.6 Scope of the Study

The study was limited to the Wera River flood plain in the Boyo catchment, which is part of the Ethiopian rift valley lake basin (ERVLB). The study was carried out in order to estimate the peak discharge of the deferred return period, to simulate flood water surface, to build an inundation map, and finally to analyze and develop a hazard map for the river flood plain. The estimation was based on tools and models such as ARC GIS and HRC-RAS, with HEC-GeoRAS GIS extension tool interconnection.

2. LITERATURE REVIEW

2.1 Historical back ground and concepts of flood

Natural disasters have always posed a significant threat to human progress and development on the planet's surface. Volcanic eruptions, earthquakes, temperature extremes, hurricanes, tropical cyclones, and flooding are just a few of the natural risks. Floods are by far the most common natural hazard on the planet. This is due to the flood's nature, timing of commencement and occurrence, and recurrence interval. Floods occur in practically every corner of the world, unlike other natural disasters, due to their nature and occurrence. According to the ISDR (2010) flood is one of the most common natural disasters, accounting for almost one-third of all natural disasters worldwide (MulugetaTeferi, 2016).

Around 80% of the world's population will reside in flood-prone areas by the middle of the century. Flood plains are periodically inundated by smaller, more frequent floods that offer nutrition to fertile agricultural regions while also supporting riparian residents' livelihoods (IWRM and Flood, 2015).

Although flood plains are extremely important on one hand, they also have a negative consequence. Floods have several negative consequences, the most serious of which is the threat to human life; nevertheless, flooding can also cause damage to homes, civic infrastructure, agriculture, water supply, and natural ecosystems, among other things (Barrientosa and Swain, 2014).

Flooding is a typical occurrence in Ethiopia's lowlands, such as ERVLB, due to topography and human-caused factors. The Boyo catchment is a part of the ERVLB that is prone to flooding. The problem is mainly confined to landslides, debris flows, and riverbank undercutting in the higher reaches of the watershed, whereas in the low-lying areas like Site zone low lands, Boyo Lake wetland area of Hadiya Zone, and the flat areas of the watershed across the river bank, the problem is mainly confined to landslides, debris flows, and riverbank undercutting. Every year during the monsoon season (June-September), floods overflow the banks, causing bank erosion, inundation, and sedimentation in the numerous streams and rivers (Kefyalew, 2003).

River flooding is a natural occurrence that occurs as a result of rainfall, surface and groundwater flow, and storage in the hydrological cycle. Floods occur when the natural or man-made drainage system's capacity is insufficient to handle the volume of water created by rainfall from the basin (Tolera and Fayera, 2019).

Rivers are fed by a network of ditches, streams, and tributaries, and flow builds up to the point where the typical course is overrun and water rushes into adjacent places when heavy rain falls over large areas. Flooding on large rivers occurs a long time after a rainstorm and lasts for a long time as massive volumes of water drain out of the watershed (Tolera and Fayera, 2019).

Flooding on large rivers occurs a long time after a rainstorm and lasts for a long time as massive volumes of water drain out of the watershed (Tolera and Fayera, 2019). Therefore, local officials will have a tough time directing construction away from the most risky locations or ensuring that building in or near the hazard areas is appropriately built and protected without precise flood maps. Neither the construction nor the insurance regulatory parts of the program can be effective without adequate, accurate, and current maps. To reduce the incidence of flood-related disaster costs, all flood hazard zones must be mapped (Nebiyu and Rabin, 2019)

In Ethiopia, natural hazard assessment is still in its early stages, with less attention paid to assessing flood threats and mapping flood inundation zones. In Ethiopia, flood risk assessment is still a work in progress. Even though some flood protection work has been done in some areas, it has largely been done without basin-scale planning and mapping. This section discusses some of the pertinent Ethiopian literature that was reviewed for this investigation (Solomon, 2012).

This flood requires competent management in order to make reasonable and equitable decisions about flooding episodes. Therefore, inundation mapping is one of the most significant phases in disaster risk reduction because it identifies disaster-prone locations so that disaster risk management can be planned (Nebiyu and Rabin, 2019).

Using the HEC-RAS hydraulic model, the study created a flood risk map by weighting flood depth, flow velocity, and flood duration. Then I made a flood map for various return durations. Flood Risk Analysis in Illu Floodplain, Upper Awash River Basin, Ethiopia by (Dawit, 2015) was carried out to analyze risk on the crop. After the study recommends that to minimize the amount of flood damage, it is recommended that areas inundated by the 100-year return period flood should not be used for agricultural activities, infrastructure development, settlement, and other investment projects during the wet season because has a high probability occurrence in the study area.

2.2 Effect of Flood Global, National and Regional perspective

Flooding is a usual and repeated occasion for a river or stream. Statistically, streams will equal exceed the mean annual flood once every 2.33 years (Leopold et al, 2002). Even if it is a short-term state and vary considerably in size and duration, several people and animal. Risk analysis can be defined as the "systematic use of available information to determine how often specified events may occur and the magnitude of their likely consequences (Granger, 2002).

A good risk analysis process yields hazard or risk maps, which are drawn using Geographical Information Systems (GIS) based on extensive surveys of vulnerability combined with topographic maps. To do this, the hazards are to be combined with the vulnerability into the risk. The vulnerability of the persons or objects (the 'elements at risk') in an area, which is inundated if a flood of ascertaining magnitude occurs, is weighted with the frequency of occurrence of that flood (Gizachew and Shimelis, 2014).

Flood risk can be assessed in quantitative terms as well as being accessible and understandable through qualitative investigation. A discussion of risk can suggest a move into the subjective world of perception, where different people and their belongings experience varying degrees of risk associated with flooding. The risk of flooding is therefore not only associated with the physical nature of the hazard. For example, frequency and magnitude, and proximity to the hazard also relate to the ability to manage, adjust and adapt to the event itself. This implies that risk is the conjunction of the natural physical hazard leading to the socio-economic vulnerability of the population in the area (Barrientosa and Swain, 2014).

Different parts of the country are vulnerable to the relatively up (UNISDR, 2009) cemented and abnormal magnitude of flooding. For example, in 2006, more than 357,000 people were affected by flooding (out of which 600 died, 200,000 became home-less) and the country lost about 40 million Ethiopian Birr (UNOCHA, 2006).

Almost all countries in Sub-Saharan Africa are exposed to one or multiple natural hazards. Flood usually affects large river basins such as the Congo, Niger, Nile, and Zambezi basins. The disproportionate impact of natural disasters on poor Sub-Saharan African countries are not been well documented (UNISDR, 2009). Published literature proposes that the magnitude and frequency of flooding increased quickly in recent years in the country. It is indicated by the intensely increased number of people and areas affected; the number of deaths; and infrastructure and property Loss. Manifestation of climate change in the form of erratic rainfall, frequent and severe floods; and droughts have grave consequences on the livelihood, security of smallholder farming communities, and making them more vulnerable in countries like Ethiopia (Gizachew and Shimelis, 2014).

Population growth, poverty, food insecurity, improper use of natural resources, and rapid urbanization are among the driving factors behind the increased exposure of Sub-Saharan Africa to natural hazards (Ashok and Saroj, 2010).

2.3 Flood problem in Ethiopia

Two fundamental factors characterize the relationship between land use and flooding. The first relationship is the presence or location of economic values and critical components on flood plains, which provides economic benefits while also posing a risk to society in terms of flood loss potential. Second, land development through various construction activities has an impact on water flow on the one hand, either by accelerating runoff by diminishing soil infiltration capacity or impeding the natural drainage system on the other, as well as sediment and pollutants. In general, large-scale land-use changes and land-use practices can significantly contribute to changes in all those processes that are hydrological processes in the catchment area. Furthermore, as the catchment area is altered and developed by humans, the runoff generation process is altered, particularly due to decreased soil infiltration capacity and changes in soil cover. As a result, there is a great

deal of concern about humans, who play a significant role in increasing flood hazards by altering catchments (WMO, 2009).

The Awash River, which flows across the Rift Valley, is a large river basin with serious concerns. Irrigation is well advanced in the river basin, and it is concentrated in the flood plains on both sides of the Awash. Almost all of the sites demarcated for irrigation expansion in the Awash Valley are prone to flooding, according to estimates. During high Awash River flows, an area of about 200,000250,000 acres is at risk of flooding. The Wabi Shebelle River in southeastern Ethiopia, near the Somali border, and the Baro Akobo/Soba t River in western Ethiopia, near the Sudanese border, are two more rivers that experience considerable flooding. The Baro-Akobo Plain (also known as Gambelia Plain) is a region of the Gambelia Plain. Floods typically occur at irregular intervals and vary in severity, duration, and flood area affected. Floods in Ethiopia's multiple river systems can have a variety of consequences and concerns, including contamination of drinking water, death and injury, disruption of homes and communities, displacement, and distraction of the populace and wildlife. During the rainy season, several sections of Ethiopia are frequently affected by flash, urban, and river floods induced by severe rainfall occurrences. Several reasons could be to blame for the seeming rise in flood risks and disasters. Increased population and asset exposures result in increased hazard frequency and intensity (Kundzewicz et al., 2014).

2.4 Consistency test of data

Double mass analysis was employed as a consistency method for flood data in the watershed by (Searcy J K and Hardison C H, 1960). This analysis is being done on the stations for the watershed to see if there are any data corrections that need to be made. They discovered that the double mass analysis applied to all stations showed good time behavior, indicating that data collecting processes or other local variables have no substantial impact on the data.

2.4.1 Double mass curve test

The theory of the double mass curve is based on the assumption that, as long as the data are proportionate, a graph of the accumulation of one quantity versus the buildup of another

quantity over the same period would show as a straight line. The constant of proportionality between the quantities will be represented by the slope of the line. A change in the constant of proportionality between the two variables, or perhaps the proportionality is not constant at all rates of accumulation, is indicated by a break in the slope of the double-mass curve. A break in the slope denotes the period when the relationship between the two quantities changes if the potential of a changeable ratio between the two numbers is neglected. The slope disparities of the lines on either side of the slope break reflect the degree of change in the relationship. Accumulations of two measurable variables shown as a double mass curve can provide indeterminate results.

The accumulation of one of the variables can be plotted against the accumulations of a pattern, which is made up of all similar records in a certain area, to get more precise results.

2.4.2 Flood Frequency Analysis

Floods, for example, are more complex natural occurrences than hydrologic processes. As a result, flood in a catchment is determined by the catchment's characteristics and antecedent conditions, which are all dependent on a variety of constituent parameters. As a result, this estimates the flood peak, which is a very difficult problem with many various techniques, but the statistical method of frequency analysis is the best approach to flood flow prediction and also applies to another hydrological process (Subramanya K, 2013).

In order to determine future choices for such incidents, it is also necessary to comprehend the prior record of flood events. The estimation of flood frequencies is required for a quantitative assessment of the flood situation. This occurrence is necessary for the proper design and placement of hydraulic structures, as well as other related studies. After a thorough examination of the gauge data and descriptive characteristics such as mean and standard deviation, etc., and the application of probability theory, reasonably predict the probability of any major flood events in terms of discharge or water level for a given return time (Singh, S. K., 2004). One of the most difficult tasks for hydrologists is to accurately predict major flood events (Leš˘cešen and Dolinaj, 2019). One of the most important topics in river hydrology is flood frequency analysis. The goal of flood frequency analysis is to calculate the flood magnitude that corresponds to any necessary return time of occurrence (Demissie,Negash and Behailu, 2016).

It is critical to analyse flood records in order to assess the likelihood of future recurrence. Flood low-frequency analysis can be used for a variety of engineering purposes, including the design of dams, bridges, culverts, and flood control structures; determining the economic value of flood control projects; and delineating flood plains and determining the impact of encroachments on the flood plain (Chow Vent et al, 1988).

Long series data is required to analyze peak flood data. In essence, there is no mechanism for calculating the precise amount of flood. The catchment's magnitude. Then there are certain ways that rely on probability or empirical equations. Gumballs, Log-Normal, and Log Pearson III type methods are all based on Probability Theory. (Manandhar, 2010) used these methods to examine flood risk zoning of the Kwando river, and (IPCC, 2007) (Osti, 2004) used them to do a feasibility study on Integrated Community Based Flood Disaster Management of Bankes, District.

2.5 Tools for Floodplain Analysis and Mapping

For numerical modeling and analysis in GIS, a variety of commercial and noncommercial software packages are available. The models can be further classified into dimensional and two-dimensional models based on information on the lateral distribution of flow across cross sections. Below are descriptions of some of the software tools that are available.

2.5.1 Geographical Information System

A Geographical Information System (GIS) is a fast-evolving tool with several applications in various disciplines of study today. GIS stands for Geographic Information Systems, which are computer systems capable of assembling, storing, manipulating, and displaying spatially referenced data (ESRI, 1990).

GIS is a powerful tool because of the incredible clarity with which it presents and analyzes data. It includes not just the GIS package, but also the database, graphing, and imaging software, and the capability of the software used to manage the GIS determines the kind of problems that the GIS can handle. The software must be tailored to the end-demands users and abilities. Vector-based GIS, such as Arc GIS (ESRI), ArcView, and Map Info, and raster-based GIS, such as Erdas Imagine (Leica), ILWIS (ITC), and IDRISI, are the most used GIS software (Clark Univ). A powerful, user-friendly, point-and-click graphical user

interface for loading spatial and tabular data and displaying it as maps, tables, and charts (Murayama and Estoque, 2010). These provide the tools for querying and analyzing data, as well as presenting the results as high-quality maps. The project, which may include views, tables, charts, layouts, and scripts, organizes all of the activities in ArcView/ArcGIS, GIS. We can alter ArcView's menus, buttons, and tools for unique applications by using Avenue. In Arc View GIS, different extensions, or add-on programs, can provide extra capabilities (ESRI, 1997).

2.5.2 Global Positioning System (GPS)

The Navigation Satellite Time and Ranging (NAVSTAR) Global Positioning System (GPS) was developed by the United States Department of Defense (DOD) to provide navigation, position, and timing information for military activities across the world. Specifications of Selected Models (Vail,Parsons,Striggow,Deatrick and Johnson, 2015).

2.5.3 Hydro Dynamic Models

The HEC RAS stands for Hydrologic Engineering Center's River Analysis System, and it may be downloaded for free from the Hydrologic Engineering Center's website, much like the other applications. The HEC-RAS hydraulic model was developed by the US Army Corps of Engineers' Hydrologic Engineering Center (HEC). For various flow circumstances, the model is used to calculate water surface profiles (USACE, 2016).

2.6 Data analysis for flood estimation

Before beginning statistical analysis, it's important to think about sample size and quality, such as completeness and consistency. For higher precision and accuracy in statistical analysis, it is preferable to use a sufficient sample and complete homogeneous data. In extreme flood analysis, such problems of sample completeness and homogeneity can be solved by extracting the daily annual extreme series, identifying and estimating the missing year's data, testing the consistency of the record, and finally reconstructing the data for any gaps and inconsistencies of records (Quraishi S and Berhane M, 2014) and (Subramanya, 1988).

2.6.1 Estimating missing data

The daily observed data time series is reviewed for potential abnormalities over time before estimating the observed daily yearly maximum flood time series. Weather stations having 30 percent or more missing daily data and/or 3 or more years of consecutive gaps are ineligible for analysis (Quraishi S and Berhane M, 2014).

Data Outlier Analysis An outlier is a data point that deviates greatly from the majority of the data, which could be due to data collecting, recording, or natural reasons, among other things. Outliers should be explored since they can provide useful data or process knowledge. Outliers may provide incorrect results in trend tests and time series modeling unless they are identified and remedied.

Several reasons for the occurrence of outliers, according to Javari (2017), can be found. Improper data entry: Re-analyze the data after fixing the error. Issue with the process: Look into the process to see what's causing the anomalies. Determine whether you filled in the blanks to account for a process-influencing factor.

2.6.2 Fitting Data to the Probability Distribution Function

The yearly daily maximum Flood data was analyzed using frequency analysis techniques (Gebremedhin Y G ,Quraishi S and Itefa, 2017). The relevant plotting point supplied in Table 2.2 is used to fit the theoretical probability distribution to the observed data.

2.6.3 Plotting position

Either empirical or analytical methods can be used to conduct a probability analysis. The plotting position formula is used to calculate the probability p at each event being equal to or exceeding (plotting position) after data is arranged in decreasing order of magnitude, and those plotting positions are also used to know the relationship between T and probability of occurrence of various events. The following table lists many plotting position equations (Subramanya K, 2013).

Table 2.1 Different plotting positions formulae

Plotting Positions Formulae	Formulae
Hazen (1930)	$\frac{m-0.5}{N}$
Weibull (1939)	$\frac{m}{N+1}$
Gringorton (1963), Heo *et al.* (2008)	$\frac{m-0.375}{N+0.25}$
Cunnane (1978)	$\frac{m-0.4}{n+0.2}$
California (1923)	$\frac{m}{N}$
Blom (1958)	$\frac{m-0.4}{n+0.12}$
Chegodajev (1955)	$\frac{m-0.3}{n+0.4}$

2.6.4 L-moment for selection of probability distribution

L-moments are similar to moments, but they are calculated using a linear combination of an ordered set, particularly L-statistics. The advantages of L-moments are as follows: (Cunnane, 1989). L-moments, in contrast to the method of moments, can characterize a wide range of distributions. L-moment sample estimates are sufficiently robust that they are unaffected by outliers in the data set and are less susceptible to estimation bias. The L-moments that follow are defined by (Cunnane, 1989).$\tau 2=\lambda 2/\lambda 1$ (L-variation coefficient, L-Cv), $\tau 3 = \lambda 3/\lambda 2$ (L-skewness coefficient, L-Cs) S $\tau 4 =\lambda 4/\lambda 2$ (L-kurtosis coefficient, L-Ck).

2.7 Method of Parameter Estimation

Parameter estimate can be done using a variety of ways. Method of the moment (MOM), Maximum likelihood method (MLM), and Probability weighting method are three of the most often utilized approaches discussed here (PWM).

2.7.1 Method of moment (MOM)

The method of moment (MOM) is a simple and natural method for estimating parameters. MOM estimates, on the other hand, are frequently of worse quality and less efficient than MLM estimates, particularly for distributions with a large number of parameters (three or

more), because higher-order moments are more likely to be heavily skewed in small samples.

2.7.2 Maximum likelihood method (MLM)

When compared to other methods, the maximum likelihood method (MLM) is considered the most efficient since it gives the smallest sampling variance of the estimated parameters and hence of the calculated quantiles. The MLM technique necessitates more computing work, however this is no longer a serious issue thanks to the widespread usage of high-speed personal computers (Bobee and Ashkar, 1991).

2.7.3 Probability weighting method (PWM)

The PWM approach (Greenwood J A, Landwehr J M, Matalas N C and and Wallis J R, 1979) and (Hosking J R, 1986) produce parameter estimates that are comparable to MLM estimates, but the estimation procedures are less complex and the calculations are easier in some circumstances. PWM estimations of parameters from small samples are sometimes more accurate than MLM estimates (Landwehr J M, Matalas and Wallis, 1979).

2.8 The Probability Distribution

The WMO (2009) suggested distribution models for the annual maximum data series are listed below (Cunnane, 1989). Gamma distribution (GAMA2), General Extreme value type distributions, Normal distribution (NOR), two parameter Log-Normal distribution Extreme value type one distribution (EVI) or Gumbel.

2.9 Goodness of fit test

The goodness of fit (GOF) tests determine if a random sample is compatible with a theoretical probability distribution function. In other words, these tests determine how well the chosen distribution fits the data. The results are presented in the form of interactive tables that aid in the understanding of the data. Choose the model that best describes your data. Several goodness-of-fit tests have been performed. The Kolmogorov-Smirnov test, Anderson-Darling test, and the chi-square test have all been used. For selecting the optimum probability distribution, a square test at a significance threshold of 0.05 was used (Alem, 2018).

2.10 Previous Related Study

Flooding is a natural occurrence that can affect people, property, infrastructure, and the environment in many regions of the world as river, flash, urban, and coastal floods. As people seek the benefits of living near water, they encroach on flood-prone areas, increasing the risk of flooding.

(Solomon, 2012); used 2D hydrodynamic flood modeling to work on flood risk mapping and vulnerability analysis of the Megech River. Using the HEC-RAS hydraulic model, the study created a flood risk map by weighting flood depth, flow velocity, and flood duration. Then I made a flood map for various return durations. (Dawit, 2015) Conducted a flood risk analysis in the Illu Floodplain, Upper Awash River Basin, Ethiopia, to assess the risk to the various crops in the study area.

They conclude that, in order to reduce the amount of flooding, areas inundated by the 100-year return period flood should not be used for agricultural activities, infrastructure development, settlement, or other investment projects during the wet season due to the high probability of occurrence in the study area. Ethiopia Flood hazard and risk assessment were investigated using GIS and remote sensing in the lower Awash sub-basin by (Yirga, 2016) to identify the land mass inundated by the unexpected flood.

The research found that low, moderate, high, and very high flood threats existed in 107,145.01 ha (5 %), 522,116.92 ha (23%), 897388.95 ha (39%), and 763045.31 ha (33%) of the region considered in the Lower Awash Sub-basin, respectively. According to the study's findings, one shortcoming of this method of flood hazard and risk mapping is that the GIS output is not paired with an appropriate hydrologic/hydraulic method for estimating stages. As a result, there is no hydrodynamic modeling or estimation of flood depth inundation in this work.

In the study of middle and upper Awash sub-basins, it recommends as the future study for the lower Awash Sub-basin and focus on generating flood hazard maps to identify the depth of inundation through hydrodynamic simulation. Thus, most of flood hazard research in Ethiopia have been concentrated in the Tana sub-basin specifically (Yirga, 2016).

(Demissie,Negash and Behailu, 2016) they studied on collaborative effort on the assessing of the influence of climate change on flood frequency in the Binate River Basin, Ethiopia, they used the HEC-HMS model and HEC-SSP software found that the study area's precipitation and temperature had altered, resulting in floods in the basin for the next 30 years. Floodplain modeling was completed for the Awitu River sub-basin in Oromia, Ethiopia (Tolera and Fayera, 2019). They concluded that upstream and downstream right banks are more vulnerable to flood inundation, with findings of 130.7 ha and 185 ha for return periods of 5 and 1000 years, respectively, using the HEC-RAS model and HEC-GeoRAS ArcGIS tool. (Bucha and Selvaraj, 2019) , used the HEC-RAS model and the GIS tool to map flood inundation in Galena, Ethiopia's Rift Valley. Their findings suggest that the watershed size of 3.99, 2.32, 2.21, 2.13, and 2.04 ha corresponds to very high, high, moderate, low, and very low flood dangers, respectively. Flood-prone sections of the Boyo watershed were mapped using a combination of multicriteria analysis and GIS techniques (Muse,Getaneh and Abiy, 2018). The weighted overlay function of the five criteria generated a final result that identified three flood-prone zones in the watershed as high, moderate, and low flood-prone areas, respectively, spanning 28.5 percent (1603.16 Km2), 61.4 percent (3453.82 Km2), and 10.1 percent (568.14 Km2). Flood hazard and risk mapping employing multicriteria analysis and GIS results is not combined with an applicable hydrologic /hydraulic approach for evaluating flood hazard relative to stages, resulting in overestimation of the area itself.

As a result, studying river plain flood inundation mapping and hazard assessment using GIS and HEC-RAS on Wera River, Boyo Flood Plain is a viable and timely research topic. There was also no additional research in this area by employing these tools and models to analyze the Wera River and the Boyo flood plain using the GIS tool and the hydrodynamic model HEC-RAS model. Floodplain modeling was completed for the Awitu River sub-basin in Oromia, Ethiopia (Tolera and Fayera, 2019).

They used the HEC-RAS model and HEC-GeoRAS ArcGIS tool to conclude that upstream and downstream right banks are more exposed to flood inundation with their finding of 130.7 ha and 185 ha for the return periods of 5 and 1000 Yrs. respectively. Flood inundation mapping in Galena, Rift valley in Ethiopia was done by (Bucha and Selvaraj, 2019) was

done using the HEC-RAS model and GIS tool. Their findings suggest that the watershed size of 3.99, 2.32, 2.21, 2.13, and 2.04 ha corresponds to very high, high, moderate, low, and very low flood dangers, respectively. Flood-prone sections of the Boyo watershed were mapped using a combination of multicriteria analysis and GIS techniques (Muse,Getaneh and Abiy, 2018).

The weighted overlay function of the five criteria generated a final result that identified three flood-prone zones in the watershed as high, moderate, and low flood-prone areas, respectively, spanning 28.5 percent (1603.16 Km2), 61.4 percent (3453.82 Km2), and 10.1 percent (568.14 Km2). Flood hazard and risk mapping employing multicriteria analysis and GIS results is not combined with an applicable hydrologic /hydraulic approach for evaluating flood hazard relative to stages, resulting in overestimation of the area itself. As a result, studying river plain flood inundation mapping and hazard assessment using GIS and HEC-RAS on Wera River, Boyo Flood Plain is a viable and timely research topic. There was also no additional research in this area by employing these tools and models to analyze the Wera River and the Boyo flood plain using the GIS tool and the hydrodynamic model HEC-RAS model.

3. Description of Study Area

3.1 Materials and Methods

3.1.1 Location

The Boyo catchment is located in the northeast of Ethiopia's Rift Valley Lakes Basin, which is one of the country's 12 major basins. According to the topography digital map, the catchment extends from 7 °15'37" N to 8° 05' 50"N and 37° 40' 45"E to 38°14' 0"E, with the highest elevation range of 3341m above sea level at the High lands of Site and Gurage zones and the lowest elevation 1789m above sea level near Alaba Kulito. The catchment area is approximately 1641.08 km2, and it encompasses five administrative zones: Kembata, Hadiya, Site, and tiny portions of Gurage and Alaba.

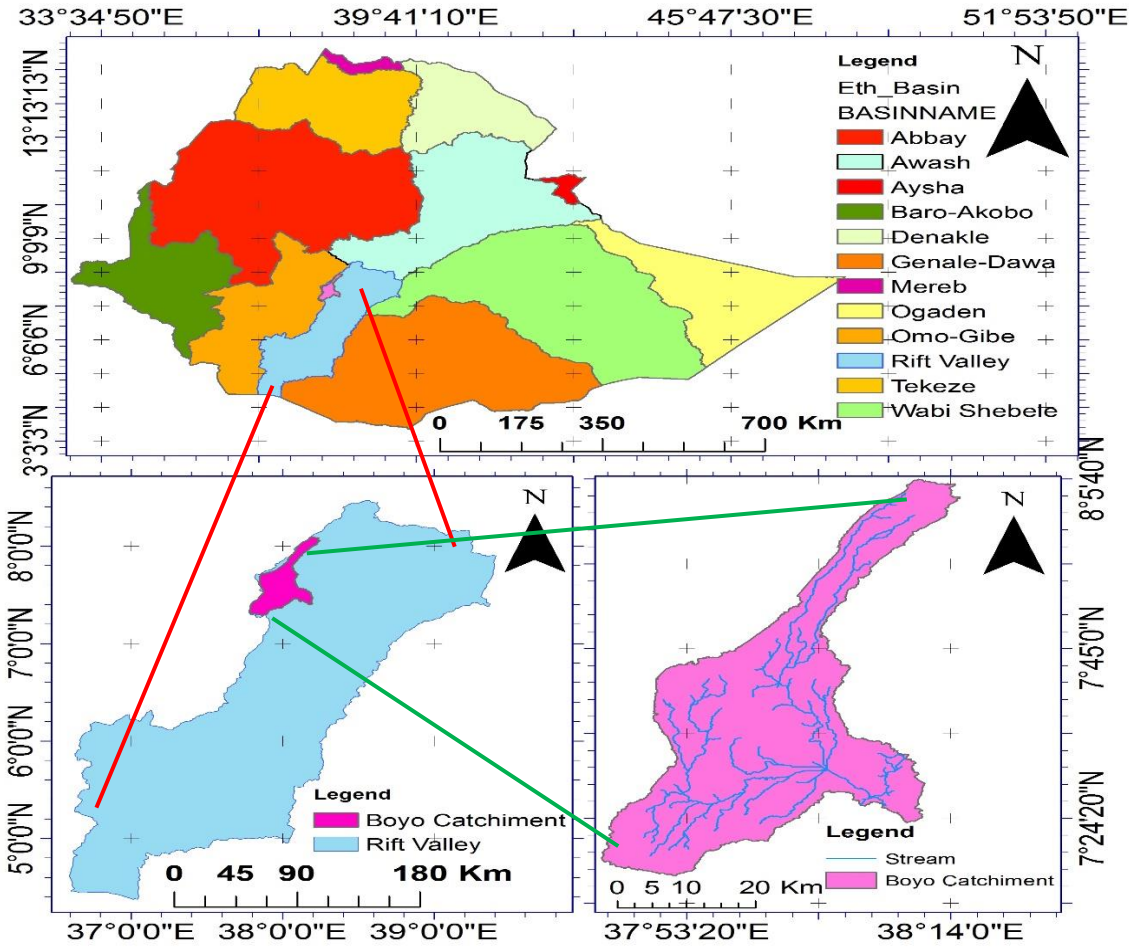

Figure 3.1 Location Map of study Area

3.1.2 Natural Vegetation and Water Resources

Acacia species, Cordia-Africana, and eucalyptus species are the most regularly seen residual tree species in the area. Because of the area's long history of agriculture and large population, most of the tree species seen during the study are cultivated, and vegetation cover is quite low. As a result, erosion risks on steep slopes are extremely high.

Huge gullies may be seen near the wear River and the southern end of the watershed, where soils have been completely gone. Wear, Guder, Metenchose, and Menarche are four rivers that r with the exception of Bilate, all rivers are seasonal. Bilate is a year-round river, despite the fact that the volume of water drops dramatically during the dry season.

According to recent investigations, the Shashogo Woreda's water table is shallow. Boyo Lake Swamp, which covers around 3,210 hectares, is also present. The study district's remaining tree species are witnesses to the land cover/land-use change that has happened as a result of human activities through the secure zone with the exception of Bilate, all rivers are seasonal. Bilate is a year-round river, despite the fact that the volume of water drops dramatically during the dry season.

According to recent investigations, the Shashogo Woreda's water table is shallow. Boyo Lake Swamp, which covers around 3,210 hectares, is also present. The study district's remaining tree species are witnesses to the land cover/land-use change that has happened as a result of human activities.

3.1.3 Topography

Mountain Ambericho to the west, Mugo ridge to the north, and mountain Dato to the east define the study area in the rift valley bottom. Rifting, erosion, and deposition processes have resulted in the area's physiographic setting. The Boyo plain is mostly located between elevations of 1789 and 2,491(a.s.l) meters above sea level. The location is bordered by high hills, making it vulnerable to soil erosion at higher altitudes and deposition in the Hadiya zone's Boyo flood plain.

3.1.4 Agriculture and LULC

Crop cultivation and livestock such as cattle, cows, and other livestock, as well as production, are the main economic activities. Low productivity due to soil degradation, reliance on rain-fed agriculture, and poor socio-economic services are among the area's primary development concerns.

Maize, teff, wheat, pepper, haricot bean, sorghum, and millet are the principal crops farmed in the area, with maize, teff, wheat, pepper, haricot bean, sorghum, and millet being the most common. In the research area, pepper is the predominant cash cropping method for bolstering food production and creating additional money. As indicated in Fig. 3.2.

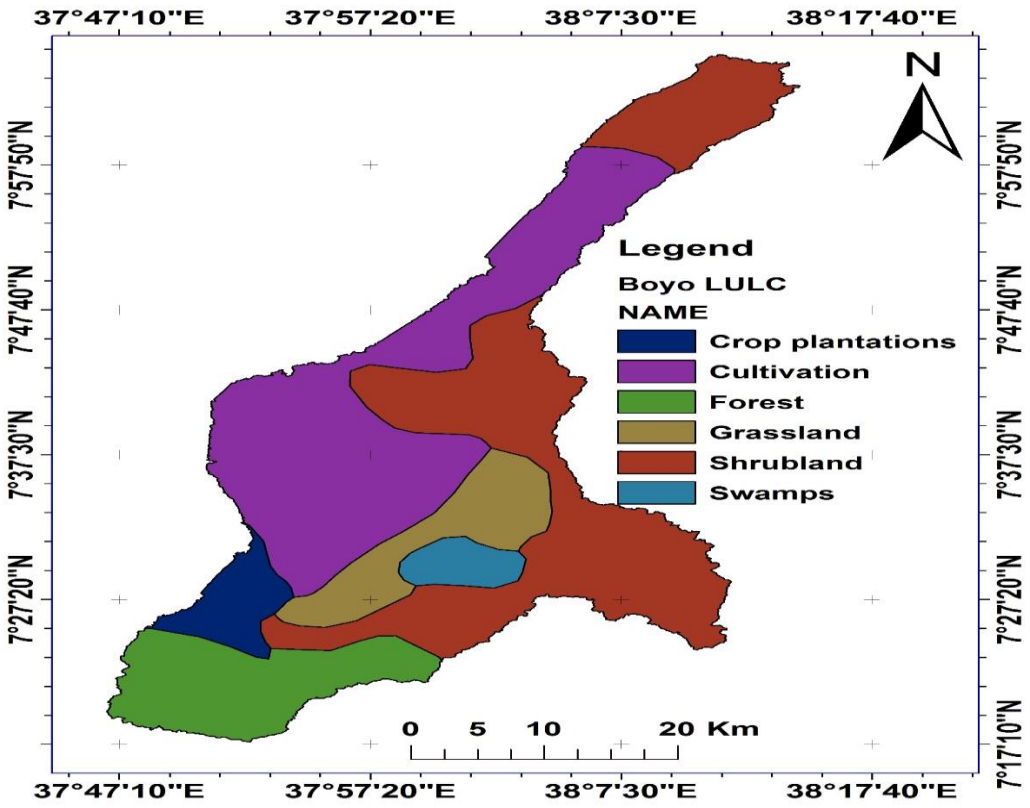

Figure 3.2 Boyo LULC Map study area

3.1.5 Physiography

The study region offers a variety of topography formations, ranging from very flat to rough terrain. Mountainous lands exist in the northwestern and southwestern parts of the territory, and they are relatively rugged. The lowest elevation is in the southern part of the territory,

on the flood plains of Shashogo Woreda in the Main Ethiopian River Rift Valley (MERRV). From west to east, there is a general decrease in altitude.

The studied area's geomorphology is primarily influenced by geological formations and rock kinds. The majority of the elevated ridges in the study region are formed by normal fault escarpments and volcanic domes. Boyo plain, severely rugged terrain, ridges, plateau, and hilly are the key geomorphological features that describe the research region.

3.1.5.1 Boyo Plain

The trough extends about north-south and is bounded on the east by the Lemo structural ridges and on the west by the Ambericho fault. In the north, the Ambericho fault scarp forms a cliff, although it gradually slopes down to the Bilate River, south of Bonshaw town. Lacustrine and alluvial, debris flow, or talus deposits cover much of the plain's floor.

3.1.5.2 Ridges

The area's northwestern and southern sections, particularly Misha Woreda, are mountainous and crisscrossed by parallel and sub-parallel drainages. Rhyolite and ignimbrite are the most common rocks found in the area. Sharp Crested Ridges are structurally controlled ridges that run north-south in the northeast corner of the basin. They are the Nazareth and Dino formations lithological.

3.1.5.3 The Plateau

This is where the mouth of the Guder River and the western edge of the Boyo plain meet. Acidic to moderate to intermediate lava rock types, as well as pyroclastic deposits such as ignimbrites and secondary tuff, characterize this region. The cliffs facing Boyo plain abruptly cease at this point, and the lithology quickly changes to lacustrine deposits.

3.1.5.4 Mountainous

The lithological features of the mountainous features are ignimbrite and rhyolite, and they are found in the northwestern, southwestern, and southeastern regions of the catchment.

Figure 3.3 Mountainous Forest which divide lemo and shashogo woredas (source capturing photo from site observation 6/ 24//2020 at 10:45AM).

3.1.5.4 Soil

There are five soil types in the study region, according to FAO (1997) soil classification: vertic and osol, eutricvertisol, chromic luvisol, and lithic leptosol. The major type of soil in the northern areas of the research region, including Lemmo, Analemma, Wulbarge, Misha, and Mierabazerinet Woreda, is chromic luvisol. Vertic, as well as the entire Shashogo Woreda, are covered. The southern areas of the study region, including most of

Doyogena and Agatha, are covered in eutric vertisol. Danboya Woreda, as well as sections of Lemmo, Doyogena, and Agatha, are covered in humic nitisols.

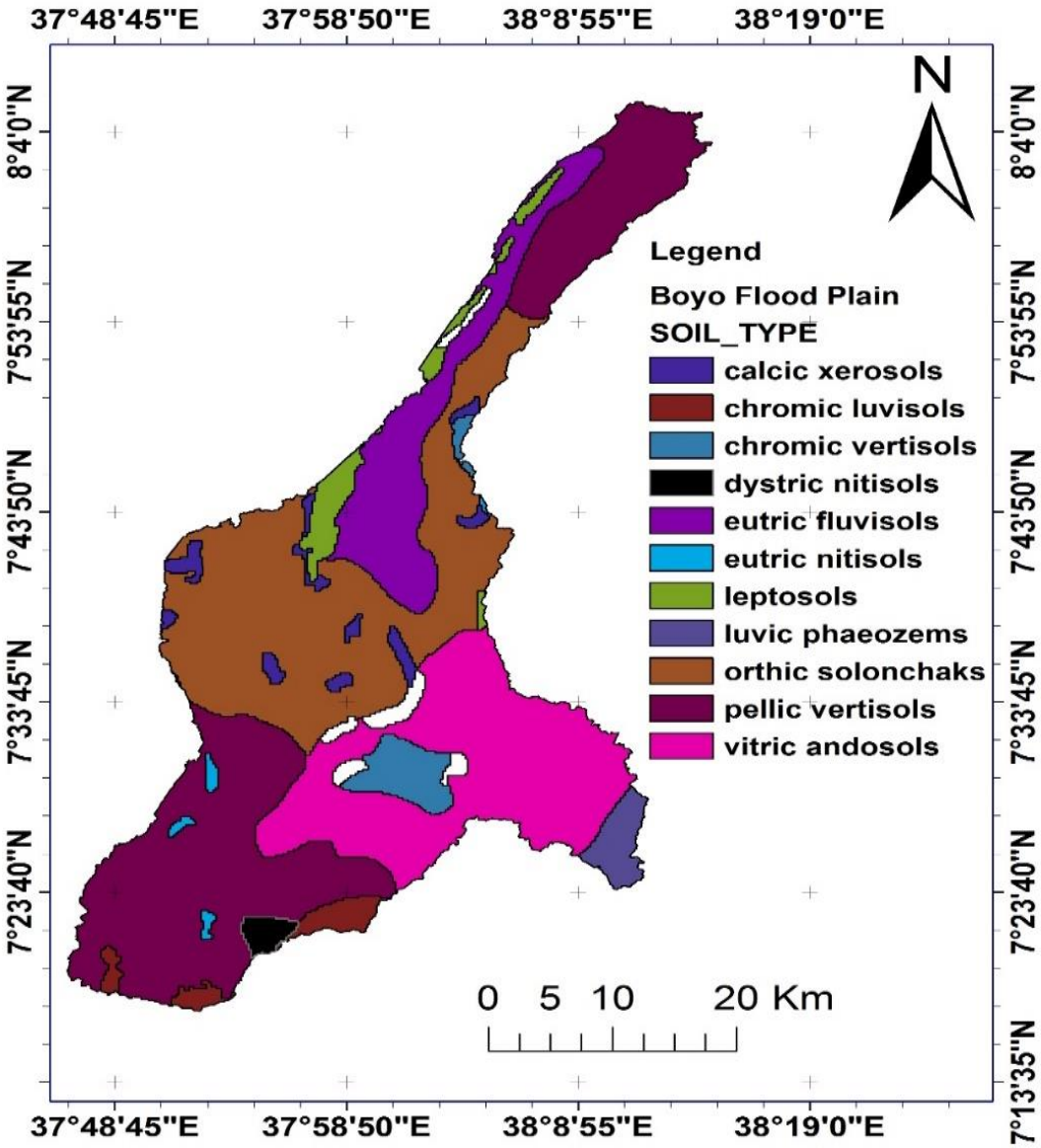

Figure 3.4 Soil map study area

3.1.5.6 Drainage and River System

The geologic characteristics of the study region have an impact on the drainage pattern. It was scanned from the area's topographic map and depicts dendritic drainage patterns. The principal streams drain to Lake Boyo in parallel drainage patterns aligned in a general north-south direction, following the orientation of key structural lines.

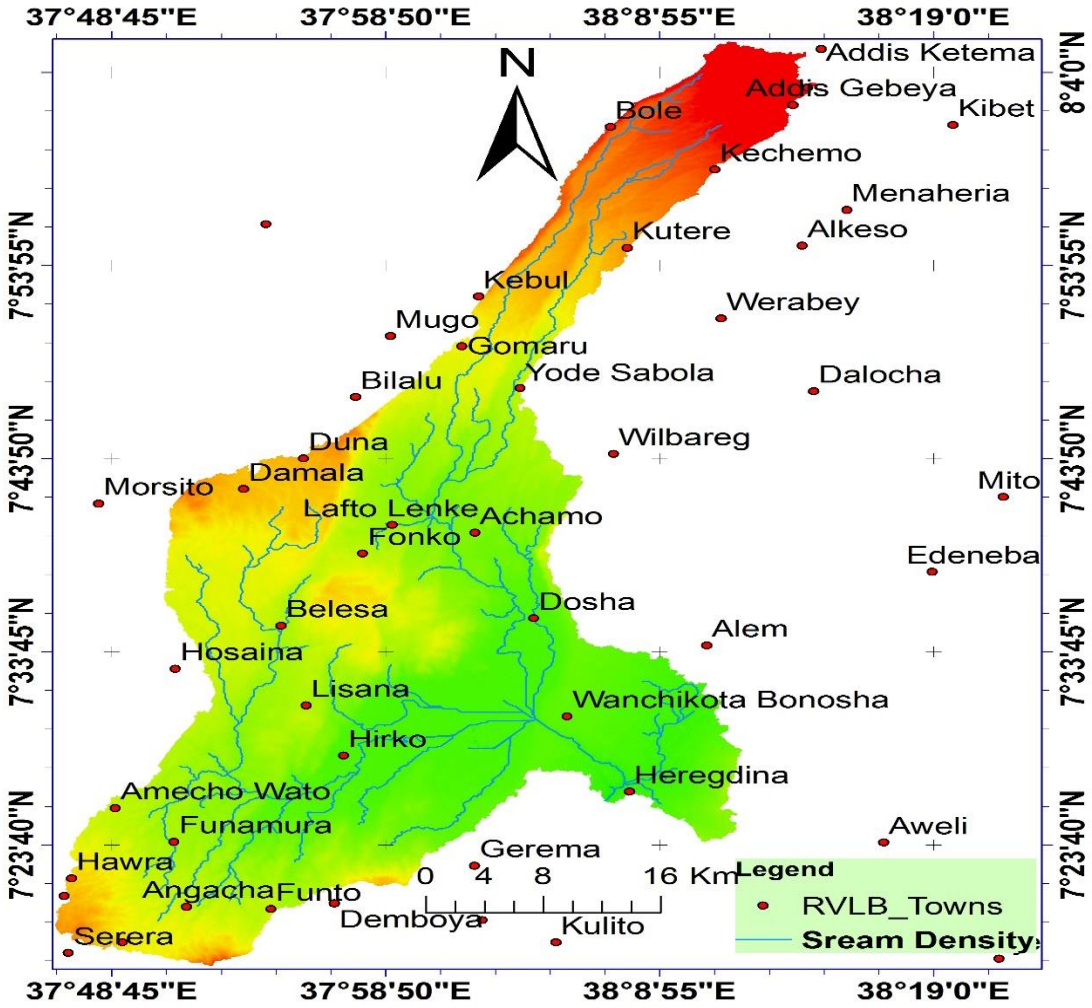

Figure 3.5 Drainage Density map of the Study Area

The Guder River and the Metenchose are the two primary rivers in the study area's river system. Rive Guder emerges near Hosanna and flows east to Lake Boyo, whereas Metenchose emerges from the Site zone and flows south to Lake Boyo. The Fofo stream feeds Lake Boyo's water into the Bilate River.

3.2 Materials and Tools Used

Literature, the internet, a book, and a computer were primarily used to conduct this research. To conduct this study, major tools were Microsoft Excel 2010, Global Mapper 18, DEM (Digital Elevation Model), GIS 10.4 software, HEC-RAS Version 5.0.7, and HEC-GeoRAS 10.3.

3.3 Data Types and Sources

3.3.1 Hydrological Data

Hydrological data, particularly streamflow data from stations within or near the catchment, (1990-2017) was legally obtained from MoWIE via a JIT request letter.

3.3.2 Topographic Data

MoWIE provided a digital elevation model with a resolution of 30m by 30m to generate TIN on ArcGIS10.41 for the compilation of river geometric data as HEC-RAS input. Correct topography representation is required as impute data in the HEC-RAS model to accurately reflect the river channel bed and other flood plain features in the catchment. As a result, MoWIE or the Ethiopian map authority were consulted for information on river and flood plain topography.

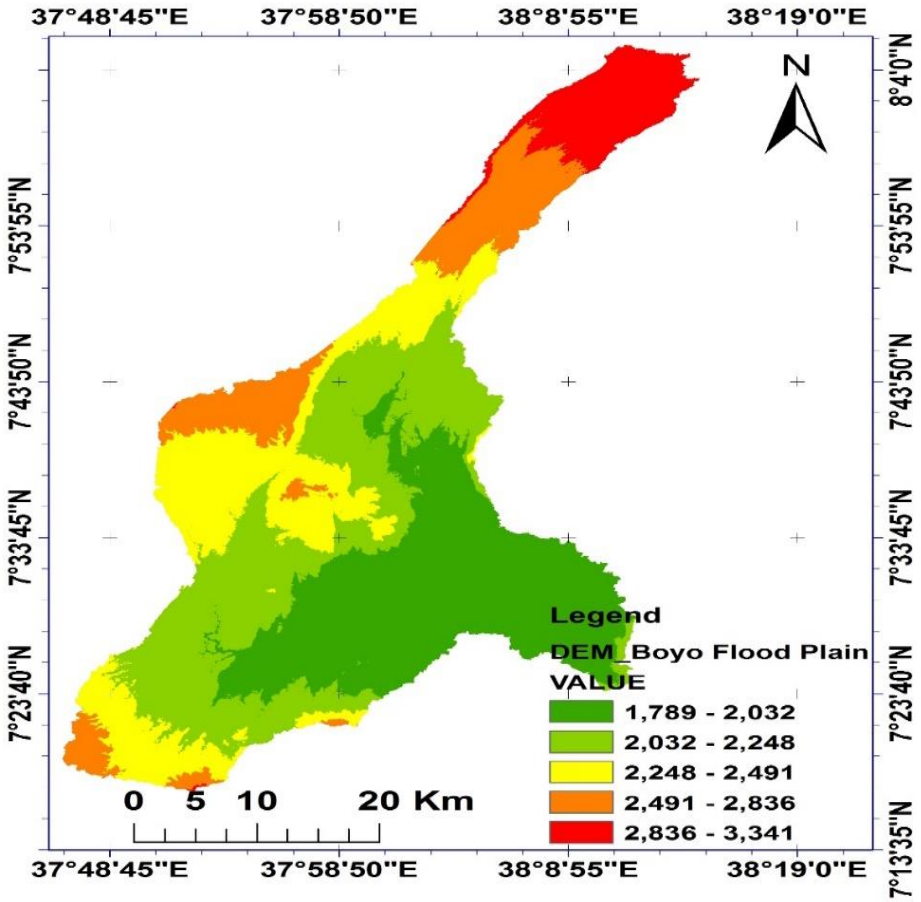

Figure 3.6 DEM of the Study Area

3.3.3 Spatial Data

Topography was defined by a DEM which describes the elevation any point in a given catchment area at specific spatial resolution. This high resolution of DEM 30mx30m was Correct topography representation is required as impute data in the HEC-RAS model to accurately reflect the river channel bed and other flood plain features in the catchment. As a result, MoWIE or the Ethiopian map authority were consulted for information on river and flood plain topography**.**

3.4 Data Preparation and Analysis

Following the collection of all data, the raw data was prepared and investigated in order to make it valuable for the research study. Identifying and filling missing data, ensuring data consistency, and data analysis were all part of the data preparation and analysis process for the flood hazard assessment study.

3.4.1 Filling Missing Data

Missing data refers to a situation in which some values from a specific point in time are missing owing to a variety of factors. Missing data, also known as missing values, occurs when no data values for a variable time period are stored in an observation. One of the most essential inputs in hydrological analysis is daily rainfall data. Most daily rainfall data series, on the other hand, are too short to undertake reliable and useful analyses, and they have a large number of missing records (Hasan M M and Croke B, 2013).

Different circumstances, such as extreme natural occurrences and human-induced phenomena, could cause hydrological data records to be lost: - field personnel misuse of observed data, wars, etc. As a result, filling in the missing observation is the first step in any hydrological data analysis. There are numerous ways to fill in the missing observation. These methods include the Arithmetic method, normal ratio method, weighted distance interpolation method, time series analysis method, and regression method for filling hydrological data (Sattari et al., 2016). The Regression Method, Station Average Method, and Normal Ratio Method are all used to fill in missing data.

3.4.2 Regression Method

A multiple linear regression of the form

$$P_X = a_o + p_1 a_1 + p_2 a_2 + \cdots + p_{nan} \quad \text{.....3.1}$$

Where; a_1, a_2, ·····, an can be calculated by the least square method. The equation can be used to compute rainfall Px of the missing station. This method is more efficient when the digital computer is available at the rain gauge site. A random standard error may be added to the equation when a large amount of missing data is to be estimated.

3.4.3 Normal Ratio Method

This method of data infilling is given as following equation 3.2

$$P_X = N * M\,[P_1 N_1 + P_2 N_2 + \cdots + P_N N_n] \quad \text{.....3.2}$$

Where: Nx is annual average precipitation at the gage with missing values $N1$, $N2$, ····· Nn is annual average precipitation at neighboring gauges if the annual precipitations vary

Considerably by more than 10 %, the missing record is estimated by the Normal Ratio Method, by weighing the precipitation at the neighboring stations by the ratios of normal annual precipitations.

3.4.4 Station Average Method

$$\mathrm{P_X} = \frac{1}{\mathrm{N}}[\,\mathrm{P_1} + \mathrm{P_2} + \cdots\cdots + \mathrm{P_n P_n}] \quad \text{.....3.3}$$

Where, is the missing precipitation record P_1, P_2, ····· P_n are Precipitation records at N is Number of neighboring stations. Where, is the missing precipitation recordP_1, P_2, ····· P_n are Precipitation records at the neighboring stations N is Number of neighboring stations.

3.5 Tests for data quality

Because of changes in the physical condition of the catchment, the method of data collection, and the observer's ignorance, any hydrologic or meteorological time series data will be inconsistent over time. To adjust such a kind, several data screening techniques and data quality within the data series are applied. Before using raw recorded data directly, verify for inconsistency, homogeneity, and outliers for a given hydrologic dataset

3.5.1 Homogeneity test

Hydrological data records may be lost due to a variety of factors, including extreme natural events and human-caused events such as field staff mishandling observed data, conflicts, and so on. Homogeneity was examined when missing data was filled in. As a result, the homogeneity test is critical in detecting data variability.

When data is homogenous, it signifies those measurements were taken at the same time with the same instruments and in the same environment. However, dealing with rainfall data is difficult since it is always influenced by changes in measuring techniques and observational procedures, as well as environmental factors and structures. The following equation be able to important to test homogeneity of Wera river flood plain of Boyo catchment. So, Mann Whitney test using two samples of size p and q.

$N = p + q$……...3.4

P and q are ranked increasing order. Where R is sum of rank of element of first sample.

$V = R - \frac{(p(p+1))}{2}$…….3.5

Then after W, $U_{varance\ and}$ $U_{statist}$ was calculated

$W = pq - V$……3.6

U_{var}=$[\frac{pq}{N(N-1)}\ ][\frac{N^3-N}{12}\ ]$…….3.7

$Ustatist = \frac{[U-Ubar]}{U_{statist}^{½}}$……..3.8

3.5.2 Test on Outlier

Data points known as outliers deviate greatly from the trend of the remaining data. When fitting a static distribution function for a given stable region, the presence of either higher or lower outliers in the hydrologic data poses problems. Outliers should be adjusted, according to the water resource council's methods.

If the station skew is more than +0.4, the water resources council (1981) recommends looking for low outliers first. Before removing any outliers from the data set, test for both

high and low outliers where the station skew is between +0.4 and -0.4. The following frequency equation be able to important identify high outliers:

$$YH = \bar{y} + KnSy \quad \text{.....3.90}$$

Y_H is higher outlier's threshold units, S_y is standard deviation, and Kn is constant which find from table, $\bar{y}$ mean of station, n sample size. The following frequency equation can be used detect lower outliers

$$YL = \bar{y} - KnSy \quad \text{.....3.10}$$

YL stands for low outlier's threshold units, Sy for standard deviation, and Kn for the constant found in the table, the station's means, a n sample size of the station, and n sample size. Low outlier flood peaks are removed from records, and a condition probability adjustment established by the Water Resource Council (1981) can be implemented.

3.5.3 Consistency test

The record of steam flows is made up of a series of observations recorded at a specific rainfall station during a certain phase of the hydrologic cycle. The majority of hydrological analyses prefer a long dataset record, which can lead to more discrepancies.

The most appropriate technique to check the consistency or non-consistency of a record is to utilize a double mass curve. Except when the lack of other old documents makes it impossible, it was considered one of the first steps in the examination of a long record.

The slope of the line represented the constant of proportionality between the quantities; the slope of the line represented the constant of proportionality between the quantities. The analysis of the double mass curve was based on the fact that a graph of the cumulative of the target station against the cumulative of another respective behavioral neighboring station data during the same period plots as a straight line as long as the data are proportional (Searcy JK and Hardisan C H, 1960).

Table 3.1 Fitted Equation for consistency of all station

S. No	Name of stations	Fitted Equation type	Fitted Equation	R^2 value
1	Fonko	Linear Equation	Y=0.2402X-53.438	0.9939
2	Batena	Linear Equation	Y=0.0407x+641	0.9734
3	Alaba kulito	Linear Equation	Y=0.2096X+21.477	0.9972
4	Bilate Tena	Linear Equation	Y=0.3779X+27.024	0.9856
5	Wulberage	Linear Equation	Y=0.116X-18.344	0.9743

3.5.4 Flood Frequency Analysis

According to flood frequency analysis laws, flooding is one of the world's most dangerous natural disasters, and its prevention and control are critical for the construction of massive hydraulic systems (Rizwan, Guo, Xiong and Yin, 2018). The flood plain of the study river gauging station was analyzed using flood frequency analysis, which is one of the peak flow estimation methods.

3.5.4.1 Pearson type III method Pearson

One of the three-parameter gamma family distribution functions used to estimate peak flood occurrence in a river basin is the three-type statically distribution approach. Equation 3.9 gives the peak flood estimation for these three-parameter distribution functions.

$$X_T = \alpha\beta + \gamma K_T\sqrt{\alpha^2\beta} \quad \text{.....3.11}$$

Where, and parameters are return period frequency factors determined using various empirical methods based on the value of the coefficient of skewness, and KT is the frequency factor for the return period. Cs is greater than zero in these circumstances, and the Wilson-Hilferty transformation is used (Hilferty, Wilson and, 1931). Equation was used

$$K_T = \frac{2}{C_s\left[\left\{\frac{C_s}{6}\left(u-\frac{C_s}{6}\right)+1\right\}^3-1\right]} \quad \text{.....3.12}$$

Where $C_s > 0$ and u is standard normal variate.

3.5.6 Gumbel's method (distribution)

In hydrologic and meteorological studies, the Gumbel distribution is the most extensively utilized probability distribution function for extreme values in the prediction of flood peaks, maximum rainfalls, and maximum wind speeds (Subramanya, 1988). The general equation of hydrologic frequency analysis for finite length records of data N can be used to apply Gumbel's technique in practice:

$$X_T = \bar{X} + K\sigma_{n-1} \quad \text{.....3.13}$$

Where, σ_ (n-1) is standard deviation sample of size, N is sample size and K is frequency factor.

$$\sigma_{n-1} = \sqrt{\frac{\sum(X-\bar{X})^2}{N-1}} \quad \text{.....3.14}$$

$$K = \frac{y_T - \bar{y}_n}{S_n} \quad \text{.....3.15}$$

Where, Y_T is reduced variate as a function of T and given by the equation 2.5 as:

$$y_T = -\left[\ln \ln \frac{T}{T-1}\right] \quad \text{.....3.16}$$

Where; $\bar{y}_n$ is reduced mean as function of N and S_n is a reduced standard deviation as function of N.

3.5.4.2 Log Pearson III method (distribution)

This distribution function method is extensively used in the USA for projects sponsored by the US government (Subramanya, 1988). In this distribution method, the first variate X is converted to and the transformed data is analyzed. For X variate random hydrologic series

Z variate series is given by:

Then reduced Z series:

$$Z = \log xi \quad \text{.....3.17}$$

$$Z_T = \bar{Z} + K_Z\sigma_Z \quad \text{.....3.18}$$

Where K_Z is frequency factor as function of T and coefficient of skew of variate Z, C_s and Standard deviation of variate Z, $\bar{Z}$ is means of Z value, N is sample size or number of records year of data.

$$\sigma_Z = \sqrt{\frac{\sum(Z-\bar{Z})^2}{N-1}} \quad \text{.....3.19}$$

$$Cs = \frac{N(\sum(Z-\bar{Z})^3}{(N-1)(N-2)(\sigma_Z)^3} \quad \text{.....3.20}$$

3.5.4.3 Log Normal method (distribution)

The Log –Person Type III distribution is simplified to a lognormal distribution when the skew is zero, which means Cs is zero (Subramanya, 1988). All processes in this method follow the Log-Person Type III distribution for zero skewness.

3.5.4.4 Exponential distributions

The exponential distribution is one of the spatial forms of the gamma family, which also includes the three-parameter Pearson and log Pearson, one-parameter and two-parameter gamma, and generalized gamma distributions (Hamed, 1998).

$XT = \varepsilon + \alpha + \alpha * KT$…….3.21

Where KT is frequency factor giver by $K_T = \log_{(T)} -1$, ε and α are parameters estimated by methods of parameter estimation.

3.5.4.5 Gamma (2p) distribution

This distribution is also another special form of Pearson (3) distribution with ε is equaled to zero and its quantile of T-year is given by

$XT = \alpha\beta + KT\sqrt{\alpha\beta}$……3.22

Where and are parameters, and KT is the frequency factor calculated using a variety of empirical techniques based on the skewness coefficient (Hamed, 1998).

3.5.4.6 Generalized extreme value

Another form of distribution method based on the sing of parameters is the GEV. The distribution function is reduced to GEV (2) when k in the distribution function is negative, which is suitable for bounded parameters. The T-year flood is calculated as follows:

$$XT = \bar{X} + \frac{\alpha}{K}\left[1 - \left\{-\log\left(1 - \frac{1}{T}\right)\right\}^{k}\right]$$…….3.23

Where x, α, and k are parameters commuted by parameter estimation methods.

3.6 Best fit distribution function selection

For a successful outcome, the fitting of a statically distributed function for a given watershed or station should be done both graphically and analytically, with the output being used for the next hydraulically and structurally study of water-related activities.

For graphical selection, such as the L-Moment ratio and the D-index, a test was employed to discover the best-fit distribution function for the catchment. During the analytical solution, parameter estimation methods such as MOM, PWM, and MLM, which are extensively used in flood frequency analysis, were used to estimate parameters for graphically selected optimal distribution methods.

Using annual maximum flood data for the catchment and the L-moment ratio, the best fit probability distribution function was chosen for this study. The distribution function's computed values L-Cs and L-Ck are plotted in the diagram. The curves depict the candidate distribution's putative connections between L-Cs and L-Ck, as well as the observed site at the diagram, which was identified using the L-moments technique parent distribution function identification. Because the site moments and site mean are moving around them, log Pearson type three distribution functions are the best-fitting techniques, according to the L-moment diagram. To identify the best-fitted distribution function for streamflow data from gauging stations, the D-index analytical method and three commonly used parameter estimate methods are employed in this study. The L-moment ratio diagram of Alaba kulito, which shows the results in figure 3.7 as well as the other supplementary stations shows Appendix figure 9 (A-B).

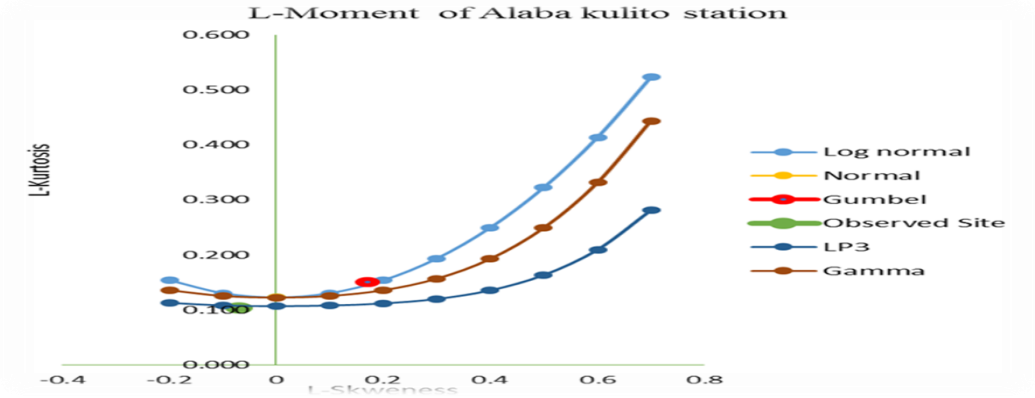

Figure 3.7 shows the L-moment ratio diagram of Alaba kulito station

3.6.1 D-Index analytical method

D-Index Method for the identification of upper limit of the data is given as;

$$D - \text{Index} = \frac{1}{\bar{X}} * \sum_{i=1}^{6} |X_i - X^*_i| \quad \text{.....3.24}$$

Where X_i and X_{i*} and ẋ are the highest observed and simulated values for the distributions and the smallest value is taken as best fit the distribution. The D-Index method was calculated by selecting six highest values from both observed and calculated data, ranging from 1 to 6 highest to least order, computing probability $p = \frac{m}{(N+1)}$, N as data record length and m as rank order), computing corresponding z value, calculating X_T value, computing the absolute value of the difference between observed and calculated data, and finally computing D-Index. The distribution with the lowest D-index is determined to be the best fit for estimating the likely maximum flood (USWRC, 1981).

3.6.2 Goodness fit test

In the estimate of MFD, the GoF tests are critical for ensuring that probability distributions are appropriate for the recorded series of AMD. The commonly known GoF tests are and KS, which were employed in the study out of various GoF tests available. The following are the theoretical descriptions of the GoF tests statistic: O (Q) $_j$ is the observed frequency value of jth class, E (Q) $_j$ is the expected frequency value of j^{th} class.

$$\sum_{j=1}^{NC} \frac{\{O_j(Q) - E_j(Q)\}^2}{E_j(Q)} \quad \text{.....3.25}$$

$$KS = Max\big(Fe(Q_i) - FD(Q_j)\big) \quad \text{.....3.26}$$

Where, Fe (Q_i) is the empirical CDF of (Q_i) and FD (Q_i) is the computed CDF of Q_i (Zhang, 2002).

3.7 Flood Plain Analysis

Using the powerful GIS version 10.4.1 tool in this study, data preparation for flood plain analysis and flood plain analysis after steady-state flow simulation was done. Hydraulic model for river analysis HEC-RAS 5.0.7 was used to calculate water surface profiles of the Wera River, Boyo flood plain. HEC-RAS and GIS were circuited with the help of the HEC-In this work, data preparation for flood plain analysis and flood plain analysis following

steady-state flow simulation were completed using the sophisticated GIS version 10.4.1 tool. Water surface profiles of the Wera River, Boyo flood plain, were calculated using the HEC-RAS 5.0.7 hydraulic model for river study.

With the help of HEC-GeoRAS version10.3, one of the GIS extension tools, HEC-RAS and GIS were connected. Because they are most widely applicable in river flood plain analysis and data processing, very accurate in 1D flood plain analysis, and freely available, these model software and tools were employed in this work. The general approaches for flood plain analysis and hazard assessment employed in this study are shown in the workflow diagram of 1D hydraulic river flood plain analysis above. The following topics are covered in depth: study area preparation, elevation TIN formulation, LULC and soil Map extraction on a GIS tool, HEC-RAS Pre-processing, HEC-RAS Processing, Post-processing of HEC-RAS data, floodplain mapping and hazard and assessment.

3.7.1 Study area delineation

The first and most crucial step in watershed research is to determine the geographic breadth of the study region. The scoped watershed, Boyo Flood plain across Wera river root, was found from a DEM of 30m resolution using GIS technology. For each watershed research area, the following steps were completed in order: filling, flow direction, flow accumulation, map calculation, flow sink, stream order, stream to feature formation, snapping outlet point, watershed forming, conversion to polygon, and clipping polygon. Delineated Watershed of study Area is presented in figure 3.8

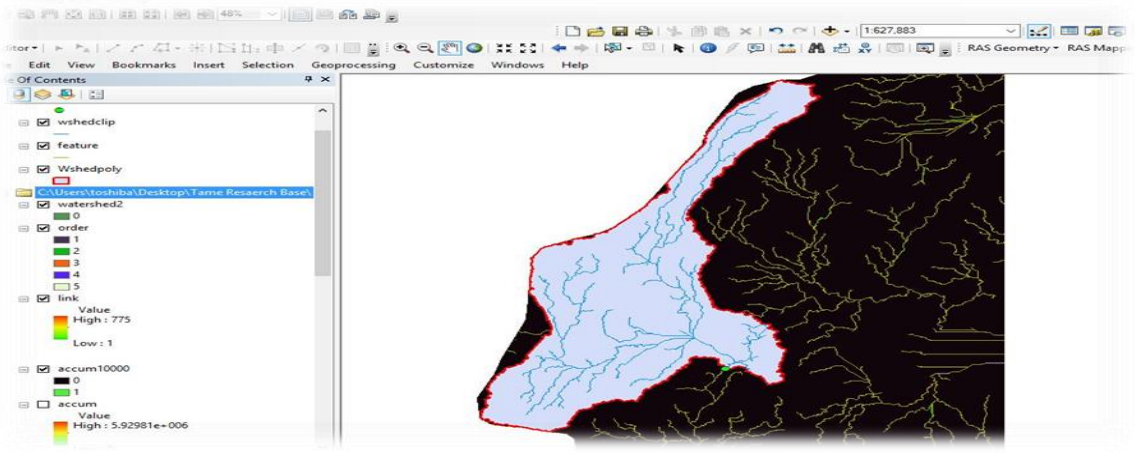

Figure 3.8 Delineated Watershed of study Area

3.7.2 Preparation of LULC Map

The Ethiopian LULC map obtained from MoWE was used to create the LULC map for this study work's watershed. The Boyo flood plain area verification has six LU classes, as shown in Figure 3.2. For this project, the Ethiopian LULC raster map was trimmed by the study area's watershed polygon. Out of the overall watershed area of 1641.08 km^2, Table 3.2 shows the area occupied by each of the trimmed map's outputs. Figure 3.3, 8 LULC shares in the study area for each type.

Table 3.2 Area of LULC is expressed in km^2 and percentage

Name	Area(km^2)	% Each
Crop Plantation	73.432473	4.474648554
Shrub Land	603.651072	36.78381357
Cultivation	557.846353	33.99267756
Grass Land	147.832807	9.008274256
Swamps	46.560506	2.83719031
Forest	211.754429	12.90337382
Total	1641.078	99.99997806

3.7.3 TIN Preparation

The HEC-RAS model with a DEM resolution of 30m x 30m was used to infer TIN, one of the most fundamental raster data for river flood plain analysis. This digital elevation model was good enough to provide TIN, which indicates the best precise river bed and banks, which is critical information in flood plain hydraulics. Two tools that can be used to generate TIN are GIS and RAS Mapper.

The following actions were taken in order to create TIN for this thesis: Open a new GIS project, import a DEM map, go to Arc Toolbox, 3D analysis tool, and save. Converts raster to TIN, then invokes the DEM to raster to TIN menu, and finally delivers the outcome. HEC-RAS pre-processing Geometric HEC-RAS import data are pre-processed as a GIS file on the Geo-RAS before initiating RAS analysis to model flow. River layer parameters such as stream centerline, bank lines, XS Cutline, and flow path centerline were created using the Wera River Boyo flood plain catchment's TIN. All of the activities were

completed as described above, and pre-processing was completed in accordance with the standards of the (USACE, 2016).

3.7.4 RAS Processing and Flow Simulation

The Hydraulic Engineering Center River Analysis System (HEC-RAS) model, which comprises procedural steps to simulate steady flow or unsteady flow analysis, is a fundamental powerful model for flood inundation mapping. Defining up a new project, importing a geometric file, modifying geometric data, inputting maximum flow data for return periods, setting boundary conditions, and conducting steady flow data analysis were all employed in this thesis work. Finally, the completed process data was exported to a GIS program in the form of an SDF file format for post-processing.

3.7.5 HEC-RAS project setup and geometric data importing

For specific research work, the HEC-RAS model was set up, followed by importing the RAS import file into HEC-RAS, creating a new project, saving it in a folder, and converting the measurement system from US customary units to SI units. Initial projections were set up, and geometric data was imported into HEC-GeoRAS. On the HEC-RAS menu, click View/edit geometric data, then import geometry file, select folder, and the data will be imported as a GIS data format. The RAS import file was created as GIS data using GIS and HEC-GeoRAS tools. TIN was produced from a DEM raster, and XS data was pre-processed using HEC-well-thought-out GeoRAS's methods.

3.7.6 Editing geometric data

The following procedures were accomplished when the geometric data was imported into the HEC-RAS edit menu: Going to tools, all reaches' XS points were filtered, then open table, manning's n value was inserted, LOB, ROB, and reach lengths were edited, and the model itself calculated contraction and expansion coefficients.

3.7.7 Flow data imputing and steady flow analysis

For return periods of 5Yrs, 10Yrs, 25Yrs, 50Yrs, 100Yrs, 200Yrs, and 500Yrs, the HEC-RAS menu offers the peak occurrence of stream flow data generated using the Pearson (III) distribution function technique. Normal depth boundary conditions with slopes of 0.003,

0.0021, and 0.004 were chosen for Batena, Wera downstream and upstream, and were averaged from both ends of the ground profile of the study region. Finally, the steady flow analysis was conducted successfully, as shown in appendix Figure 2.

3.7.8 Inundation Mapping

After successfully simulating steady flow in the HEC-RAS model and exporting it as a RAS export SDF file, post processing of the river flood study to generate inundation area began. Going to the RAS Mapping option, the RAS layer was set up, RAS data was imported in XML format, and inundation mapping was completed.

To convert an SDF file, use the converter tools on the Geo- RAS menu, then navigate to the folder where the RAS export file was saved after the flow simulation in HEC-RAS and add it. This converts the data to an XML file that can be read by a GIS tool.

Setting up the RAS map for steady flow analysis was done for this study by going through the procedures of establishing a folder, adding the RAS export file from that folder, adding the TIN that was used first on Pre-RAS processing, setting cell size 30 and running the tool. Finally, after RAS, water surface creation as TIN and inundation mapping in raster format were completed. Post-RAS was accomplished passing the steps like changing.

3.7.9 Flood Hazard Assessment and Mapping

Flood hazards are linked to hydraulic variables (depth, velocity, slope, boundary condition, and elevation) as well as hydrological factors (stream flow or rain fall) (Glard, 1996). The analysis categorized the depth grids in the hazard map into five depth levels, indicating mild to very severe levels, because the inundation depth grows directly proportional to the severity of the peak flood.

These reclassified inundation depth grids were intersected with the land use land cover map for inundation in the research area, and the resulting attribute table in the GIS tool was evaluated for hazard severity. To construct hazard maps for specified return dates, the depth grid raster was reclassified as follows: less than half is low, half to one is moderate, one to one and half is high, one and half to two is severe, and more than two is extremely severe flood magnitude.

3.7.10 Conceptual Frame work

The general work flow showing the methodology to delineate flood inundation mapping and flood hazard area mapping was described in Figure 3.10, which illustrates the steps of Wera river flood plain of Boyo catchment.

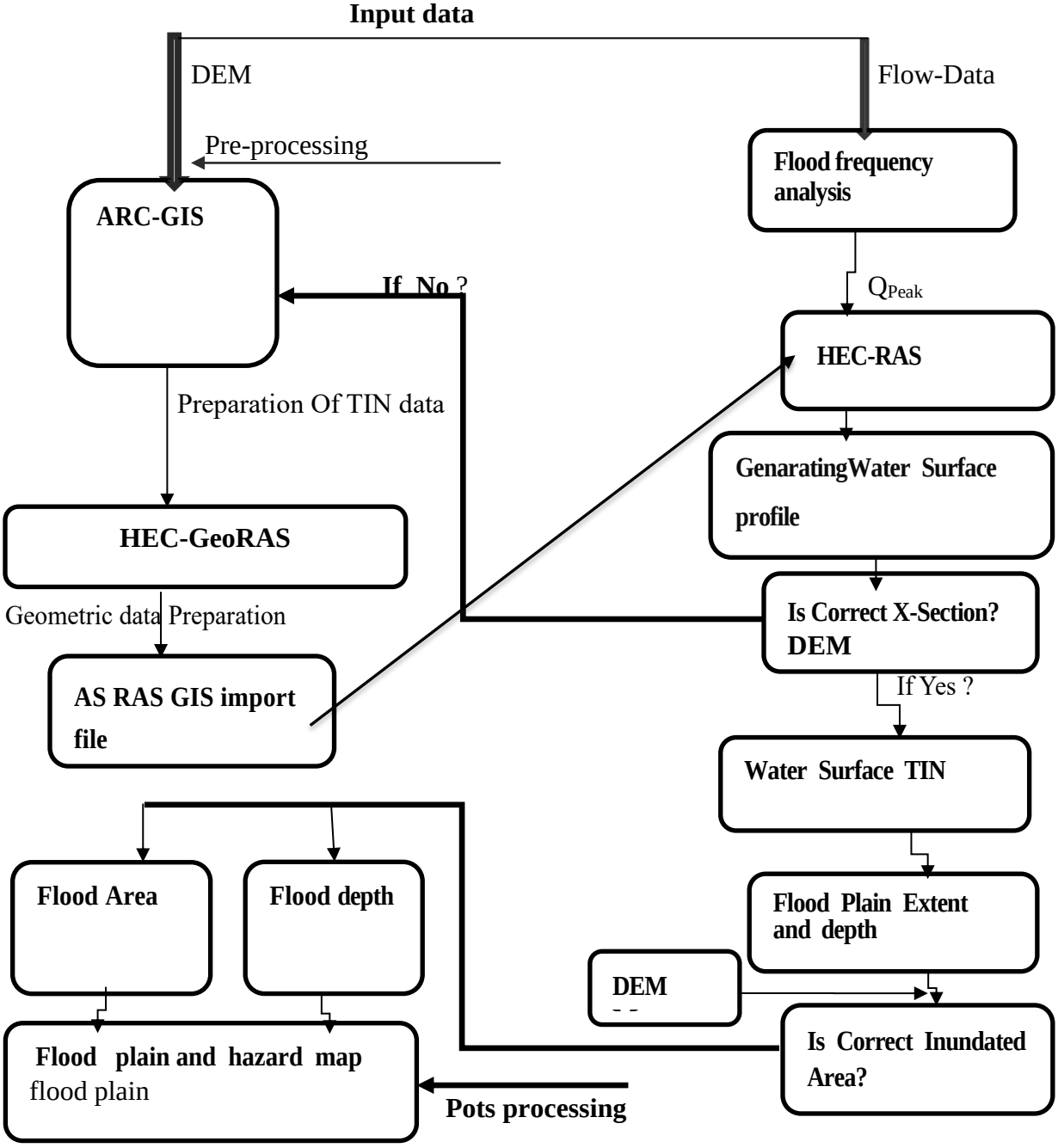

Figure 3.9 Conceptual Framework of the Study

4. RESULTS AND DISCUSSION

4.1 Determination of Stream Flow Accuracy

4.1.1 Test for Outlier of Data

The missing data was filled using the station average method in XLstat 2015 before estimating outlier and consistency tests for this investigation. The top and lower bounds of outliers' values were examined using equations 3.9 and 3.10, and the results were shown in table 4.1 and table 4.2 for Alaba, Batena, and Wera stations, respectively.

Table 4.1 Statistical test result of outlier for gauging stations

	Observed discharge		Calculated discharge		
Name of Station	Max-Yearly Max. Discharge(m^3/s)	Min. of Max. yearly Discharge(m^3/s)	High outlier(m^3/s)	low outlier(m^3/s)	C_S value
Alaba kulito	283.54	5.120	376.3019953	10.07047625	0.01214
Fonko	239.48	2.611	346.0973175	8.476350571	0.01952
Batena	101.3	3.777	86.63466291	2.555633147	0.02614

Table 4.2 Maximum and minimum data record in respective year

	Alaba kulito		Wera		Batena	
	Q_{max} 283.54 m^3/s	Q_{min} 5.120 m^3/s	Q_{max} 239.48 m^3/s	Q_{min} 2.611 m^3/s	Q_{max} 24.871 m^3/s	Q_{min} 3.777 m^3/s
Year	1993	1992	2006		1987	2013

The greatest measured flow at the Alaba kulito gauging station in 1993 was 283.54 m3/s, which did not surpass the calculated value of outlier in table 4.1. As a result, there are no high outliers in this station, however there are around five data points with low outlier values. The maximum recorded flows of 239.48 m^3/s at Fonko station in 2006 were not exceeded by a computed value of outlier reported in table 4.1.

As a result, there are no extreme outliers in this station. The computed lower outlier value for this gauging station surpasses the minimum observed values, as shown in table 4.1 above. The maximum reported flows of 101.3 m3/s at Batena station in 1987 surpass the predicted value of outlier, indicating that there is an upper outlier in the gauging station. However, because the computed lower outlier value is greater than the minimum value in table 4.1, the data does not need to be removed.

4.1.2 Test for consistency of Data

A double mass curve analysis was performed to ensure that the streamflow data was consistent. This implies that the missing data technique and the station's recorded data were adjusted by deleting extraneous data or outliers from the data series. On Excel, a scatter plot was made showing the cumulative average yearly streamflow for targeted or disturbed stations vs an accumulated average of the other four index stations. The Alaba kulito streamflow data was consistent with the other streamflow data stations, as shown in plot figure (4.1). The result of other stations consistency double mass curve was presented in Appendix of Figure 8 (A-D).

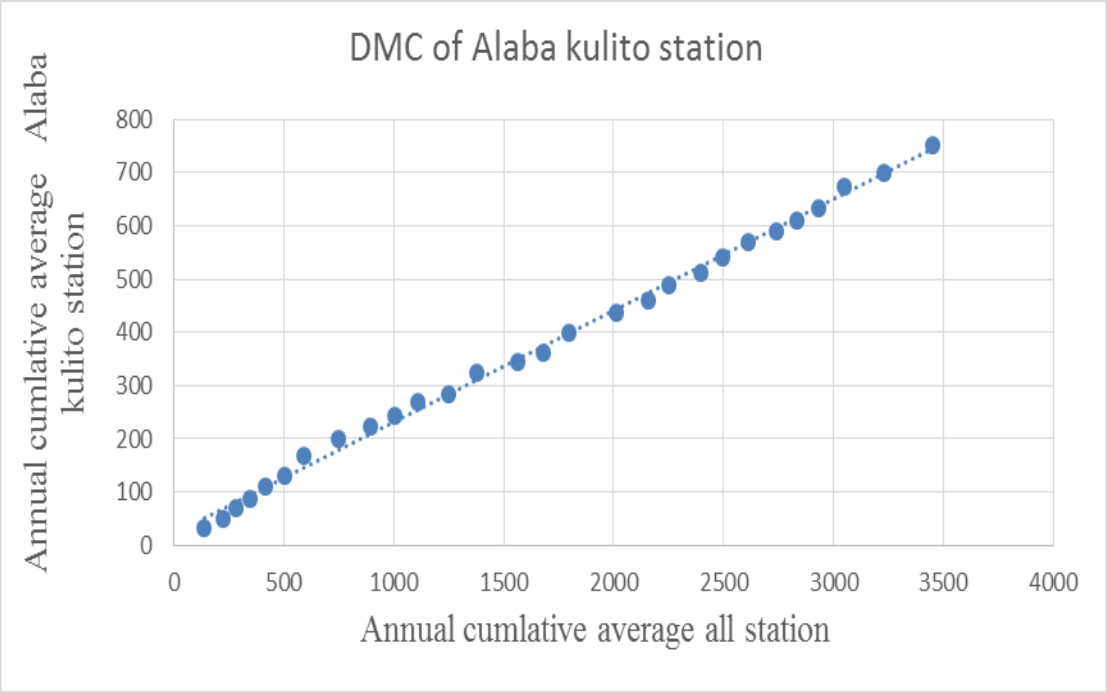

Figure 4.1 Double mass curve for consistency of Alaba kulito

Table 4.3 Consistency Test Equations for double mass curve of all stations

S. No	Name of stations	Fitted Equation type	Fitted Equation	R^2 value
1	Fonko	Linear Equation	Y=0.2402X-53.438	0.9939
2	Batena	Linear Equation	Y=0.0448X+33.592	0.9666
3	Alaba kulito	Linear Equation	Y=0.2096X+21.477	0.9972
4	Bilate Tena	Linear Equation	Y=0.3779X+27.024	0.9856
5	Wulberage	Linear Equation	Y=0.1179X-17.755	0.9705

4.1.3 Test for homogeneity of data

Hydrological data records can be destroyed as a result of extreme natural disasters and human-caused events such as field staff mishandling observed data, disagreements, and other causes. Homogeneity was tested when missing data was filled in. When data is homogeneous, it means measurements were taken at the same time, with the same instruments, and in the same place. Stream flow data, on the other hand, is difficult to deal with because it is always changing due to changes in measuring techniques, observing procedures, and environmental factors and structures. In thesis this work, homogeneity was tested using the Mann Whitney test with two samples of size p and q.

Table 4.4 The Mann-Whitney test result for homogeneity test of all stations

Name of Station	Sample	R Value	$Vv_{ariance}$	Us_{tatic}	$U_{critical}$	standard value	Remark
Alaba kulito	27	1583.97	471.251	0.6441	1.0256	1.96	Homogenous
Fonko	27	628.364	464.166	0.6499	1.0256	1.96	Homogenous
Batena	27	246.933	471.251	0.6449	1.0256	1.96	Homogenous
Wulbarge	28	87.8953	493.541	0.6305	1.0256	1.96	Homogenous
Bilate Tena	28	1267.7	451.916	0.6585	1.0256	1.96	Homogenous

4.1.4 Goodness of fit test (GoF)

Calculated using Equations (3.25 and 3.26) and GoF tests, quantitative assessment of the fitting of probability distributions to data sets of the distribution is judged to be appropriate for modeling the series of annual peak flood discharge (PFD) if the computed values of GoF tests statistic produced by the distribution are fewer than the theoretical values at the desired significance level (Vivekanandan, 2015).

To see if the hypothesized distribution function fit the sample data, goodness of fit tests such the chi-square X^2 and Kolmogorov-Simonov (K-S) test were used. The findings of GoF were reported in Appendix table 3 from A to C for Batena, Fonko, and Alaba kulito gauging stations fitted whether the hypothesized distribution function.

The computed values of X^2 statistic result of EVI, NOR, LN2, LP3 distributions, the calculated value is less than the theoretical value of Alaba kulito at 5% significance level, then those probability distribution functions were accepted for Alaba kulito station, but the gamma distribution function was not accepted for Alaba kulito station.

Similarly, if the computed values of the KS test statistic value for all five probability distributions are less than the theoretical value at the 5% significance level, then all of those distribution probability functions were accepted by Alaba kulito station. Similarly, the computed values of the X2 test statistic value for all five probability distributions are less than the theoretical value at the 0.05 significance level, as shown in Appendix table-3B Fonko station. For Fonko station, all five probability distribution functions were accepted.

Similarly, if the computed values of the KS test statistic value for all five probability distributions are less than the theoretical value at the 0.05 significance level for Fonko station, then all of those distribution probability functions were acceptable.

Finally, there is an appendix table. 3C Batena station It should be noticed that the computed values of the X^2 test statistic value for each of the five probability distributions are less than the theoretical value at the 5% significance level. For Fonko station, all five probability distribution functions were accepted. If the computed values of the KS test statistic value for all five probability distributions are less than the theoretical value at the

5% significance level for the Batena station, then all of those distribution probability functions were accepted for the Fonko station.

To see if the hypothesized distribution function fit the sample data, the goodness of fit tests chi-square (x^2) and Kolmogorov Smirnov KS) were chosen. As a result, all probability distribution functions were fitted in my thesis work, except the expert gamma function, which was not fitted to the sample data Alaba Station in kulito.

4.2 Magnitude of Peak Flood Estimation

Using methods of probability distribution functions of best fit, the maximum magnitude of each flood for 5, 10, 25, 50, 100, 200, and 500 Yrs. return periods were accomplished. The best fit statistical model was selected in this thesis work using graphical and numerical methods of best fit selection analysis. Plots of Recorded and Estimated Flood Discharge using G2, LN2, NOR, EV1 and LP3 Distributions was presented in Appendix of Figure 10(A-C) for respective station such as Alaba kulito, Fonko, Batena.

For several powerful functions and current internationally recommended probability distribution functions, graphical analysis was performed, and five of the best fitted were analytically solved for the best of the best using the D-Index approach. The distribution with the lowest D-index was chosen as the best and most suitable.

In comparison to the other distributions for MFD estimate, the distribution with the lowest D-index was identified as a better and more appropriate distribution (USWRC, 1981). (Rosbjerg D and Madsen H, 1995). Equation was used to calculate the discharge D-Index values of the distributions in order to select the best suited distribution for peak estimation (3.24). Appendix Table 2 shows the D-index values for five probability distributions (A-C). As a result of the aforementioned finding, the distribution's D-index values for Alaba Kulito, Fonko, and Batena stations are comparatively low when compared to the comparable values of other distributions. As a result, LP3 distribution was chosen as the best method for estimating peak discharge, based on both GoF and diagnostic test findings. As the result is shown in Table 4.4 below.

Table 4.5 Peak discharge different for return period at gauging stations by LP-3

Station	Alaba	Wera	Batena
Return Period (Year)	$Q_T(m^{\wedge 3}/s)$	$Q_T(m^{\wedge 3}/s)$	$Q_T(m^{\wedge 3}/s)$
2	61.0324514	55.184508	126.8101
5	159.819738	147.42157	160.0383
10	239.705509	218.82759	211.092
25	344.836842	307.52453	269.21
50	421.227013	368.01832	372.180
100	493.503706	422.07222	445.619
200	560.96046	469.61889	475.795
500	642.160912	522.931	507.201

4.3 HEC-RAS pre-processing

4.3.1 Preparation of TIN

For this study, TIN was pre-processed for HEC-RAS Model utilizing DEM 30m by 30m resolution, which is the backbone for river flood analysis. It depicts the best specific river bed and banks, both of which are critical elements in flood plain hydraulics. From the top elevation of 3341m to the lowest elevation of 1961m above mean sea level, TIN was classed into nine classes.

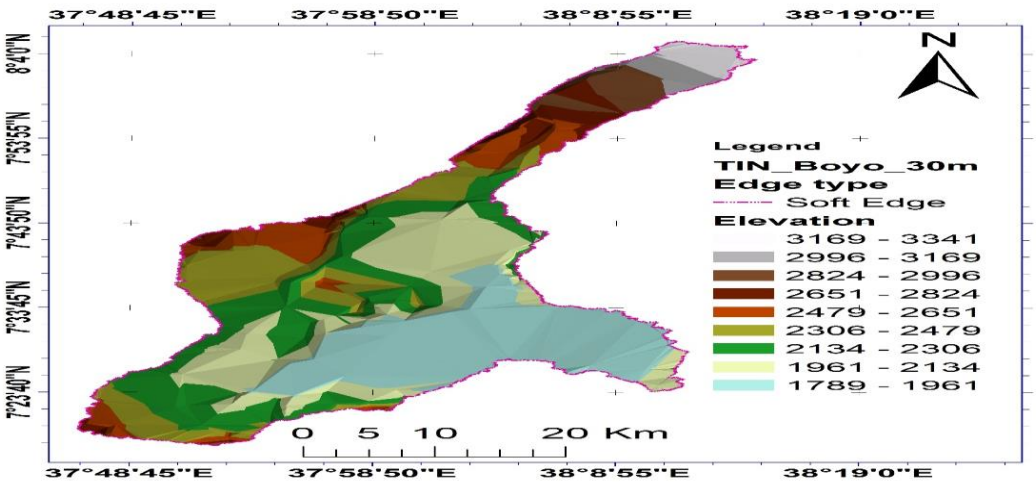

Figure 4.2 TIN of Study Area

4.3.2 Stream centerline layer

One of the required RAS layers, Stream centerline, was built using the GeoRAS geometry processing option. The stream network was built reach by reach, from upper to lower, and is based on the Wera River's river and reach network. The stream centerline is utilized to assign river stations to XS, and a schematic entered into HEC-RAS defines the main channel flow path.

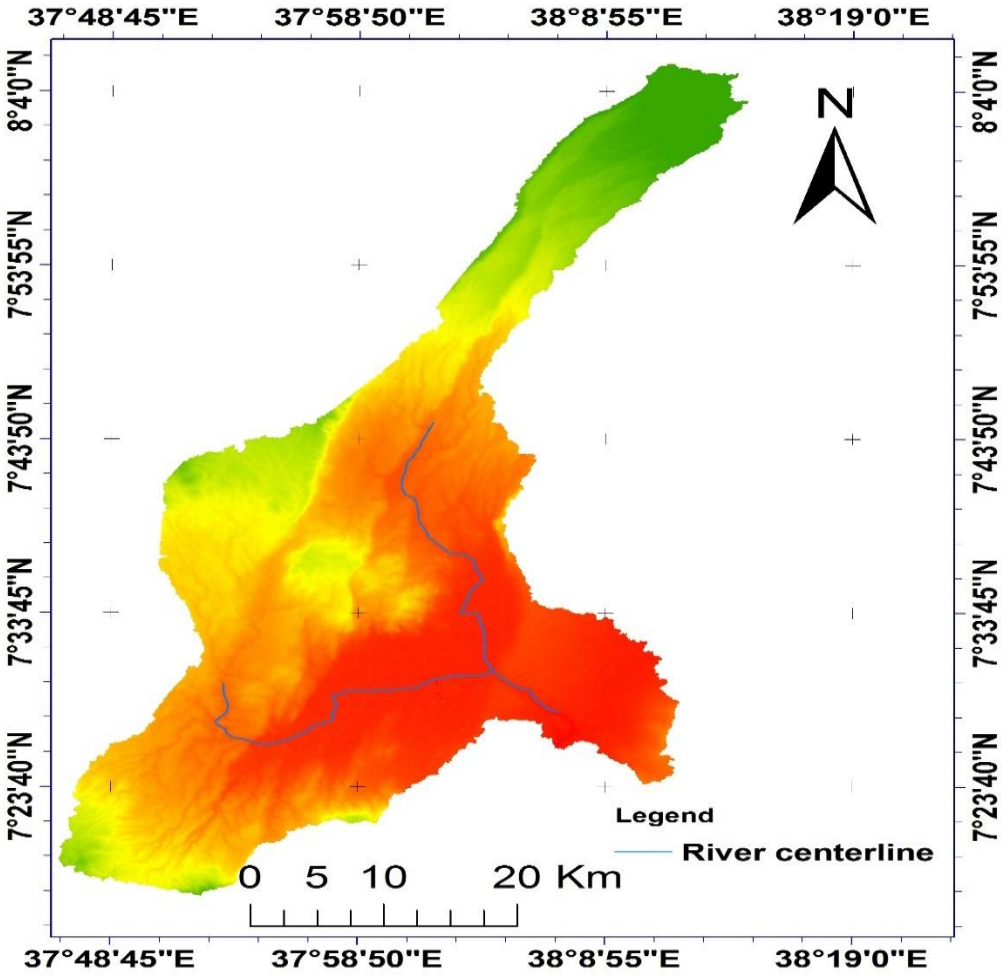

Figure 4.3 Stream Center Line

4.3.3 Bank lines layer

The bank lines are a RAS layer that separates two overbank flows from the main channel flow. The junction of bank lines with cut lines determined which bank stations were

assigned to each XS. In this study, the two bank lines intersect with each cut line exactly and drown from upstream to downstream.

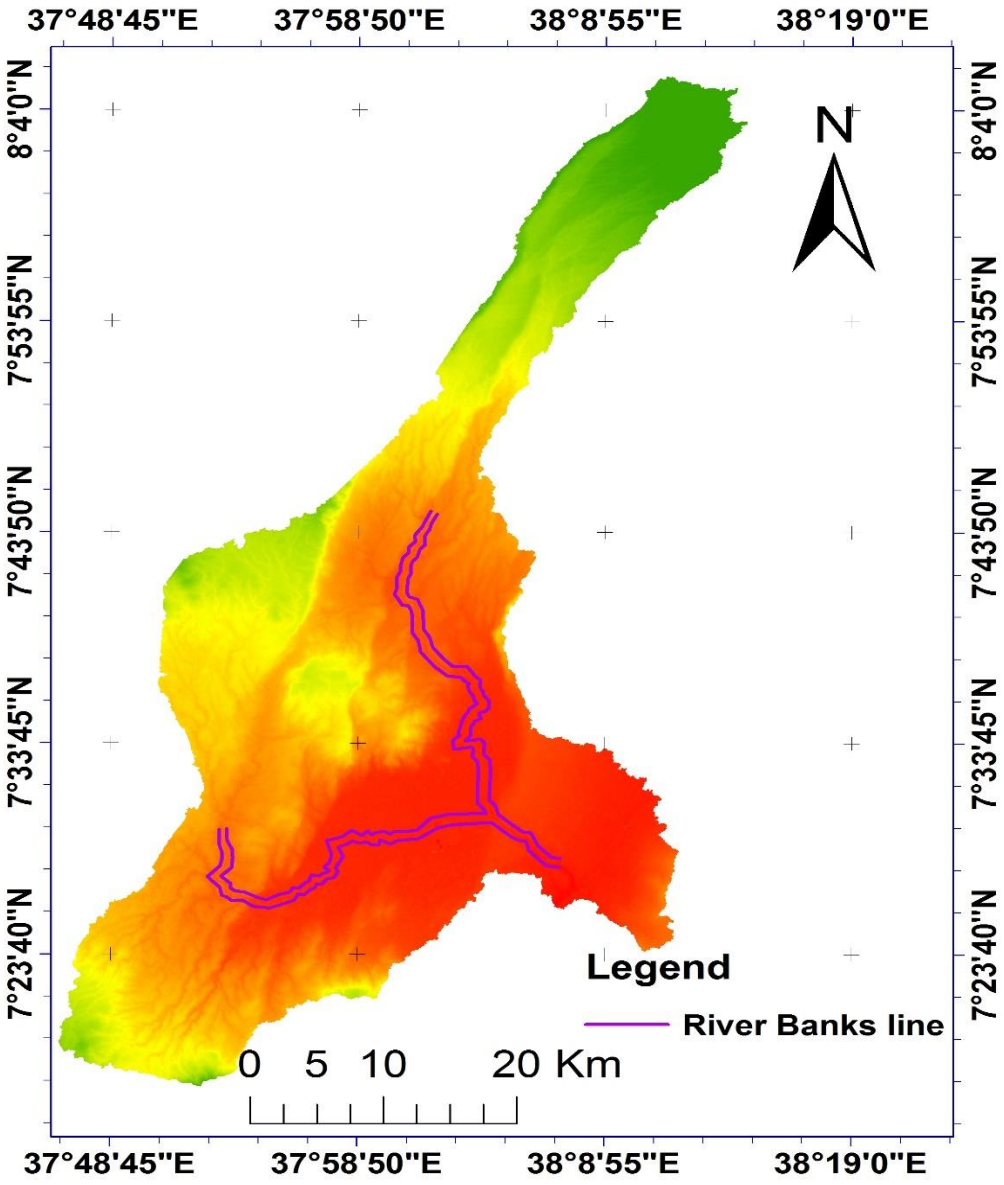

Figure 4.4 River Bank Line

4.3.4 Flow path layer of centerline

By defining the center mass of flow in each zone, the flow path center lines are RAS layers used to define the hydraulic flow path in the left overbank, main channel, and right over the bank. The flow route center lines aid in the precise placement of the X-sectional cut

lines. According to the manual, the path center lines were drawn in the direction of flow, which is upstream to downstream in this study.

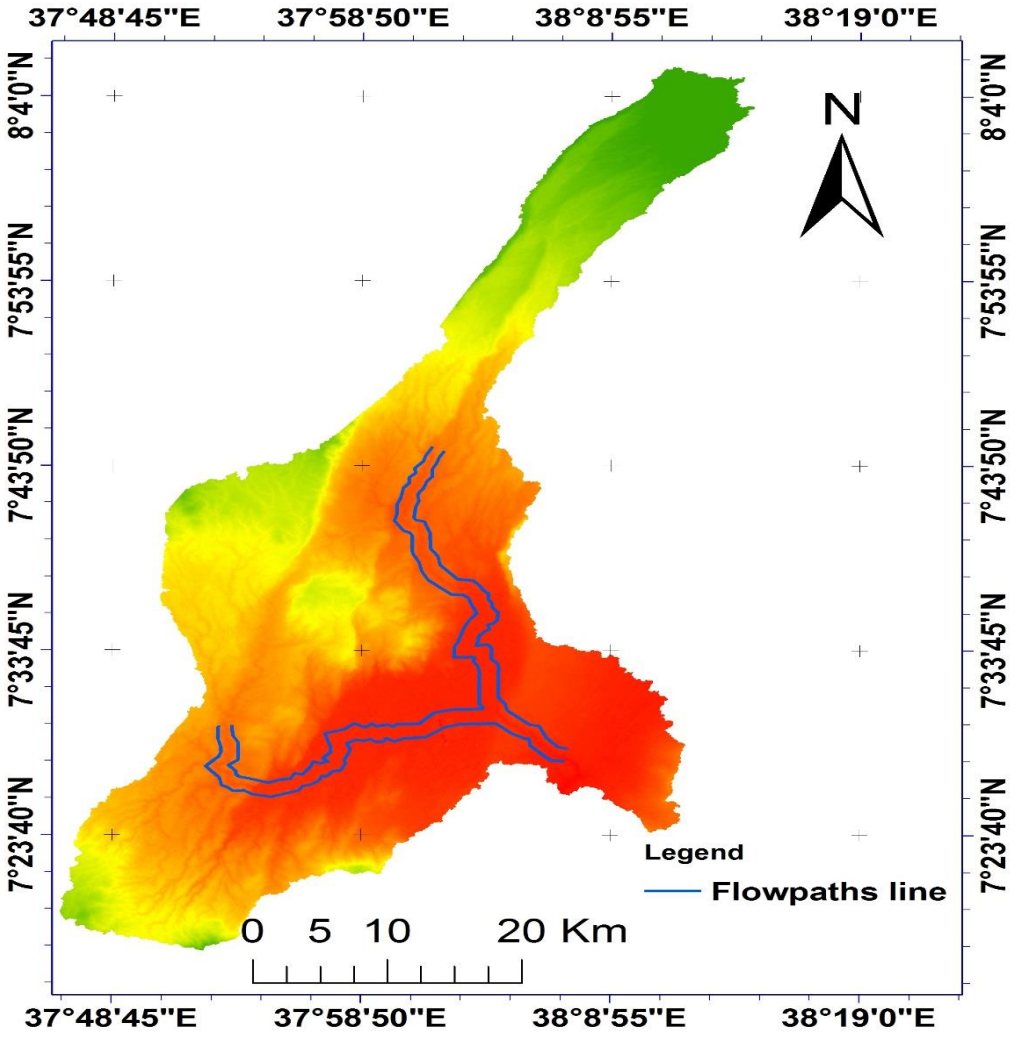

Figure 4.5 Flow Path Line

4.3.5 Cross section cut lines layer

When looking downstream, cross-section cut lines are another needed RAS layer that was drowned in the perpendicular direction of flow from left to right over bank. The study's cut lines depict the location, position, and extents of XS in the Wera River's flood plain in the Boyo basin.

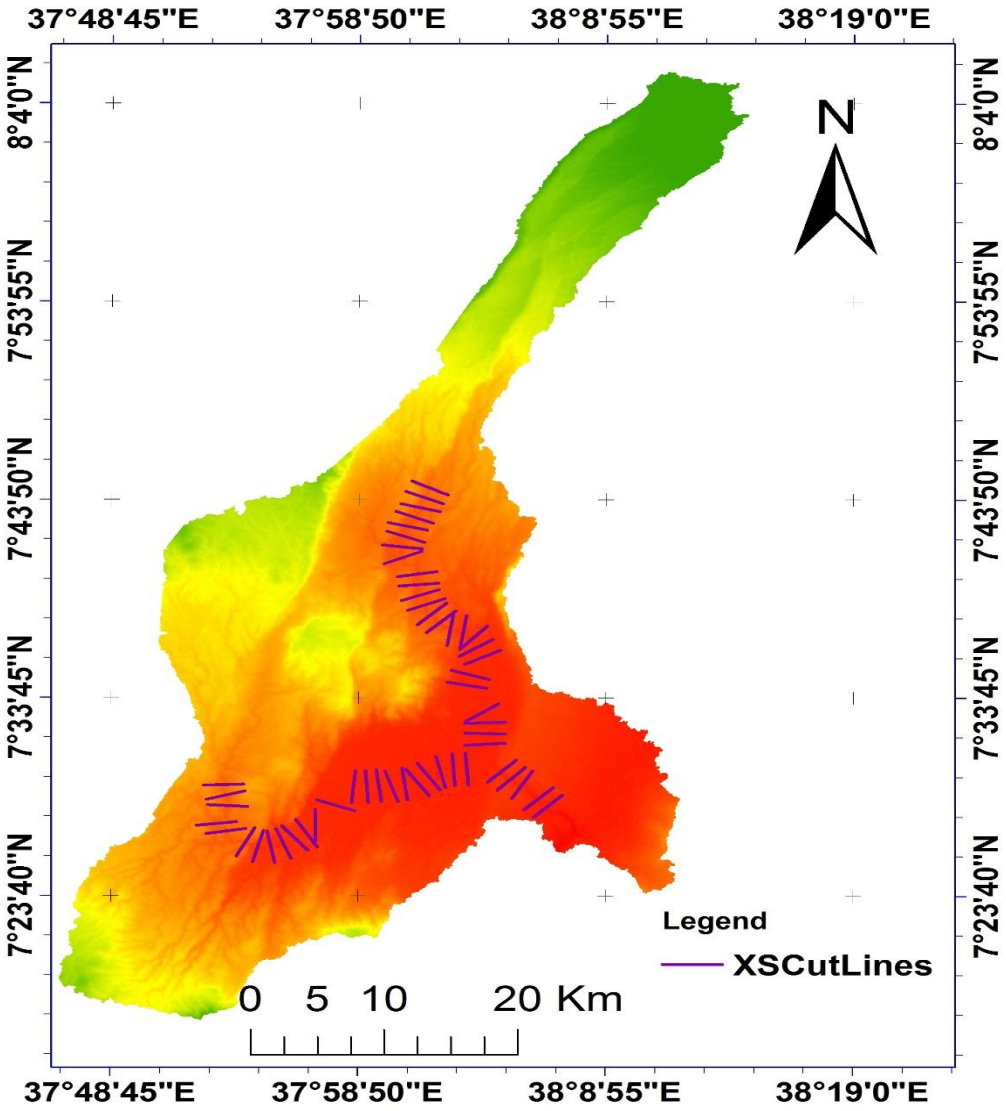

Figure 4.6 Cross Section Cut Line

4.3.6 River Geo-Metric Data

The Geo-RAS tool was used to prepare geometric data, which is a prerequisite for steady flow simulation. This data was imported into HEC-RAS and tweaked for the best results in steady flow simulation. Four basic RAS layers were applied to the HEC-GeoRAS tool

in this study and processed to provide the geometric data shown in Figure 4.7 below.

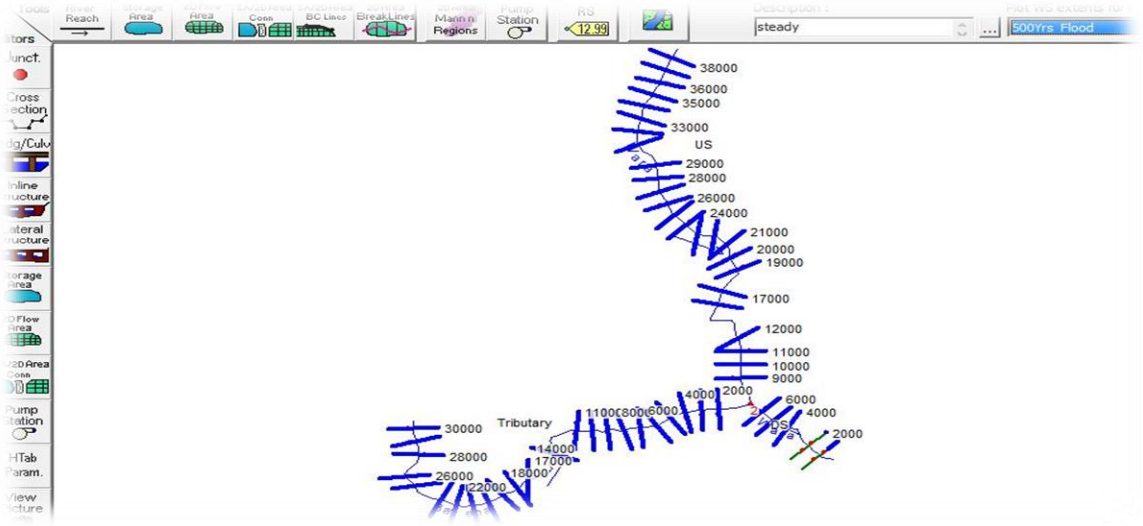

Figure 0.7 River Geometry File from HEC-RAS Menu for 500 Yrs. Return Period.

4.4 Steady Flow Simulation

After importing the geometric data from the Geo-RAS tool as well as the peak flood from the flood frequency analysis, steady-state flow was simulated one by one. As shown in figure a water surface profile was produced at several locations.

A.

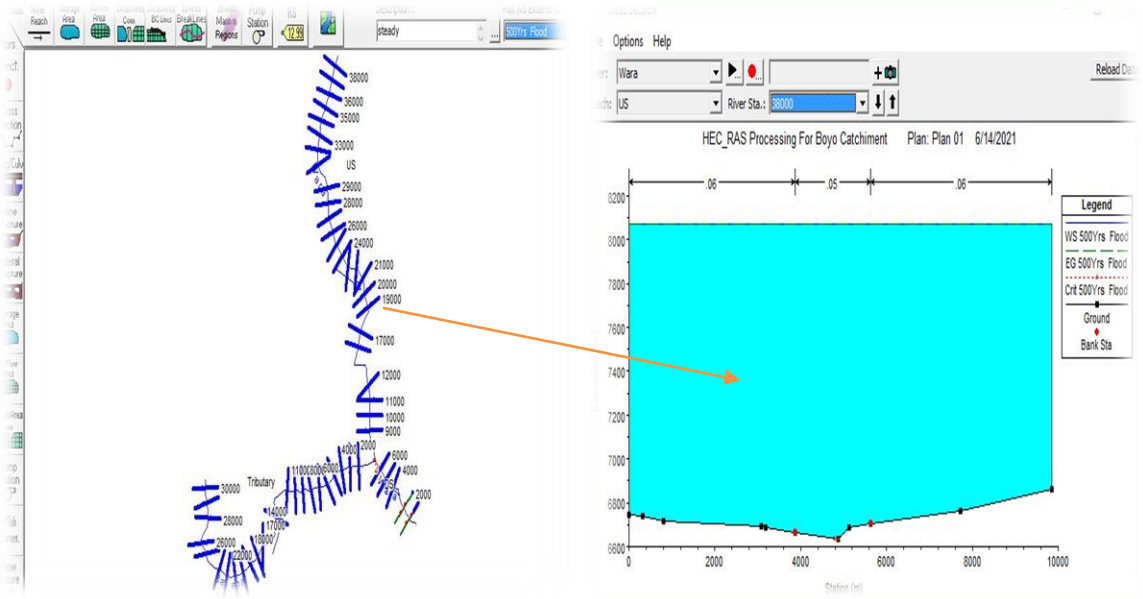

B.

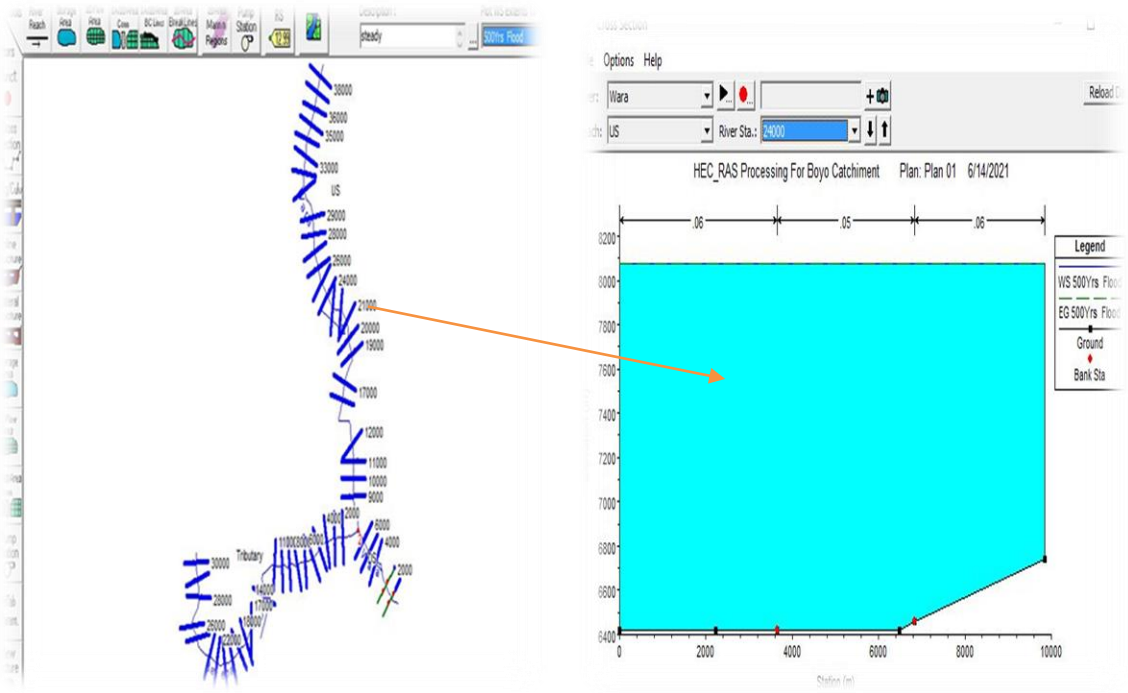

C.

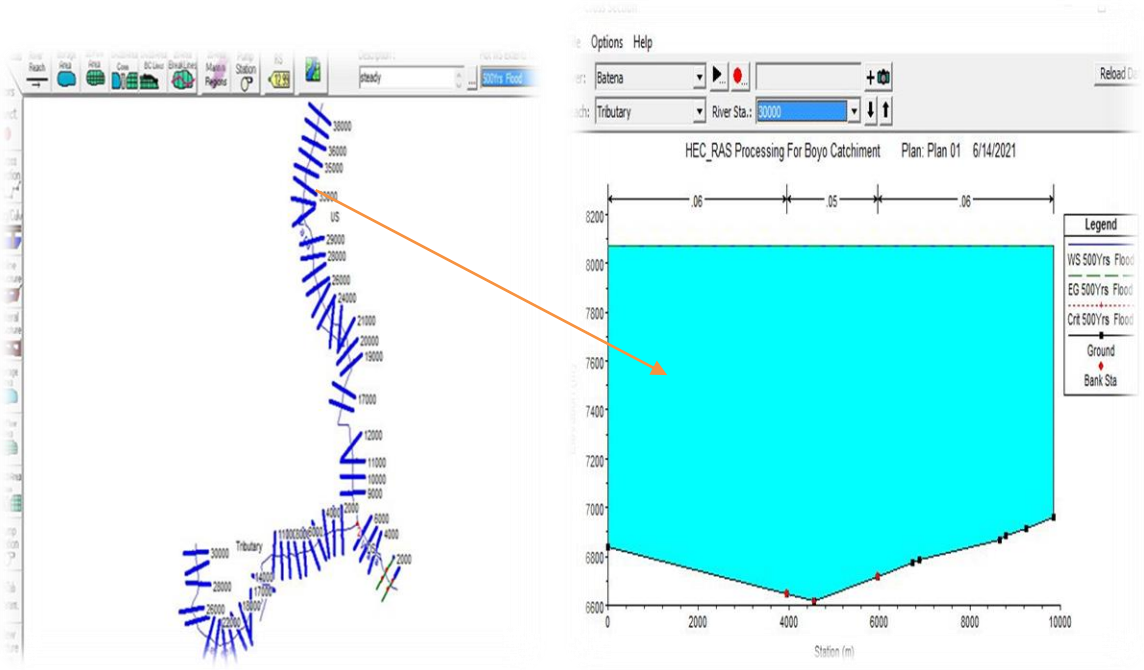

Figure 4.8 (A-C) Showing Different Water Surface Profiles Simulated on HEC-RAS

The steady-state flow was simulated sequentially after importing the geometric data from the Geo-RAS tool and the peak flood from flood frequency analysis. Figure 4.8 shows a water surface profile at various locations as a sample for a peak flood discharge with a 500-year return time (A-C).

4.5 Post-RAS Analysis

4.5.1 Water Surface TIN

For this study, TIN was constructed for all additional reaming water surface profiles based on heights of the water surface at each XS and bounding polygon collected during the import RAS export file. Enough water surface TIN was obtained for this research scope area river flood inundation mapping because it covered the outside of the area possible.

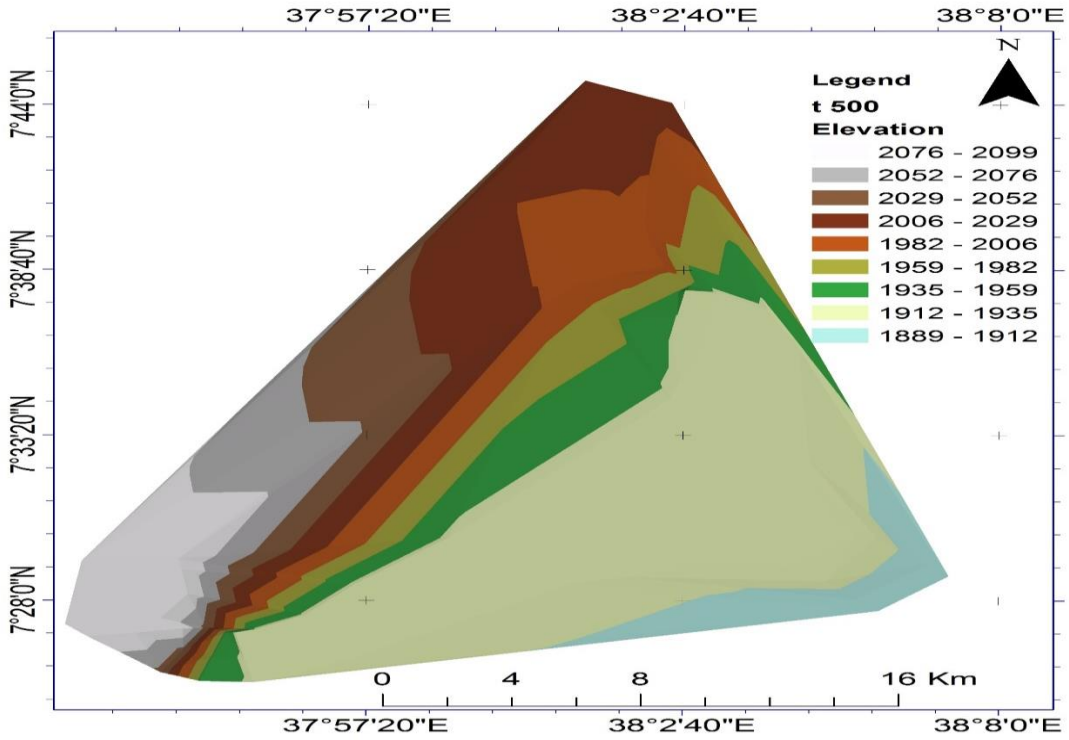

Figure 4.9 Water Surface TIN Generated

4.5.2 Flood Inundation

Inundation in the research region was delineated using the GIS extension tool HEC-GeoRAS as a raster after the steady flow analysis in HEC-RAS for varied discharges of

the respective return period. Then, at a return period of peak discharge, the area flooded was calculated from the bounding polygons of this raster, and the result is given in Table 4.5. Figures 4.10 to 4.16 illustrate how the inundation map for each return period was overlapped on the bounding polygon of post-RAS processing for better visibility.

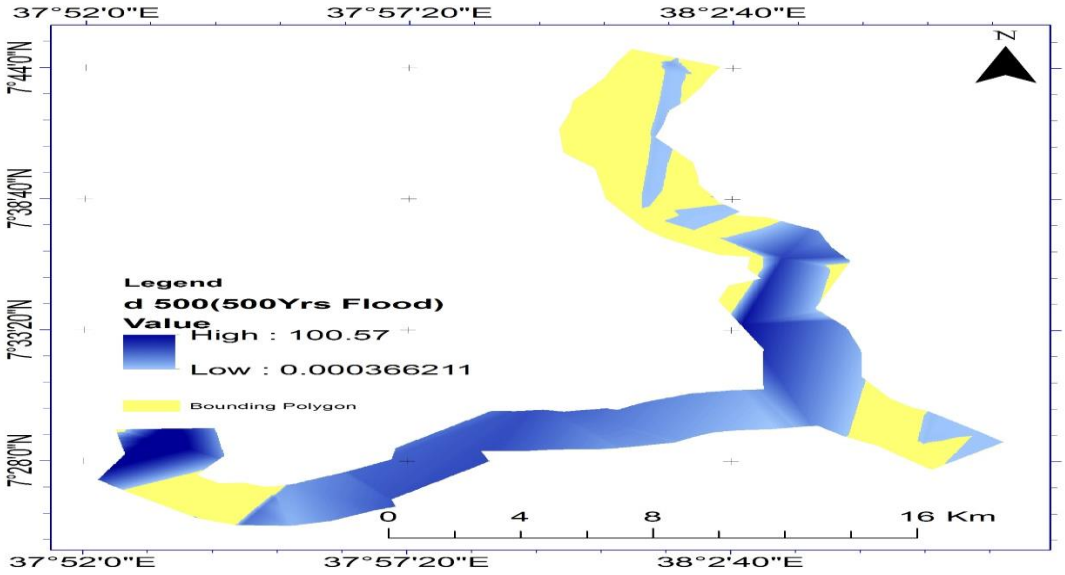

Figure 4.10 Flood Inundation Map for 500 Yrs. Return Period

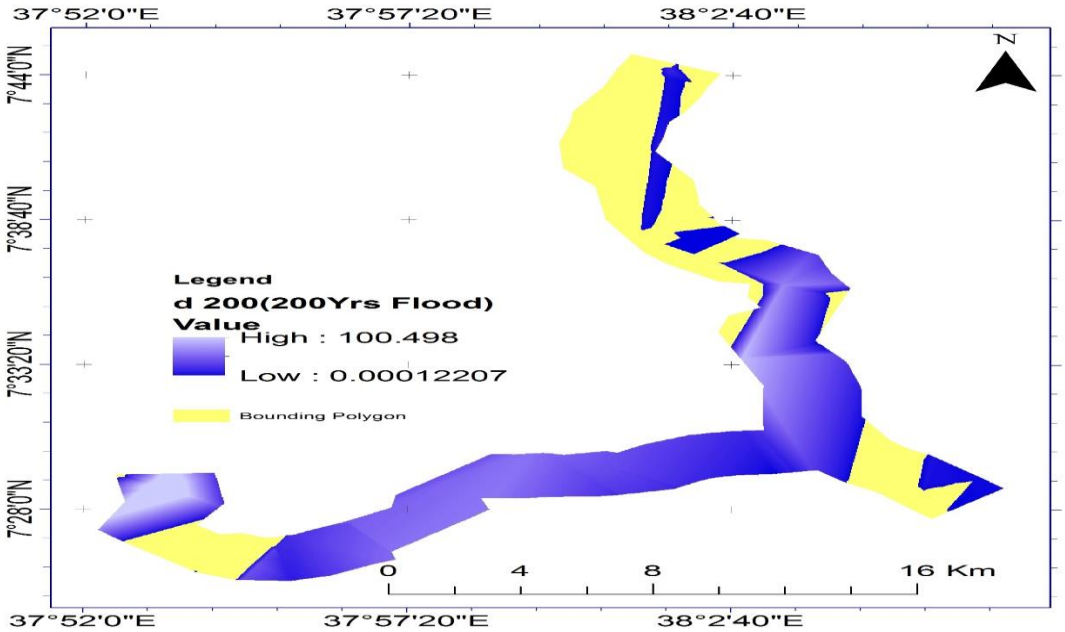

Figure 4.11 Flood Inundation Map for 200Yrs Return Period

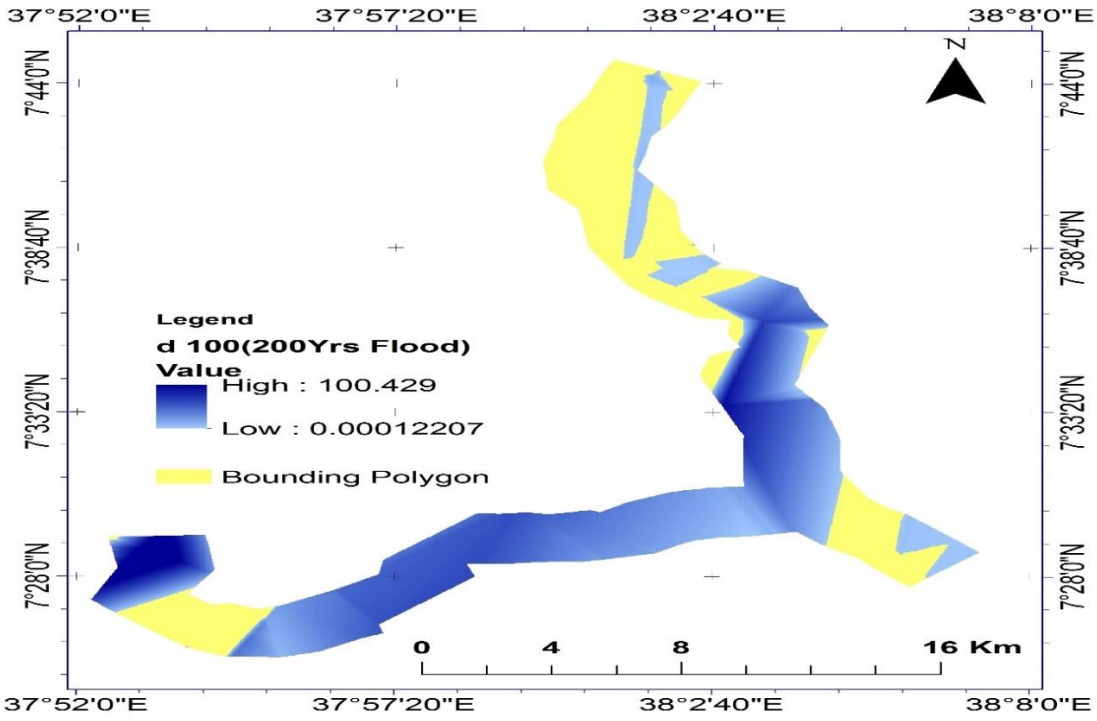

Figure 4.12 Flood Inundation Map for 100 Yrs. Return Period

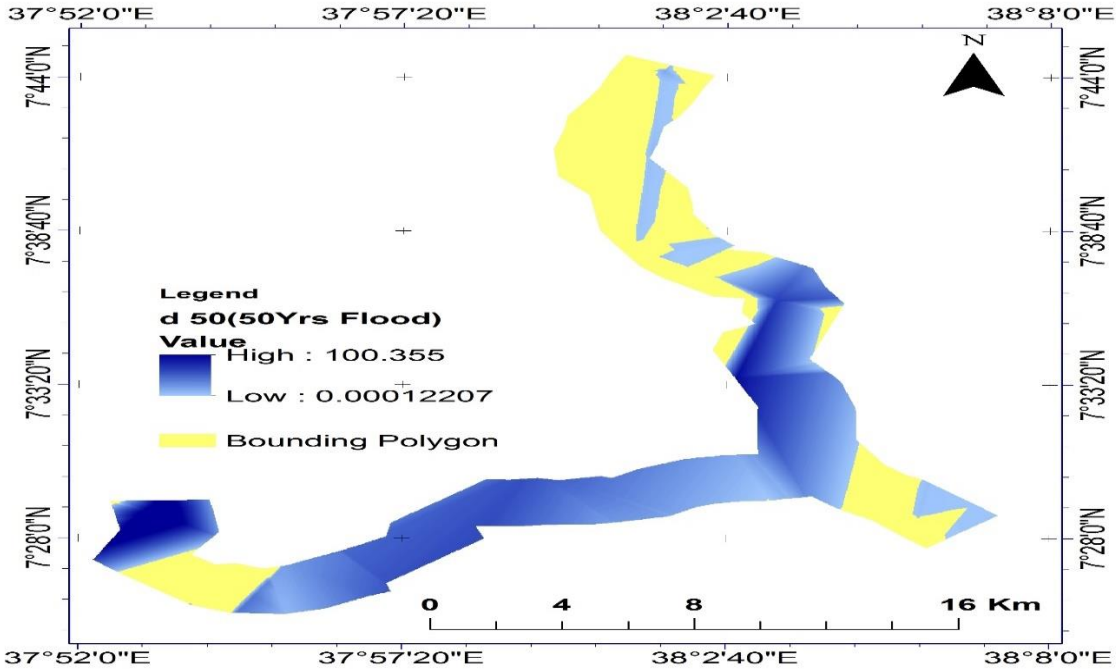

Figure 4.13 Flood Inundation Map for 50 Yrs. Return Period

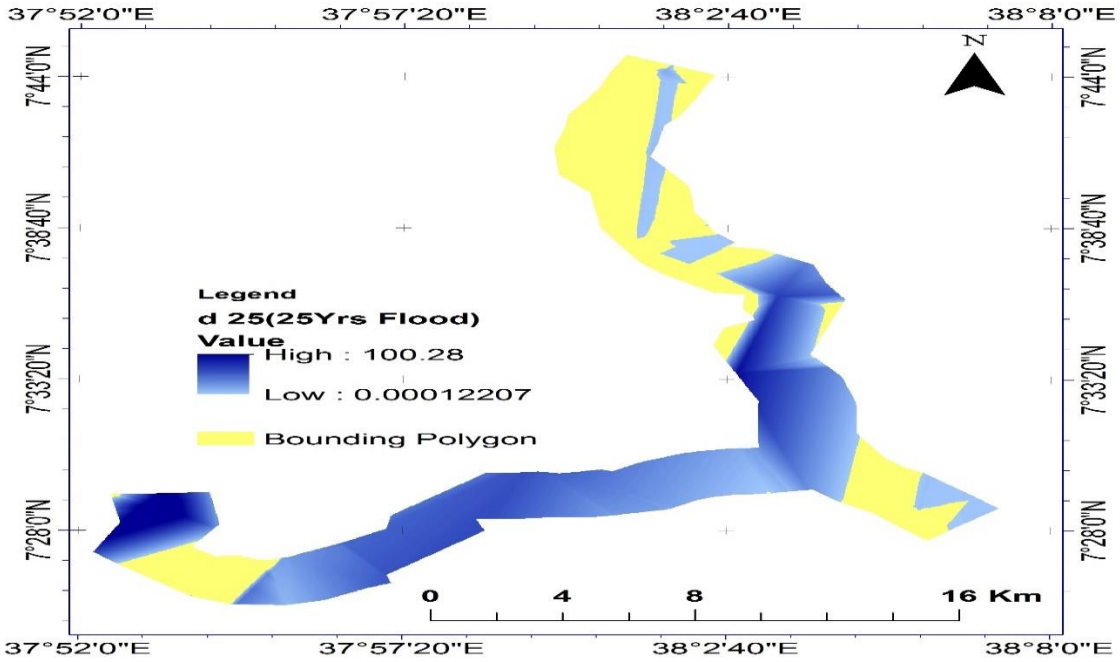

Figure 4.14 Flood Inundation Map for 25 Yrs. Return Period

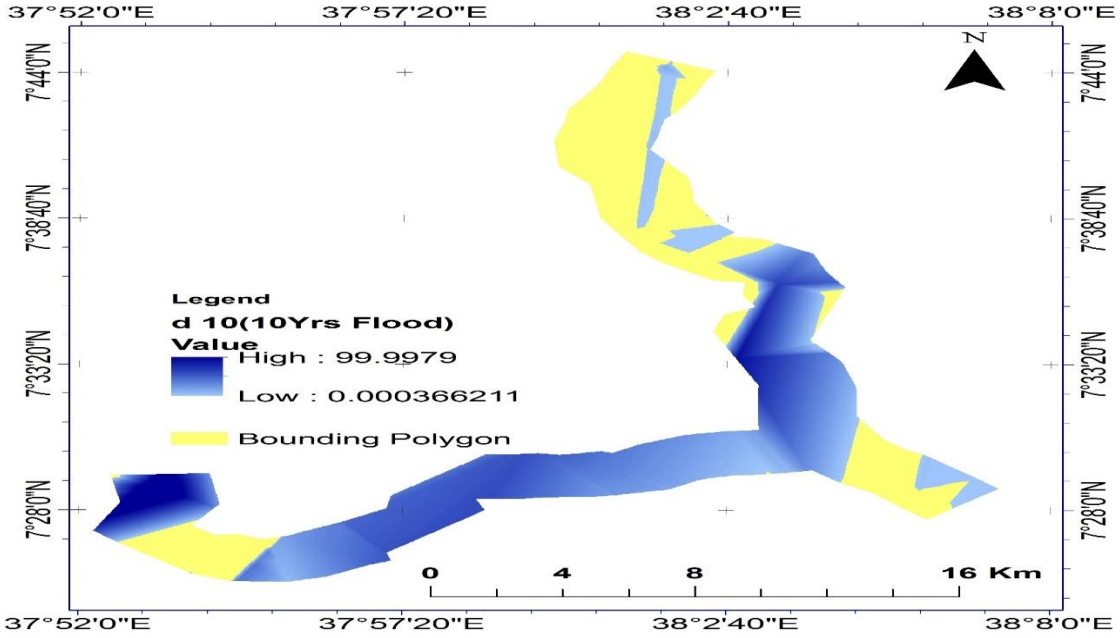

Figure 4.15 Flood Inundation Map for 10 Yrs. Return Period

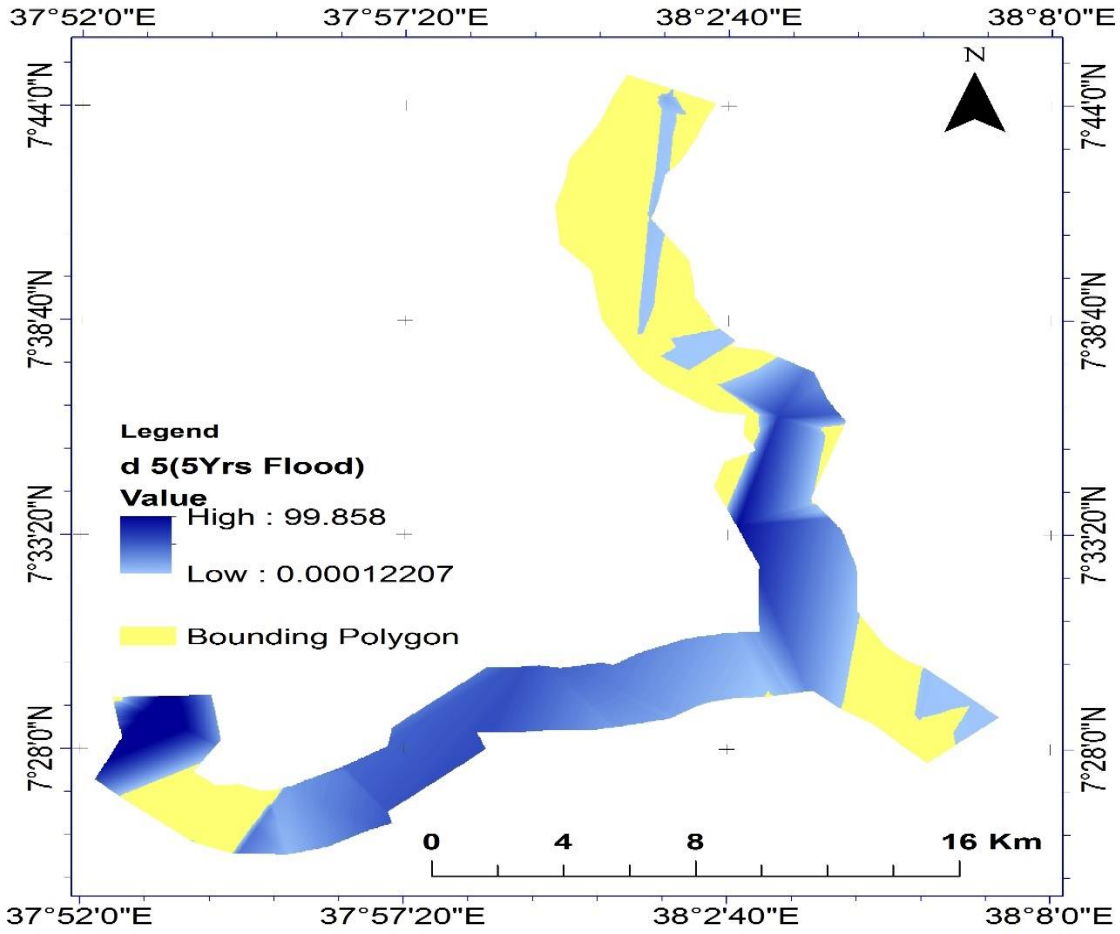

Figure 4.16 Flood Inundation Map for 5 Yrs. Return Period

Table 4.6 Flood inundation area at different return period

Return period (Yrs.)	Flood Inundation (km^2)
2	112.316446
5	112.972257
10	113.561718
25	113.85456
50	114.251455
100	114.433287
200	114.735882
500	114.77083

Observe that inundated area delineated using the model for different return period discharge was increased slightly due to increase in flood magnitude and return period as shown in both from the inundation maps and Table 4.6 above.

4.6 Flood Hazard Mapping and Analysis

Flood hazard maps for return periods of 2, 5,10,25, 50,100, 200, and 500 years were created by overlapping the water surface grid depth generated during inundation mapping with the DEM of the study area, as shown in Figure 4.17(A-B) for the 200- and 500-year floods, and the rest are in Appendix Figure 7. The severity of the effect associated to hydraulic and hydrologic parameters flood expresses the hazard element of the flood. To construct the map and flood hazard level assessment for each return, the hydraulic parameter depth was reclassified as very low, low, moderate, high, very high, and severe using the water depth grid generated from the post-RAS analysis.

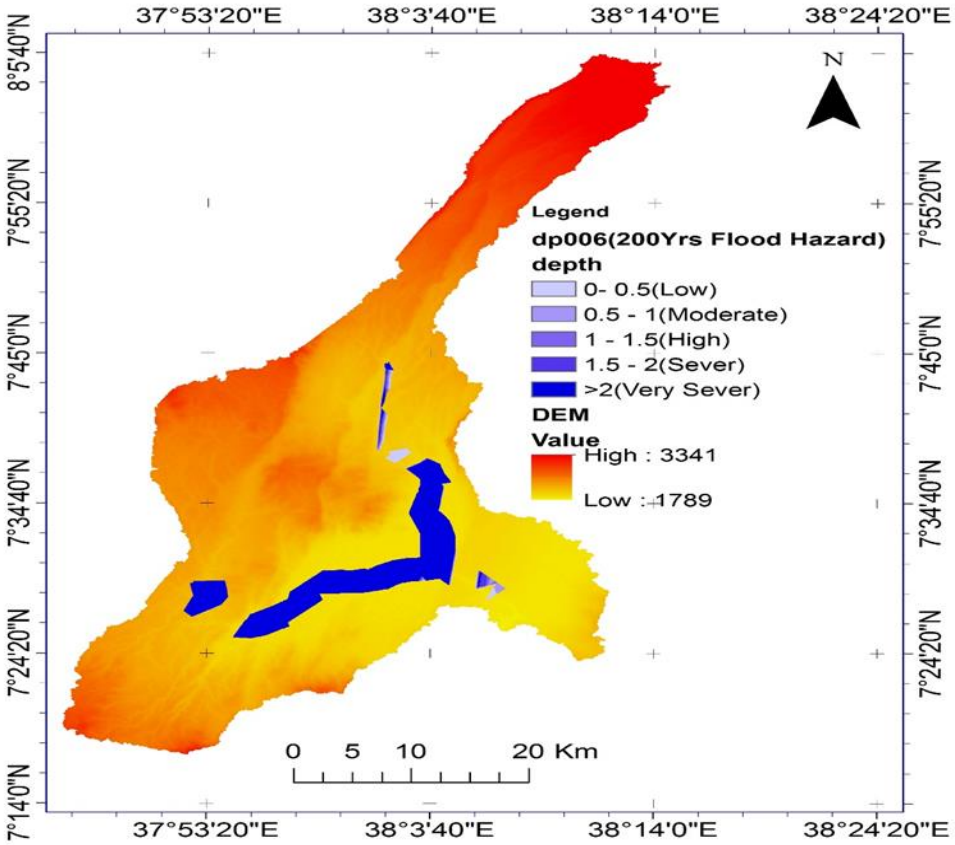

A

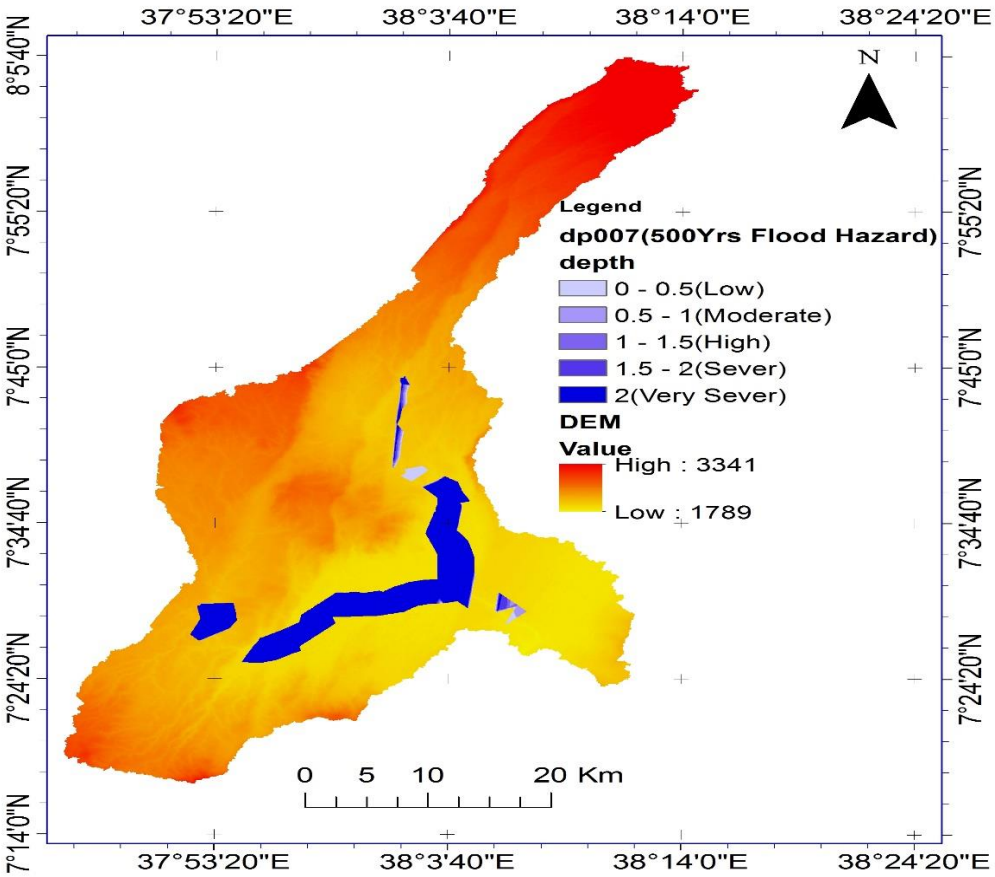

B

Figure 4.17 (A-B) Flood Hazard Maps of 200 and 500Yrs Return Periods

Table 4.7 Flood hazard for different return period

			Level Of Hazard				
Return Period		Low	Moderate	High	sever	Very sever	Total
5Yrs	Area	4.99548	2.4645	2.598366	1.21097	101.047	112.316
	% of Total	4.44769	2.1942	2.313434	1.07818	89.9665	100
10Yrs	Area	4.92592	2.5564	2.593171	1.50806	101.389	112.972
	% of Total	4.36029	2.2629	2.295404	1.3349	89.7465	100
25Yrs	Area	4.80065	2.6418	2.318614	2.01547	101.785	113.562
	% of Total	4.22735	2.3263	2.041722	1.77478	89.6298	100
50Yrs	Area	4.71376	2.6545	2.081627	2.33946	102.065	113.855
	% of Total	4.14016	2.3315	1.828321	2.05478	89.6452	100
100Yrs	Area	4.69533	2.6825	2.045186	2.49227	102.336	114.251
	% of Total	4.1097	2.3479	1.790097	2.18142	89.5721	100
200Yrs	Area	4.58047	2.6851	2.055436	2.50323	102.609	114.433
	% of Total	4.00286	2.3465	1.796239	2.18757	89.6697	100
500Yrs	Area	4.52372	2.6862	2.029258	2.50593	102.991	114.736
	% of Total	3.96817	2.3563	1.780051	2.19819	90.3428	99.9999

Almost all areas inundated from the inundation mapping result indicates that the flood hazard level around the Wera River, Boyo flood plain is a very severe level. For the return periods used in this research the more than 90% flood hazard level is categorized under severe level as it was tabulated in Table 4.7 above.

4.7 Flood hazard management system in study area

Flood defenses are being erected for the Boyo catchment as time goes on to guard against flooding. Flood protection structures built around flood-prone settlements appeared to be both locally and environmentally acceptable, as observed during the field assessment. However, the buildings' holding capacity and strength appeared to be restricted in terms of the volume of water infiltrating those places and the level reached during heavy rain, and the tiny defenses built through the safety net program appeared to be of poor quality and size. The holding capacity and strength of the buildings appeared to be limited in terms of the volume of water infiltrating those places and the level obtained during heavy rains, and the tiny fortifications erected through the safety net program appeared to be of inadequate quality and size. As a result, a particular program focusing on flood protection must be developed in order to create the groundwork for the construction of dependable and locally sound structures.

Figure 4.18 Flood protection structure on flat area of Shashogo, in Suta Kebele (source capturing photo from site observation 6/ 24//2020 at 10:45AM).

5 CONCLUSION AND RECOMMENDATION

5.1 Conclusion

Mass curve technique to test the consistency of the data, outliers test to identify the outliers in the data series with respect to all stations for flood plain analysis. Estimation peak discharge for different return periods developed flood inundation mapping, and preparation of flood hazard map and re-classification hazard level was included in the study. The results of GoF and diagnostic test analysis LP3 distribution are better suited for estimation of flood estimation method for Wear flood plain Boyo catchment. So peak discharge yield by using LP3 was 159.820, 239.710, 344.840, 421.230, 493.510, 560.960, 642.161m3/s for Alaba, 147.420, 218.830, 307.525, 368.018, 422.072, 469.620, 522.931 m3/s for Wera and 24.830, 37.750, 61.27, 85.572, 117.236, 158.301, 231.465m3/s for Batena for 5, 10, 50, 100 and 200 Yrs. return period was produced respectively. The flooded areas along the Wera River flood plain of Boyo catchment was mapped based on the using the HEC-RAS (5.0.7) model, GIS (10.4.1) and HEC-GeoRAS for spatial data processing. The flood hazard assessment map was produced by flood generating powerful GIS-based tools which produce the area of flood 112.316446, 112.972257, 113.561718, 113.85456, 114.251455, 114.433287, 114.735882, 114.77083 Km^2 for return periods 2, 5, 10, 25, 50, 100, 200 and 500Yrs respectively. The flood hazard assessment on the river flood plain was done by GIS tool which is effective in reclassifying to give good results and the map shows that very severe, severe, high, moderate, and low flood hazards around 90%, 2%, 2% 2.33% and 4%, respectively for all return periods. The area inundated indicates an increase from 5Yrs to 500Yrs due to an increase in peak flood, water surface depth grid, and flood velocity land use. Hazard map was prepared for all return periods and its assessment was done for each return period by reclassifying the resulted depth grid polygon and land use land cover change map. Finally, from this study was concluded that preparing and evaluating hazard mapping is important for decision-makers to implement the strategic plan, flood warning, and its mitigation measure for preventing flood hazards. Due to this reason floodplain mapping and its assessment is a basic concern for this research work that was done in keeping the scientific guidance of water-related research.

5.2 Recommendation

Estimation annual maximum floods for different return periods over Wera River flood plain Boyo catchment presented in this thesis work will be useful in planning, designing and management of different hydraulic structures for exercise of water resource in the basin. So, this provides information on flood hazard at Wera River flood plain Boyo catchment.

To identify flood hazard information of Wera River flood plain Boyo catchment the responsible bodies such as Kebele, Woreda, zone, and Region that could be used the relevant decision makers to act upon the current land use policy for reducing vulnerability to flood disaster of the Boyo Catchment in particular Shashogo Woreda. Thus, the responsible bodies of the Woreda as well as the Region should incorporate the flood hazard assessment studies in their development strategies.

The responsible bodies should be developing an idea Watershed management practice in the uplands of the catchment in order to alleviating future flood disasters of Wera River flood plain Boyo catchment.

Finally, the steps listed below are recommended. The bodies in charge in order to reduce reoccurring flood dangers in Shashogo Woreda, the Wera River flood plain Boyo catchment should be developed and made operational. Hillside reforestation; densely planted trees in gullies; Artificial drains that hinder river and stream movement should be blocked; the development of artificial channels will help with Lake Boyo's discharges.

References

Dilley, Chen RS, Deichmann u, 2005. Natural disaster hotspots: a global risk. *internatinal bank for Reconstration and devlopment/ The world Bank and columbia unversity, washgton.*

IWRM and Flood, 2015. *Making Integrated Flood Management Part of the Development Agenda,* s.l.: s.n.

Pathan and Agnihotri, 2019. A Combined Approach For 1-D Hydrodynamic Flood Modeling By using Arc-Gis, Hec-Georas, Hec-Ras Interface - A Case Study On Purna River Of Navsari City, Gujarat. *International Journal of Recent Technology and Engineering (IJRTE),* May.8(1).

Ahmad, Alam,Bhat and Ahmad, 2016. One Dimensional Steady Flow Analysis Using HEC RAS -Acase of River Jhelum,Jammu and Kashmir. *European Scientific Journal,* November, Volume 12, p. 341.

Alem, M. A., 2018. Best-fit probability distributions and return periods for maximum monthly rainfall in Bangladesh. Climate, 16..

Anon., 1995. Rosbjerg D and Madsen H. *Uncertainty measures of regional flood frequency.*

Anon., n.d. *United Nations International Strategy for Disaster Reduction (UNISDR). 2009. Report on Living With Risk: A Global Review of Disaster Reduction Initiative, Geneva, Switzerland,* s.l.: s.n.

Arekhi S., 2012. Run-off modeling by HEC-HMS model (Case study:Kan watershed,Iran).. *International journal of Agricuture and Crop sciences,* Issue 5.

Asadi A., 2013. Performance Evaluation of the HEC-HMS Hydrologic model for lumped and semidistributed storm flow simulation(Study Area:Delibajak Basin American). *journal of Engineering Research,* Issue 7.

Ashok and Saroj, 2010. Report on the status of Disaster Risk Reduction in Sub-Saharan Africa.. *World Bank, Global Facility for Disaster Reduction.*

Awal, 2003. *Application of Steady and Unsteady Flow Model and GIS for Floodplain Analysis and Risk Mapping: A Case Study of Lakhandei River,Nepal*, Kathmandu: IOE.

Baker, V.R., Kochel, R.C., Paton, P.C., Flood Geomorphology. Natural Hazards Review 7,, 1988. Flood Geomorphology.. *Natural Hazards Review*, p. 7.

Barrientosa and Swain, 2014. Linking Flood Management to Integrated Water Resource Management in Guatemala: A critical review. *International Journal of Water Governance*, Issue 4.

Bobee and Ashkar, 1991. *The Gamma family and Derived distributions applied in hydrology.* s.l.:water resources publications,Lettloton,Co.

Bras R. L., 1990. Hydrology: An Introduction to Hydrologie Science.. *Cunnane, C. (1978) Unbiased plotting positions—a review../. Hydrol.*, Issue 37.

Bucha and Selvaraj, 2019. FLOOD INUNDATION MAPPING IN GELANA IN ETHIOPIA. *Global Scientfic Research*, May.7(5).

Cameron and Ackerman, 2012. *HEC-GeaRAS GIS tool for suport of HEC-RAS using ARC-GIS.* s.l.:s.n.

Chow Vent et al, 1988. *Open Channel Hydraulics.* Singapore: McGraw Hill Inc.

Chow, 1959. *Open Channel Hydraulics.* McGraw Hill Inc., Singapore: s.n.

Cowan, 1956. Estimating Hydraulic Roughness Coefficients. *Agricultural Engineering*, Issue 37.

Cunnane, 1989. *Statistical distributions for flood frequency.* Geneva: s.n.

Dawit, 2015. Flood Risk Analysis in Illu Floodplain, Upper Awash River Basin.

Demissie,Negash and Behailu, 2016. Assessment of Climate Change Impact on Flood Frequency of Bilate River Basin, Ethiopia. *Civil and Environmental Research*, 8(9).

Elias, 2015. *FLOOD MAPPING Case Study: On Bantyeketu River In Addis Ababa.*, Addis Ababa: s.n.

Enyew, B. D. &. S. G. J., 2014. Analysing the impact of topography on precipitation and flooding on the Ethiopian highlands.. *J Geol Geosci.*

ESRI, 1996. *Introducing ArcView: The Geographic Information System for Everyone.* Redlands,California(Environmental Systems Research Institute (ESRI) Inc): s.n.

ESRI, 1997. *Using ArcView 3D Analyst,* Redlands, California: s.n.

Garcia, 2012. *Tests to identify outliers in data series,* Brazil: Rio de Janeiro.

Gebremedhin Y G ,Quraishi S and Itefa, 2017. Development Of one day Probable Maximum Periciptation(PMP) and Isohytal map for TIgray Region,Ethiopia. *Global Journal of Science Frontier Research: H Environment & Earth Science.*

Gizachew and Shimelis, 2014. Analysis and mapping of climate change risk and vulnerability in Central Rift Valley Ethiopa. *African Crop Science Journal,* Volume 22, pp. 807-818.

Glard, 1996. *Flood risk Managment:Risk chartography for objective navigations.* 3rd IHP/IAHS George Kovacs colloquium ed. Paris: UNESCO.

Granger, 2002. Community Risk Assessment in Mackay, a Multi Hazard Risk Assessment. *www.ga.gov.au/image_cache/GA4177.pd f . Access Date: November.*

Greenwood J A, Landwehr J M, Matalas N C and and Wallis J R, 1979. Probability weighted moments: definition and relation to parameters of several weighted moments distributions expressable in inverse form. *Water Resources Research .*

G, S., 2013. *Causes and Consequences of Flooding in Dire Dawa City, Eastern Ethiopia,* s.l.: s.n.

Hamed, 1998. *Flood Frequency analysis.* Boca Rotan(Florida): CRC Press LLC,2000 N.Y.corporate Blvd.

Hasan M M and Croke B, 2013. *Filling gaps in daily rainfall data: a statistical approach,* s.l.: s.n.

Hosking J R, 1986. The theory of probability weighted moments moments. *IBM Research Research Division, TJ Watson Recierch Center.*

IPCC, 2007. *Climate Change, Synthesis Report –,* Switzerland: An Assessment of theI nter governmental.

Kefeyale, 2003. *Integrated Flood Management Case Study Ethiopia:,* Addis Ababa,Ethiopia: Integrated Flood Managent.

Kefyalew, 2003. *INTEGRATED FLOOD MANAGEMENT CASE STUDY ETHIOPIA: INTEGRATED FLOOD MANAGEMENT.* s.l., s.n.

Khan et al, 2017. *regional frequency analysisof extremes precipitation using L-moments and partial L-moments Advances in Meteorology.* s.l.:s.n.

Lampros, 2009. Hydrological response to metereological drought indices in thessaly.. *Greece journal of hydrolgic Engineering.*

Lešˇcešen and Dolinaj, 2019. *Regional Flood Frequency Analysis of the Pannonian,* Serbia: 21000 Novi Sad.

Lewin, 2008. *Fundamentals of Remote Sensing and its application in GIS,* s.l.: s.n.

Manandhar, B., 2010. *Flood Plain Analysis and Risk Assessment of Lothar Khola.A Thesis submitted in partial fulfillment of the requirements for the Degree of Master of Science in Watershed Management,* Pokhara,Nepal: Tribhuvan University, Institute of Forestry.

Mayers and White, 1993. *The challenge of the Mississippi flood..* s.l.:s.n.

Merwade , 2012. *Tutorial on using HEC-GeoRAS with ArcGIS 10 and HEC-RAS Modeling,* s.l.: s.n.

Mfwango, Salim ,Kazumba , 2018. Estimation of Missing River Flow Data for Hydrologic Analysis: The Case of Great Ruaha River Catchment. *Hydrol Current Res, an open access journal,* 11 April.9(2).

Mohamed, 2015. Characterization of a Typical Mediterranean Watershed Using Remote Sensing Techniques and GIS Tools. *Hydrology Current Research.*

Mulugeta, T., 2016. *Causes of Flooding Hazards and Mitigation Adama city A GIS-Based Risk Analysis and the Way Forward, Ethiopia,* s.l.: s.n.

MulugetaTeferi, 2016. Causes of Flooding Hazards and Mitigation Techniques in. *A GIS-Based Risk Analysis and the Way Forward Ethiopia.*

Murayama and Estoque, 2010. *Fundamentals of Geographic Information System.* Tsukuba: s.n.

Muse,Getaneh and Abiy, 2018. Mapping Flood Prone Areas of Bilate Watershed Using Integration of Multicriteria Analysis and GIS Techniques. *International Journal of Scientific & Engineering Research Volume* , November. 9(11).

NDRMC, 2018. *Flood Alert #3 Federal Democratic Republic of Ethiopia National Disaster Risk Management Commission, Early Warning and Emergency Response Directorate,Ethiopia,* s.l.: s.n.

Nebiyu and Rabin, 2019. FLOOD inundation mapping in gelana in Ethiopia. *Global Scientific journals* .

Noto and Loggia, 2009. Use of L-Moments Approach or Regional Flood Frequency Analysis in Sicily. *Water Resour Managiment.*

Ohimain, E. I., 2014. *Selective impacts of the 2012 water floods on the vegetation and wildlife of wilber force island,Nigeria,* Nigeria: s.n.

Osti, 2004. Community Participation and Agencies Role for the Implication of Water Induced Disaster Management. *Protecting and Enhancing the Poor, Disaster Prevention and Managemen,* 13(1), pp. pp. 6-12.

Quraishi S and Berhane M, 2014. *Development of one Day probable maximum precipitaion and ISO hyetal map for North sheaw of Amhara Region, Ethopa HARAMAYA University.* s.l., s.n.

Rahman, 2010. Selection of the best fit flood frequency distribution and parameter estimation procedure: a case study for Tasmania in Australia. *Stochastic Environmental Research and Risk Assessment,* Julay.

Rizwan, Guo, Xiong and Yin, 2018. Evaluation of Various Probability Distributions for Deriving Design Flood Featuring Right-Tail Events in Pakistan. *Water*, 8 November.

Santosa, 2002. *The Role of GIS for Flood Disaster Management. Gadjahmada University, Yogyakarta Qihao Weng (,* s.l.: s.n.

Santosa, 2006. *Santosa The Role of GIS for Flood Disaster Management.,* s.l.: s.n.

Saroj, A. a., 2010.. *Report on the status of Disaster Risk Reduction in Sub-Saharan Africa. Washington DC, USA.*, Washington DC, USA.: World Bank, Global Facility for Disaster Reduction,.

Sattari et al., 2016. , *Rezazadeh-Joudi A and and Kusiak A Assessment of different methods for estimation missing data in precptation*, s.l.: hydrololgy researche.

Searcy J K and Hardison C H, 1960. *Double-mass curves: US Government Printing Office*, s.l.: s.n.

Searcy JK and Hardisan C H, 1960. *Double mass curve US Govermment printing office*, s.l.: s.n.

Shahiri Parsa et al, 2016. Floodplain Zoning Simulation by Using HEC-RAS and cche2dModels in the Sungai Maka river.. *Air, Soil and Water Research*, Volume 9, p. 55–62 doi:10.4137/ASWr.S36089.

Sinafikish, 2013. Causes and Consequences of Flooding in Dire Dawa City, Eastern Ethiopia.

Singh, S. K., 2004. *Analysis of Uncertainties in Digital Elevation Models in Flood*, India.: s.n.

Smith and Ward, 1998. *Integrated Flood Risk Management.* England and Wales: s.

Solomon, 2012. *Flood risk mapping and Vulnerability Analysis of Megech River using 2D hydrodynamic flood modelling*, Addis Ababa: s.n.

Solomon, 2012. Worked on Flood risk mapping and Vulnerability Analysis of Megech River using 2D hydrodynamic flood modeling.

Subramanya K, 2013. *Engineering Hydrology.* 4th ed. s.l.:s.n.

Subramanya, 1988. *Engineering Hydrology.* 3rd ed. Kanpur: Tata McGraw-Hill Campanies,New Delhi.

Subramanya, K., 2008. *Engineering hydrology.* 3rd ed. s.l.:s.n.

Tesfaye, 2015. Ground Water Potential Evaluation Based on Integrated GIS and Remote Sensing Techniques, in Bilate River Catchment: South Rift Valley of Ethiopia.. *American Scientific Research Journal for Engineering, Technology, and Sciences (ASRJETS).*

Tolera and Fayera, 2019. FloodPlain Modeling of Awitu River Sub-Basin, Jimma, Oromia, Ethiopia. *Journal of material and Environmental Science,* 01 October, 10(11), pp. 1030-1042.

Traore, 2015. STEADY FLOW SIMULATION IN ANAMBE RIVER BASIN USING HEC-RAS. *International Journal of Development Research,* July, Volume Iv, pp. 4968-4979.

UNDRO, 1991. *Mitigation of Natural Disasters: Phenomena, Effects and Options (A Manual for Policy Makers and Planners).,* New York: s.n.

UNISDR, 2009. *United Nations International Strategy for Disaster Reduction Report on Living With Risk: A Global Review of Disaster Reduction Initiative,,* Geneva, Switzerland: A Global Review of Disaster Reduction Initiative, .

UNISDR, 2009. *United Nations International Strategy for Disaster Reduction Report on Living With Risk: ,* Geneva, Switzerland: s.n.

UNOCHA, 2006. *Flood Affected Woredas in Ethiopia. http://www.ochaeth.org/Home/ downloadables/FD0014RecentFlood_WWW.pdf. (Accessed on March, 2013).,* s.l.: s.n.

USACE, 2016. *HEC-RAS River Analysis System, User's Manual for version5.0.* California(Hydrological Engineering Center): Devis.

USWRC, 1981. *Guidelines for determining flood flow frequency vol 29: US Water,* USA: s.n.

Vail,Parsons,Striggow,Deatrick and Johnson, 2015. *Global Positioning System,* s.l.: s.n.

Vivekanandan, 2015. Estimation of Maximum flood discharge using gamma and exterme value family of porbabilty gistrbuation. *International Journal of World Research.*

Vivekanandan, 2015. Flood frequency analysis using method of moments and L-moments of probability distributions. *IVIL & ENVIRONMENTAL ENGINEERING | RESEARCH ARTICL,* 16 March.

WMO, 2009. Applying Environmental Assessment for Flood Management.. *A Tool for Integrated Flood Management. Associated Programme on Flood Management.*

WMO, 2009. *Integrated Flood Management Concept. Associated Programme on Flood Management*, s.l.: s.n.

Wrachien, Mambretti & Schultz, 2011. Flood management and risk assessment in flood-prone areas: Measures and solutions. *Irrigation and Drainage*, p. 60.

Yadav, S. K., 2002. *Hydrological Analysis for Bheri-babai Hydropower Project Nepal.,* Norway: s.n.

Yirga, 2016. Flood Hazard and Risk Assessment Using GIS and Remote Sensing in Lower Awash Sub-basin, Ethiopia. *Journal of Environment and Earth Science,* Volume Vol.6.

Zewde, 2004. Development of Flood Forecasting Model in Midd Awash River Basin of Ethiopia..

Zhang, J., 2002. Powerful goodness-of-fit tests based on the likelihood ratio. *Journal of Royal Statistical Society Series B, ,* Volume 64, pp. 281-294.

APPENDICES

APPENDIX TABLES

Appendix Tables 1 from (A-D) sample calculation and value Peake discharge for each station by selected probability distribution.

A) Sample calculation of peak flood using LP III

		Alaba	Wera	Batena						
	Mean	1.79209	1.73351	1.17412						
	Skew	0.01214	0.0195	0.02614						
	Standard	0.55113	0.56962	0.34496						
	Alaba river									
T	F	p	1/p^2	w	Z	k	KT	log(QT)	QT	
2	0.5	0.5	4	1.17741	-0.16	-0.1483	-0.0119	1.78556	61.0325	
5	0.8	0.8	25	1.79412	0.70019	-0.1483	-0.7467	2.20363	159.82	
10	0.9	0.1	100	2.14597	1.15282	-0.1483	1.06616	2.37968	239.706	
15	0.933333333	0.06667	225	2.32725	1.37812	-0.1483	1.20693	2.45726	286.591	
25	0.96	0.04	625	2.53727	1.63408	-0.1483	1.35273	2.53761	344.837	
50	0.98	0.02	2500	2.79715	1.94439	-0.1483	1.51041	2.62452	421.227	
100	0.99	0.01	10000	3.03485	2.2231	-0.1483	1.6352	2.69329	493.504	
200	0.995	0.005	40000	3.25525	2.47783	-0.1483	1.73616	2.74893	560.961	
500	0.998	0.002	250000	3.52551	2.78608	-0.1483	1.84269	2.80764	642.161	
1000	0.999	0.001	1000000	3.71692	3.00202	-0.1483	1.90776	2.84351	697.44	
	Wera river									
T	F	p	1/p^2	w	Z	k	KT	log(QT)	QT	
2	0.5	0.5	4	1.17741	-0.16	-0.1745	0.01429	1.74182	55.1845	
5	0.8	0.8	25	1.79412	0.70019	-0.1745	0.74841	2.16856	147.422	
10	0.9	0.1	100	2.14597	1.15282	-0.1745	1.0435	2.3401	218.828	
15	0.933333333	0.06667	225	2.32725	1.37812	-0.1745	1.16985	2.41355	259.147	
25	0.96	0.04	625	2.53727	1.63408	-0.1745	1.29772	2.4879	307.525	
50	0.98	0.02	2500	2.79715	1.94439	-0.1745	1.43188	2.56587	368.018	
100	0.99	0.01	10000	3.03485	2.2231	-0.1745	1.53427	2.67175	422.072	
200	0.995	0.005	40000	3.25525	2.47783	-0.1745	1.61402	2.67175	469.619	
500	0.998	0.002	250000	3.52551	2.78608	-0.1745	1.69435	2.71844	522.931	
1000	0.999	0.001	1000000	3.71692	3.00202	-0.1745	1.74098	2.74555	556.606	
	Batena river									
T	F	p	1/p^2	w	Z	k	KT	log(QT)	QT	
2	0.5	0.5	4	1.17741	-0.16	0.09688	-0.2506	1.08768	12.237	
5	0.8	0.8	25	1.79412	0.70019	0.09688	0.64011	1.39494	24.8276	
10	0.9	0.1	100	2.14597	1.15282	0.09688	1.16763	1.57691	37.7495	
15	0.933333333	0.06667	225	2.32725	1.37812	0.09688	1.44687	1.67324	47.1237	
25	0.96	0.04	625	2.53727	1.63408	0.09688	1.77747	1.78729	61.2757	
50	0.98	0.02	2500	2.79715	1.94439	0.09688	2.19793	1.93233	85.5716	
100	0.99	0.01	10000	3.03485	2.2231	0.09688	2.59429	2.06906	117.236	
200	0.995	0.005	40000	3.25525	2.47783	0.09688	2.97241	2.1995	158.305	
500	0.998	0.002	250000	3.52551	2.78608	0.09688	3.45069	2.36449	231.465	
1000	0.999	0.001	1000000	3.71692	3.00202	0.09688	3.79955	2.48483	305.371	

B)

	Peak discharge of Alaba kulito (m^3/s)				
	EVI	LN2	NOR	GAMMA	LP3
T	XT	XT	XT	XT	XT
2	103.448	98.625	111.4137	132.4361	61.03245136
5	143.4056	126.105	123.486	168.1047	159.819738
10	175.9009	189.932	174.5317	189.9101	239.7055093
25	216.9587	242.648	235.438	197.8961	344.8368416
50	247.4177	281.859	316.398	252.8966	421.2270127
100	277.6519	323.909	397.784	283.2887	493.5037059
200	307.7757	352.3649	407.453	302.8541	560.9604602
500	347.5183	387.378	438.344	340.5605	642.1609124

C)

	Peak discharge of Fonko(m^3/s)				
	EVI	LN2	NOR	GAMMA	LP3
T	XT	XT	XT	XT	
2	111.678	99.2443	143.324	119.4361354	55.18450795
5	151.6356	125.0385	160.536	155.1046626	147.421569
10	184.1309	190.061	179.129	187.2401183	218.8275914
25	225.1887	241.921	191.453	195.2260617	307.5245281
50	255.6477	283.175	201.356	190.0060617	368.0183163
100	285.8819	325.401	211.564	245.0065551	422.0722231
200	316.0057	354.765	223.712	275.3987142	469.6188927
500	355.7483	367.507	232.762	294.9640824	522.9309972

D)

Peak discharge of Batena(m^3/s)					
T	EVI	LN2	NOR	GAMMA	LP3
2	57.768	36.81	85.324	122.765	12.237
5	98.326	92.0385	108.562	145.345	24.8276
10	132.061	111.092	169.786	181.211	37.7495
25	186.806	169.21	217.238	223.617	61.2753
50	231.675	242.18	287.133	295.183	85.5716
100	261.681	315.619	344.804	363.089	117.236
200	279.074	345.795	374.83	423.142	158.305
500	339.048	377.201	463.244	502.224	231.465

Appendix Tables 2 from (A to C) shows best fit selection for each station

A) Best fit selection computation for Alaba kulito, Fonko, Batena station.

D-index test for Alaba kulito station				
Type of distribution	Type of parameter	D-index value	Selected parameter	Best-fit distribution
EVI	MOL	5.6841	PWM	LP3/MOM
	MLM	13.010		
	PWM	2.1457		
LP3	MOL	0.0755	MOM	
	MLM	0.5760		
	PWM	0.3865		
Gamma 2	MOL	1.0329	MLM	
	MLM	0.2185		
	PWM	2.6467		
NOR	MOL	6.8918	PWM	
	MLM	13.717		
	PWM	0.1957		
LN2	MOL	0.6917	MLM	
	MLM	0.1407		
	PWM	3.1676		

B)

D-index test for Fonko Station				
Type of distribution	Type of parameter	D-index value	selected parameter	Best fit distribution
EVI	MOL	0.2163	MOM	
	MLM			
	PWM	0.8814		
		0.8825		
LP3	MOL	0.0697	MOM	LP3/MOM
	MLM	0.1404		
	PWM	1.3511		
Gamma 2	MOL	0.3483	MLM	
	MLM	0.2388		
	PWM	1.5399		
NOR	MOL	0.1349	MLM	
	MLM	0.1143		
	PWM	0.8163		
LN2	MOL	0.1441	PWM	
	MLM	0.2634		
	SPWM	0.1296		

C)

D-index test for Batena station				
Type of distribution	Type of parameter	D-index value	selected parameter	Best fit distribution
EVI	MOL	0.8338	PWM	
	MLM	0.8771		
	PWM	0.6811		
LP3	MOL	0.1688	MOM	
	MLM	0.4367		
	PWM	0.6255		
Gamma 2	MOM	0.4188	MLM	
	MLM	0.3394		
	PWM	4.1684		
NOR	MOM	1.0968	MLM	LP3/MOM
	MLM	0.9446		
	PWM	1.6296		
LN2	MOL	0.201	PWM	
	MLM	0.3869		
	PWM	0.1894		

Appendix Tables 3 from A to C

A) Computation x^2 and KS test best fit for Alaba kulito, Fonko, Batena gauging station.

Computed values of GoF tests result for Alaba kulito station				
Distribution	x^2 test	K-S test	Theoretical values of X^2 tests result	Theoretical values K-S test Result
EVI/PWM	14.208	0.21149	33.678	0.2749
LP3/MOM	0.6186	0.10309		
Gamma/MLM	65.644	0.93899		
NOR/PWM	4.1807	0.1899		
LN2/MLM	0.8029	0.20539		

B)

Computed values of GoF tests result for Batena station				
Distribution	x^2 test	K-S test	Theoretical values of X^2 tests result	Theoretical values of k-s tests result
EVI/PWM	11.201	0.28117	37.246	0.25438
LP3/MOM	3.7481	0.10819		
Gamma/MLM	15.648	0.29610		
NOR/MLM	3.185	0.23499		
LN2/PWM	0.784	0.16236		

C)

Goodnes test for Fonko station				
Distribution	x^2 test	K-S test	Theoretical value for X^2 test	Theoretical value for X^2 test
EVI/MLM	3.4637	0.14932	42.324	0.2407
LP3/MOL	1.8712	0.13949		
Gamma/MOM	6.7967	0.13899		
NOR/PWM	5.3852	0.21899		
LN2/PWM	16.7593	0.10539		

Appendix Table 4

(A) HEC-RAS profile output table sample

River	Reach	River Sta	Profile	Q Total	Min Ch El	W.S. Elev	Crit W.S.	E.G. Elev	E.G. Slope	Vel Chnl	Flow Area	Top Width	Froude # Ch
				(m3/s)	(m)	(m)	(m)	(m)	(m/m)	(m/s)	(m2)	(m)	
Wara	US	38000	500Yrs Flood	522.93	2021.63	2024.44	2024.44	2025.14	0.022057	3.71	140.84	100.42	1
Wara	US	37000	500Yrs Flood	522.93	2008.31	2010.85	2009.52	2010.87	0.000508	0.67	1009.44	794.98	0.16
Wara	US	36000	500Yrs Flood	522.93	2007.19	2009.55		2009.57	0.001123	0.75	811.82	687.68	0.22
Wara	US	35000	500Yrs Flood	522.93	2015.11	2008.69		2008.7	0.000443		1168.67	811.51	0
Wara	US	34000	500Yrs Flood	522.93	2022.85	2008.35		2008.37	0.000325		973.74	405.55	0
Wara	US	33000	500Yrs Flood	522.93	2022.45	2008.06		2008.07	0.000212		1046.6	350.62	0
Wara	US	32000	500Yrs Flood	522.93	2025.49	2007.74		2007.78	0.000662		647.05	245.3	0
Wara	US	31000	500Yrs Flood	522.93	2025.03	2005.98		2006.44	0.023336		175.81	136.64	0
Wara	US	29000	500Yrs Flood	522.93	2000.22	2002.9		2002.92	0.000418	0.61	974.93	726.16	0.14
Wara	US	28000	500Yrs Flood	522.93	1999.04	2001.76		2001.78	0.000379	0.55	1000.95	735.18	0.14
Wara	US	27000	500Yrs Flood	522.93	1997.84	2000.51		2000.52	0.00048	0.53	986.1	740.1	0.15
Wara	US	26000	500Yrs Flood	522.93	1997.82	1998.03	1997.62	1998.1	0.00699	0.37	453.26	636.7	0.37
Wara	US	25000	500Yrs Flood	522.93	1978.01	1978.28	1978.24	1978.36	0.02719	1.29	422.03	1628.95	0.83
Wara	US	24000	500Yrs Flood	522.93	1957.53	1957.95	1957.76	1957.98	0.005001	0.76	765.38	1978.22	0.39
Wara	US	23000	500Yrs Flood	522.93	1932.81	1934.72	1934.72	1935.21	0.025703	3.11	168.27	176.28	1.02
Wara	US	22000	500Yrs Flood	522.93	1914.87	1930.15	1911.83	1930.15	0	0.03	18906.55	1868.38	0
Wara	US	21000	500Yrs Flood	522.93	1900.7	1930.15		1930.15	0	0.01	66026.46	2566.88	0
Wara	US	20000	500Yrs Flood	522.93	1884.6	1930.15		1930.15	0	0.01	77106.65	2458.97	0
Wara	US	19000	500Yrs Flood	522.93	1897.25	1930.15		1930.15	0	0.01	64695.3	2794.11	0
Wara	US	17000	500Yrs Flood	522.93	1877.36	1930.15		1930.15	0	0.01	61796.58	2341.09	0
Wara	US	16000	500Yrs Flood	522.93	1874.09	1930.15		1930.15	0	0.01	68821.84	2361.4	0
Wara	US	12000	500Yrs Flood	522.93	1893.95	1930.15		1930.15	0	0.01	96138.23	3000	0
Wara	US	11000	500Yrs Flood	522.93	1896.77	1930.15		1930.15	0	0.01	82554.21	3000	0
Wara	US	10000	500Yrs Flood	522.93	1898.01	1930.15		1930.15	0	0.01	75638.72	3000	0
Wara	US	9000	500Yrs Flood	522.93	1899.61	1930.15		1930.15	0	0.01	66610.8	3000	0
Wara	DS	6000	500Yrs Flood	642.16	1923.93	1930.15		1930.15	0	0.03	12577.08	1656.64	0.01
Wara	DS	5000	500Yrs Flood	642.16	1936.25	1930.07	1928.94	1930.14	0.003133		526.6	349.3	0
Wara	DS	4000	500Yrs Flood	642.16	1928.42	1925.55	1924.98	1925.65	0.006831		464.13	459.01	0
Wara	DS	2000	500Yrs Flood	642.16	1898.27	1895.37	1895.37	1895.69	0.041915		255.65	403.8	0
Wara	DS	1000	500Yrs Flood	642.16	1888.22	1888.73	1888.34	1888.75	0.002003	0.46	1189.88	2514.47	0.24
Batena	Tributary	30000	500Yrs Flood	231.47	2017.1	2099.63	2019.14	2099.63	0	0	118888.4	2690.76	0
Batena	Tributary	29000	500Yrs Flood	231.47	2000.64	2099.63		2099.63	0	0	196919.4	3000	0
Batena	Tributary	28000	500Yrs Flood	231.47	2032.18	2099.63		2099.63	0	0	168426.3	3000	0
Batena	Tributary	26000	500Yrs Flood	231.47	2072.84	2099.63		2099.63	0	0	55807.68	2550.65	0
Batena	Tributary	25000	500Yrs Flood	231.47	2112.7	2099.46	2099.02	2099.61	0.010757		133.49	130.8	0
Batena	Tributary	23000	500Yrs Flood	231.47	2071.56	2046.63	2046.63	2047.12	0.038245		75.11	79.8	0
Batena	Tributary	22000	500Yrs Flood	231.47	1977.18	1954.78	1954.78	1955.27	0.038204		74.99	79.38	0
Batena	Tributary	21000	500Yrs Flood	231.47	1920.15	1930.15	1919.78	1930.15	0	0.01	20676.24	2435.3	0
Batena	Tributary	20000	500Yrs Flood	231.47	1913.81	1930.15		1930.15	0	0.01	48114.89	3000	0
Batena	Tributary	19000	500Yrs Flood	231.47	1904	1930.15		1930.15	0	0	72668.52	3000	0
Batena	Tributary	18000	500Yrs Flood	231.47	1899	1930.15		1930.15	0	0	89226.28	3000	0
Batena	Tributary	17000	500Yrs Flood	231.47	1894.41	1930.15		1930.15	0	0	103551.1	3000	0
Batena	Tributary	14000	500Yrs Flood	231.47	1893.03	1930.15		1930.15	0	0	105634.2	3000	0
Batena	Tributary	11000	500Yrs Flood	231.47	1893.41	1930.15		1930.15	0	0	106297.7	3000	0
Batena	Tributary	10000	500Yrs Flood	231.47	1892.36	1930.15		1930.15	0	0	107933.4	3000	0
Batena	Tributary	9000	500Yrs Flood	231.47	1898.46	1930.15		1930.15	0	0	91595.26	3000	0
Batena	Tributary	8000	500Yrs Flood	231.47	1904.91	1930.15		1930.15	0	0	72608.59	3000	0
Batena	Tributary	7000	500Yrs Flood	231.47	1906.76	1930.15		1930.15	0	0	65748.12	3000	0
Batena	Tributary	6000	500Yrs Flood	231.47	1909.77	1930.15		1930.15	0	0	55806.66	3000	0
Batena	Tributary	5000	500Yrs Flood	231.47	1912.4	1930.15		1930.15	0	0.01	48446.83	3000	0
Batena	Tributary	4000	500Yrs Flood	231.47	1915.91	1930.15		1930.15	0	0.01	38236.2	3000	0
Batena	Tributary	3000	500Yrs Flood	231.47	1920.48	1930.15		1930.15	0	0.01	25821.05	3000	0
Batena	Tributary	2000	500Yrs Flood	231.47	1919.13	1930.15		1930.15	0	0.01	23947.76	3000	0

APPENDIX FIGURE

Appendix 1

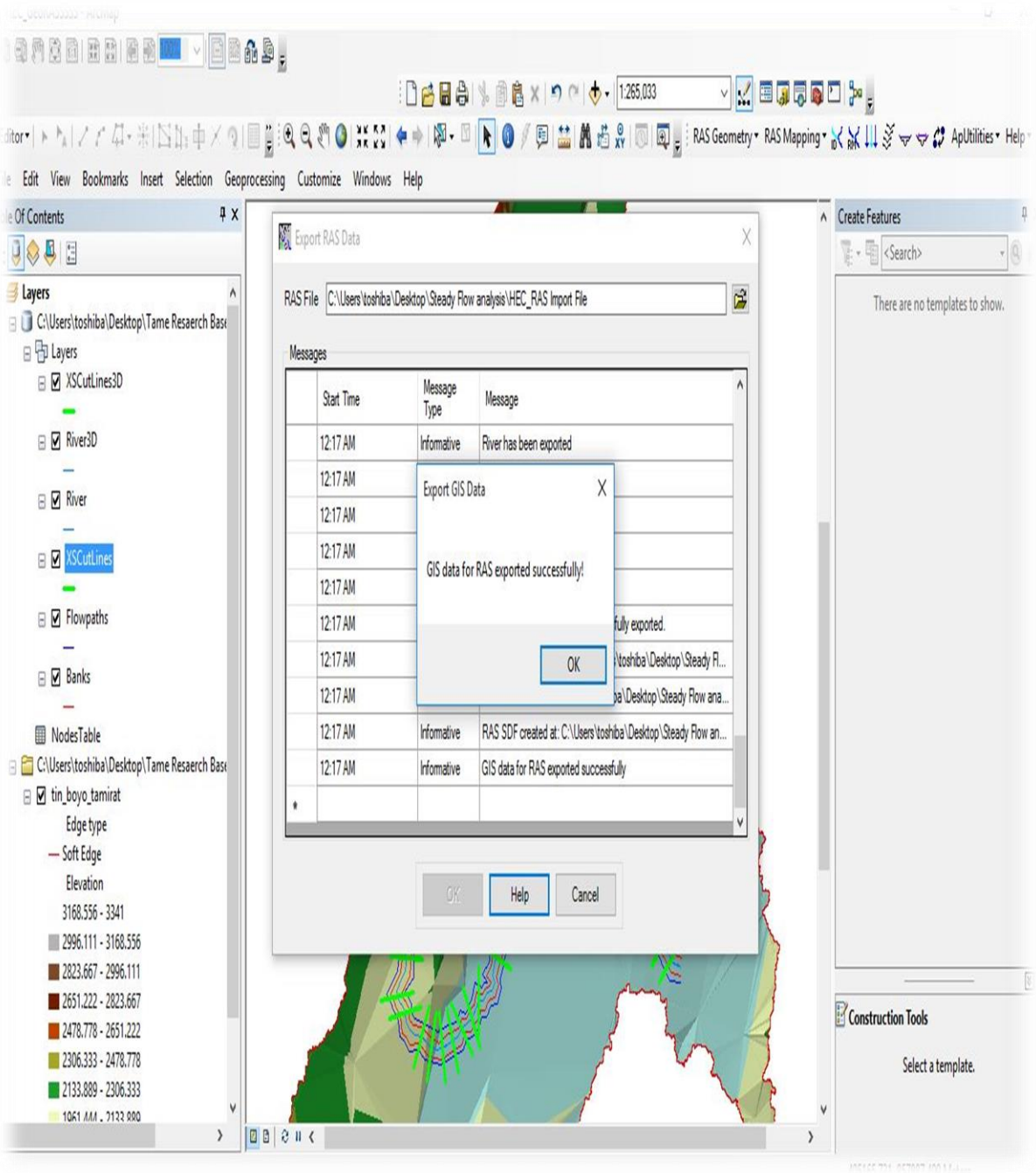

Appendix Figure 1 Post-RAS Process at Boyo catchment wear river

Appendix 2

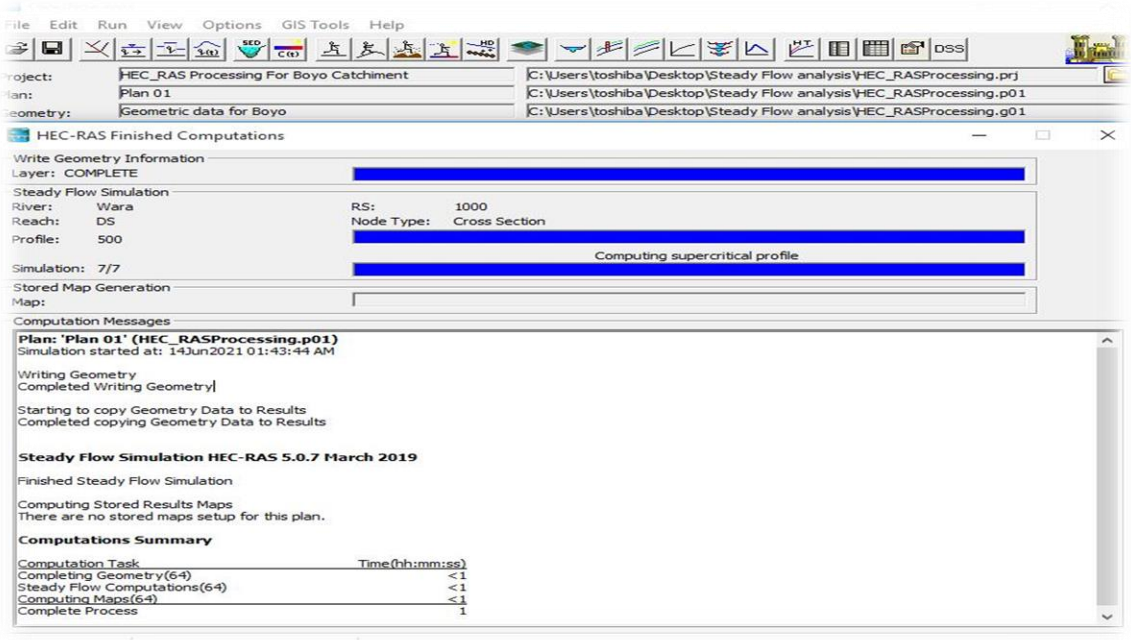

Appendix Figure 2 Steady Flow Simulation

Appendix 3

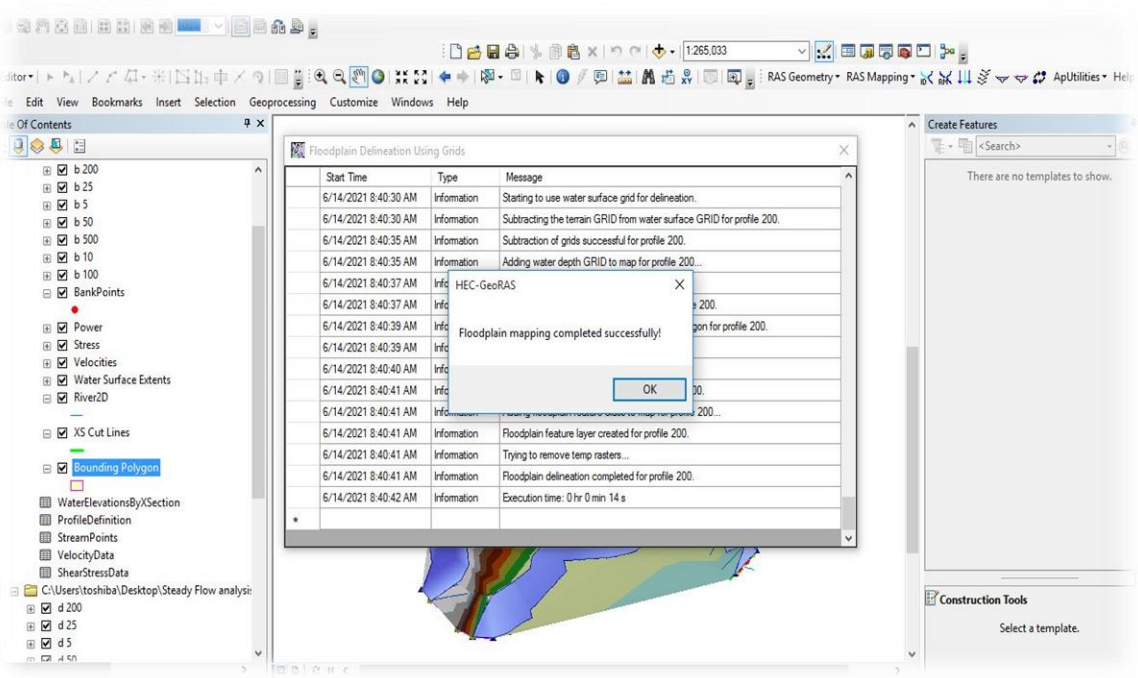

Appendix Figure 3 Flood plain mapping in HEC RAS

Appendix 4

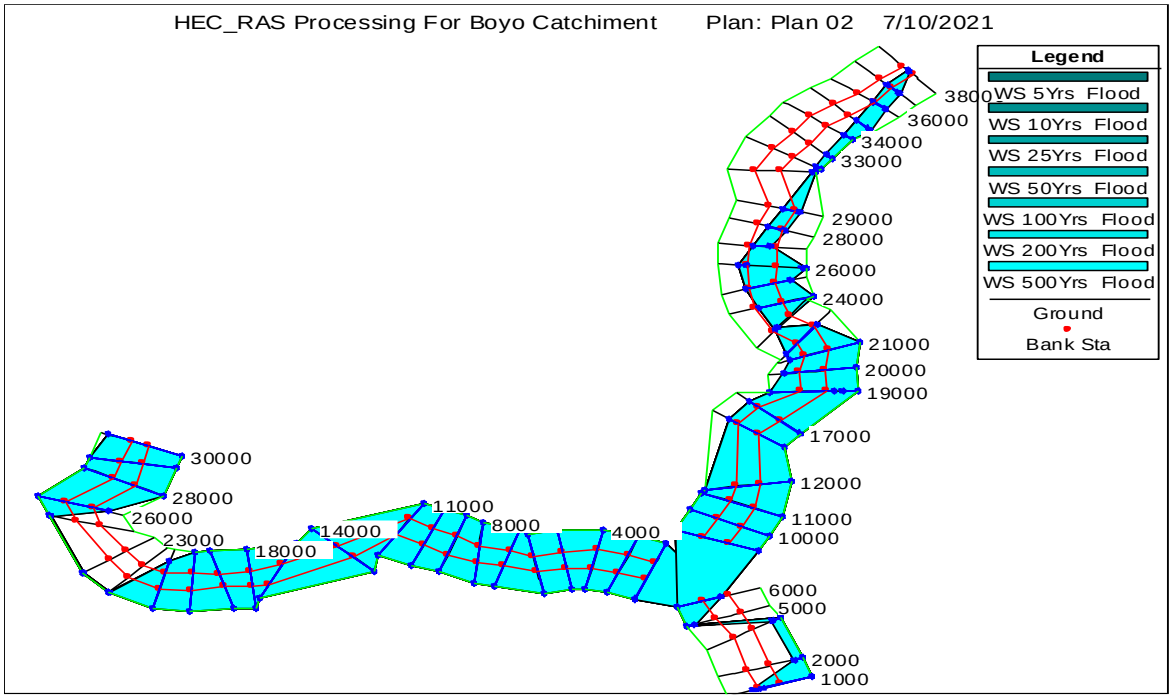

Appendix Figure 4 X-Y-Z Perspective Plot

Appendix 5

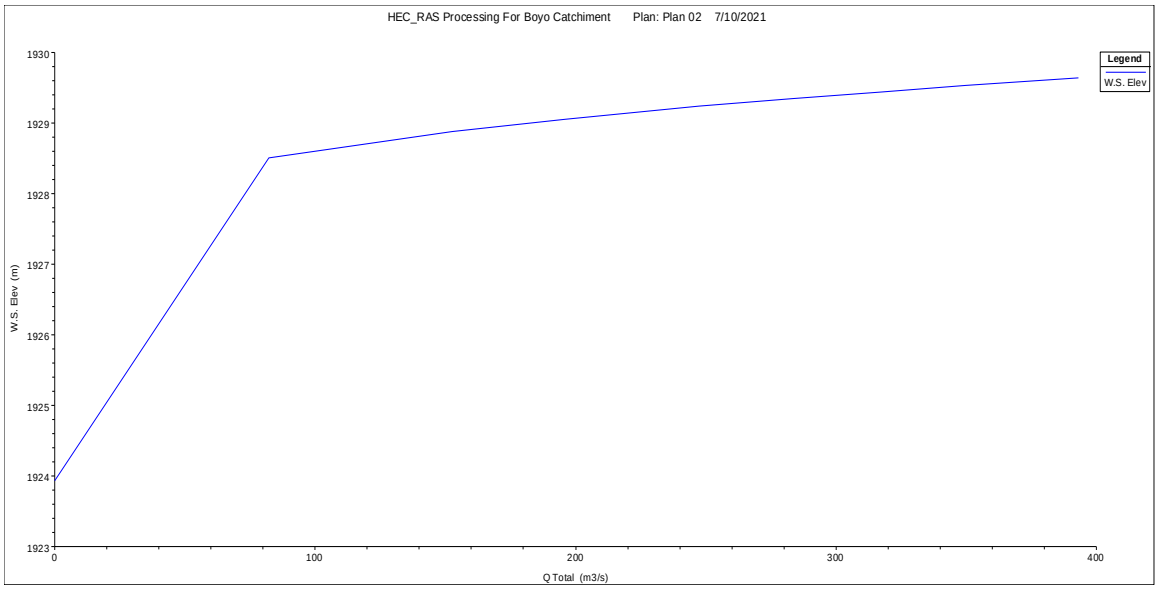

Appendix Figure 5 Sample Rating Curve at Station 6000

Appendix 6

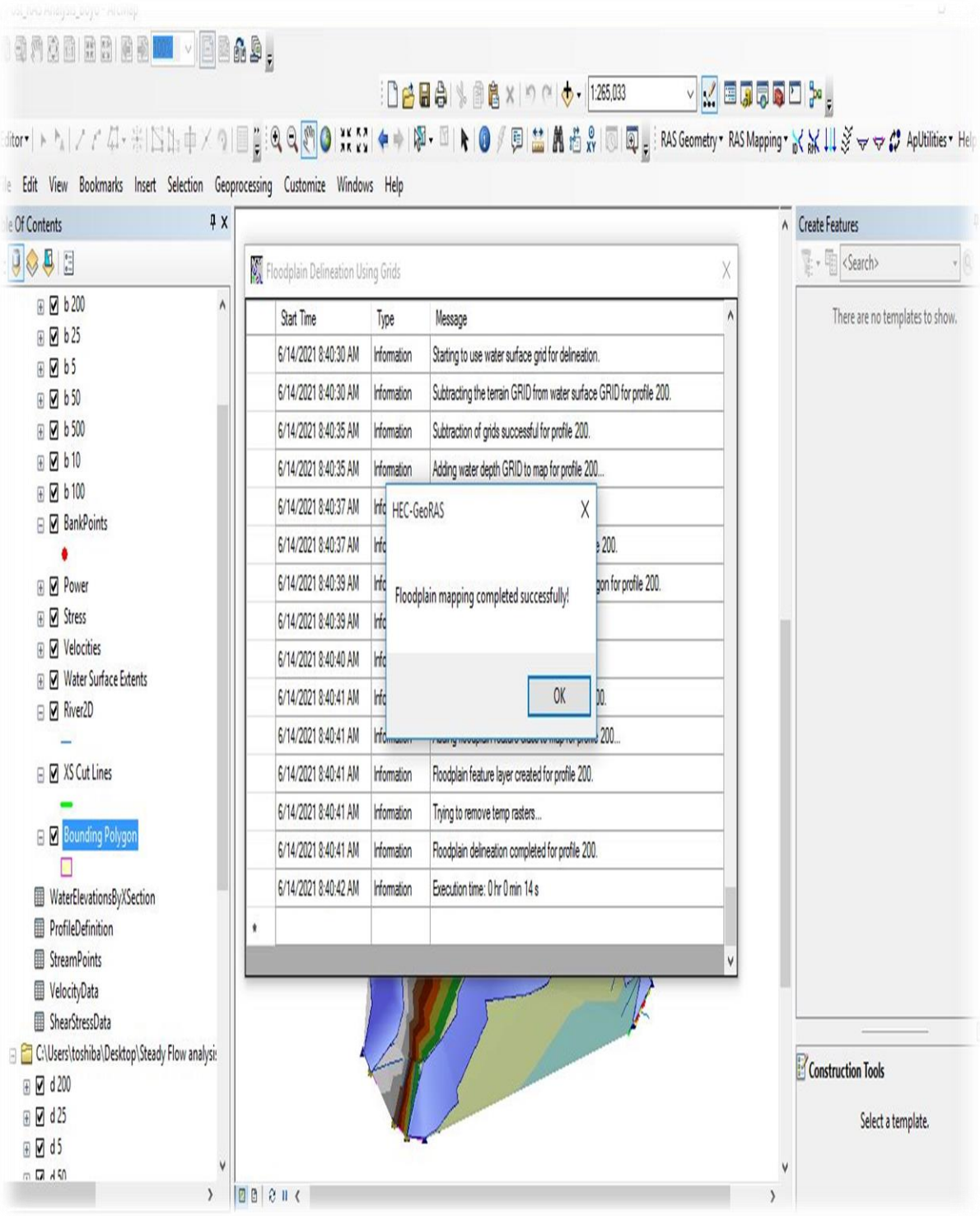

Appendix Figure 6 Post-RAS Processing

Appendix 7(A-E)

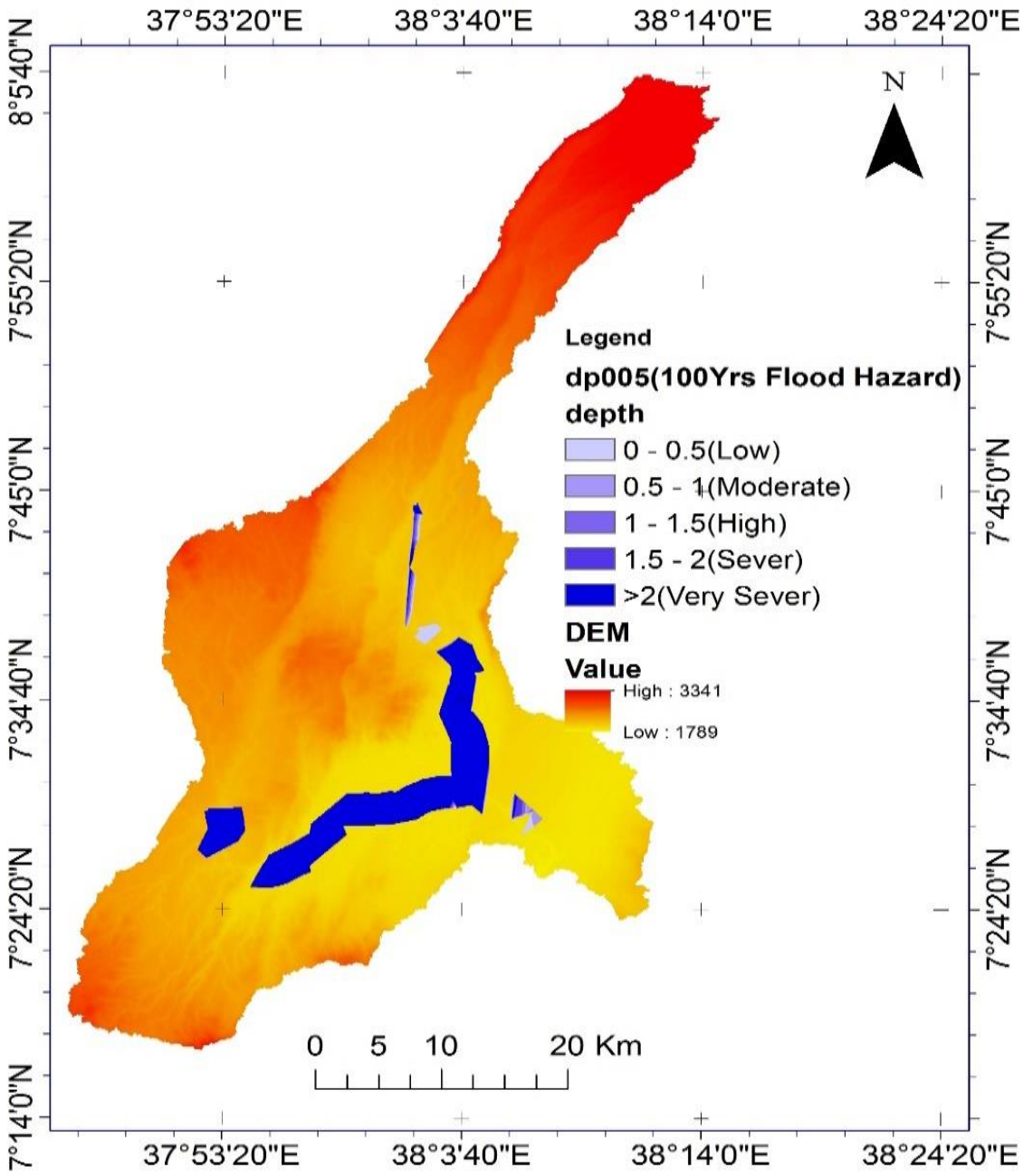

A)

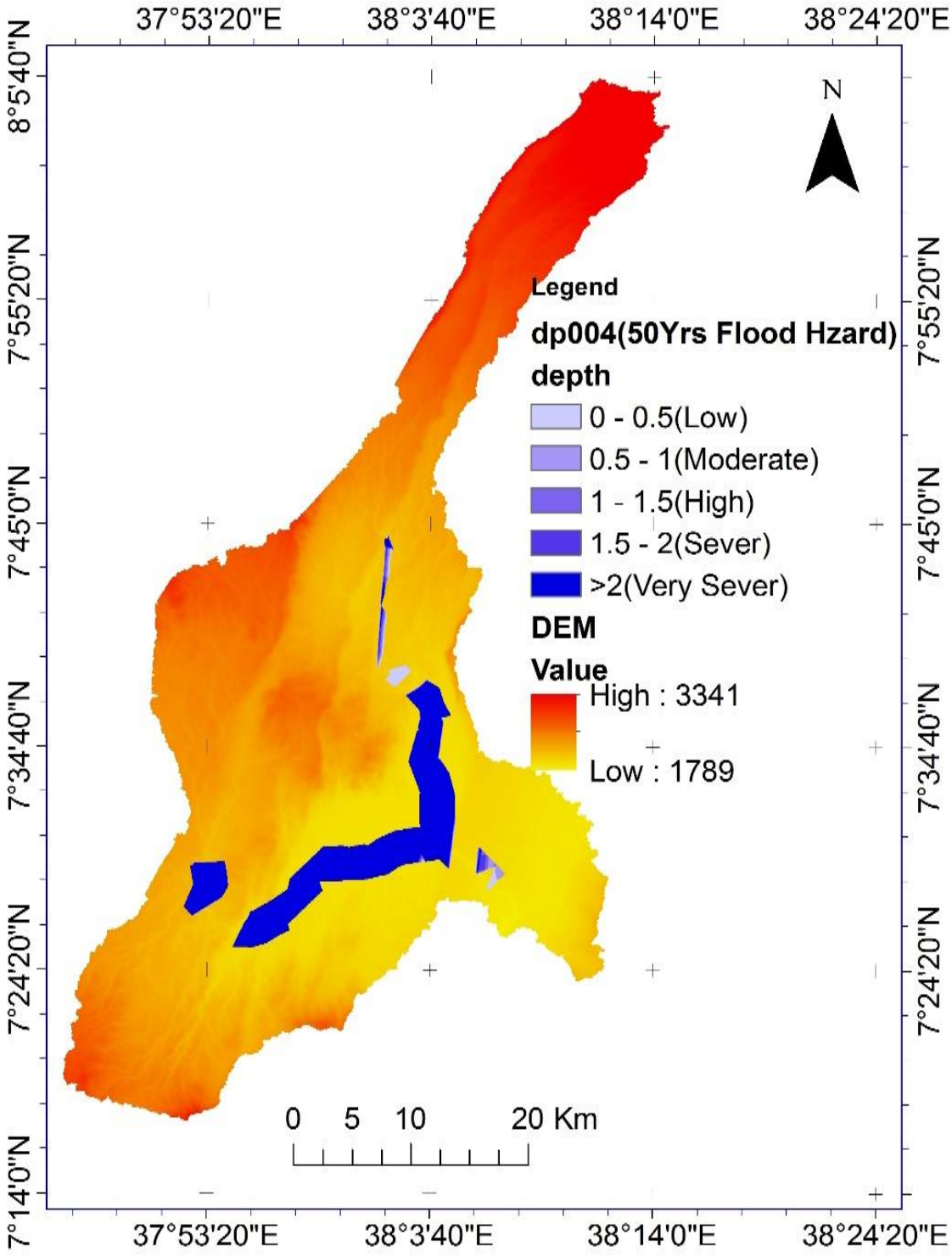
37°53'20"E
38°3'40"E
38°14'0"E
38°24'20"E
8°5'40"N
7°55'20"N
7°45'0"N
7°34'40"N
7°24'20"N
7°14'0"N
N
Legend
dp004(50Yrs Flood Hzard)
depth
0 - 0.5(Low)
0.5 - 1(Moderate)
1 - 1.5(High)
1.5 - 2(Sever)
>2(Very Sever)
DEM
Value
High : 3341
Low : 1789
0 5 10 20 Km

B)

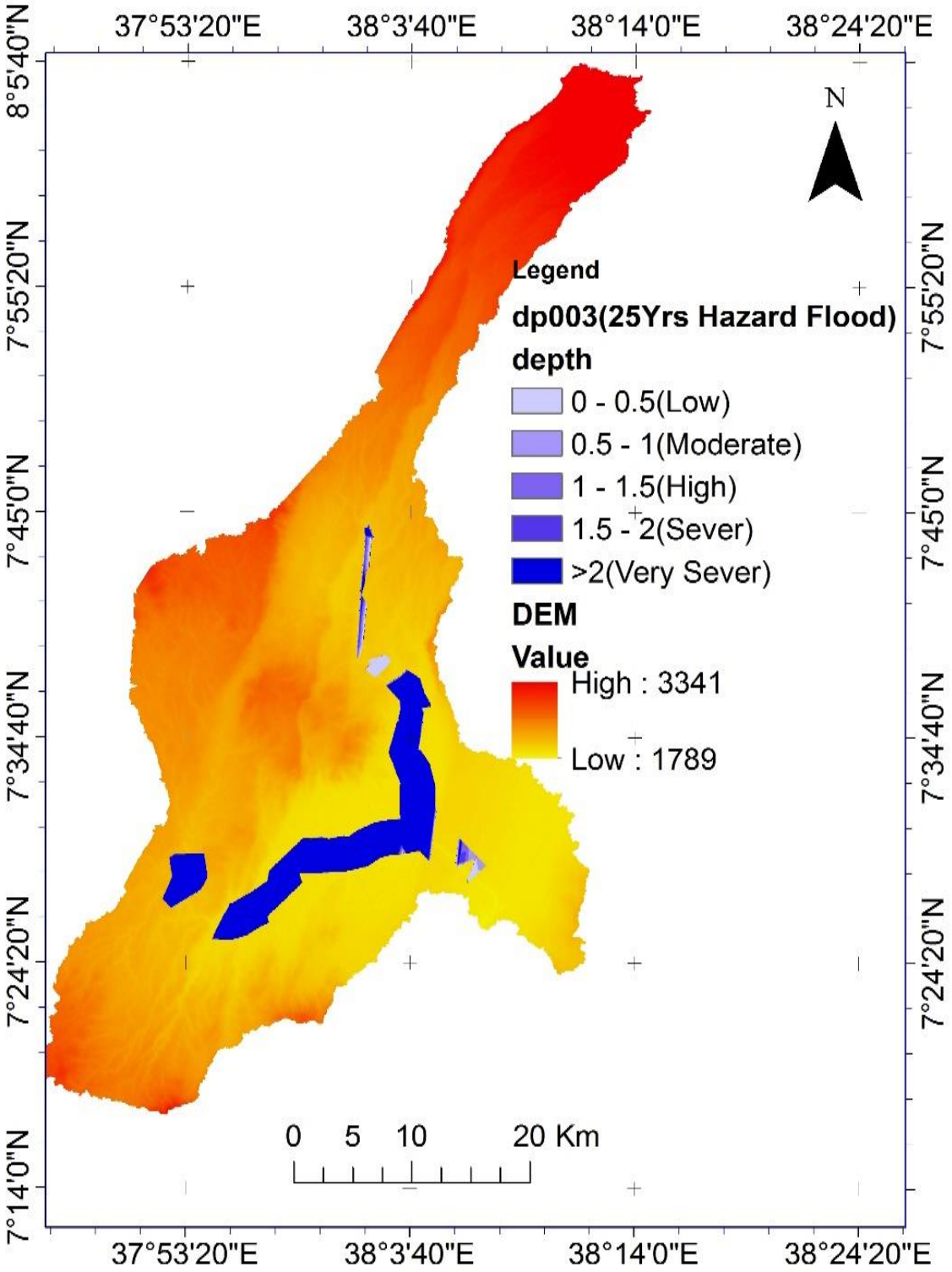
37°53'20"E
38°3'40"E
38°14'0"E
38°24'20"E
8°5'40"N
7°55'20"N
7°45'0"N
7°34'40"N
7°24'20"N
7°14'0"N
N
Legend
dp003(25Yrs Hazard Flood)
depth
0 - 0.5(Low)
0.5 - 1(Moderate)
1 - 1.5(High)
1.5 - 2(Sever)
>2(Very Sever)
DEM
Value
High : 3341
Low : 1789
0 5 10 20 Km

C)

D)

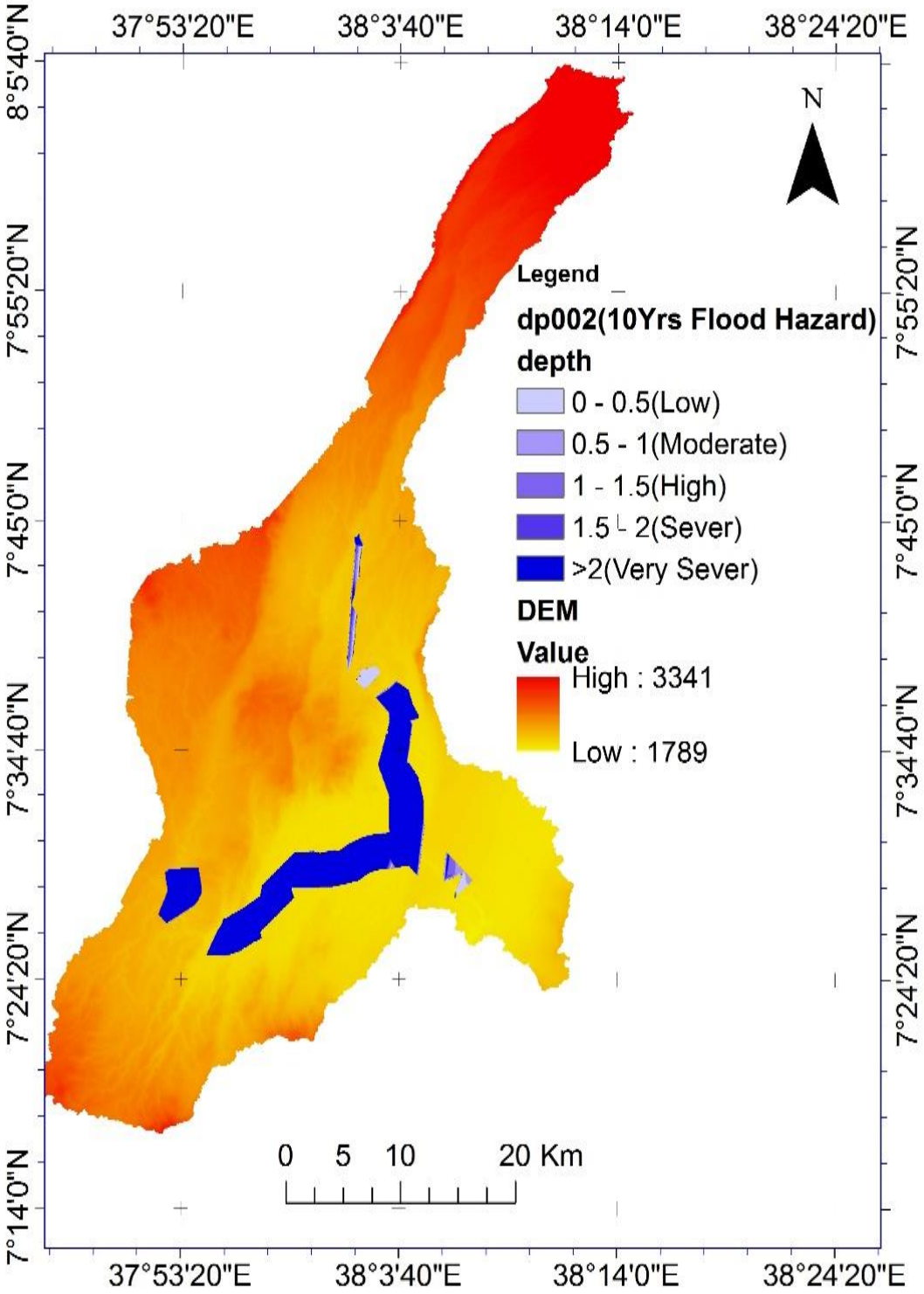
37°53'20"E
38°3'40"E
38°14'0"E
38°24'20"E
8°5'40"N
7°55'20"N
7°45'0"N
7°34'40"N
7°24'20"N
7°14'0"N
N
Legend
dp002(10Yrs Flood Hazard)
depth
0 - 0.5(Low)
0.5 - 1(Moderate)
1 - 1.5(High)
1.5 - 2(Sever)
>2(Very Sever)
DEM
Value
High : 3341
Low : 1789
0 5 10 20 Km

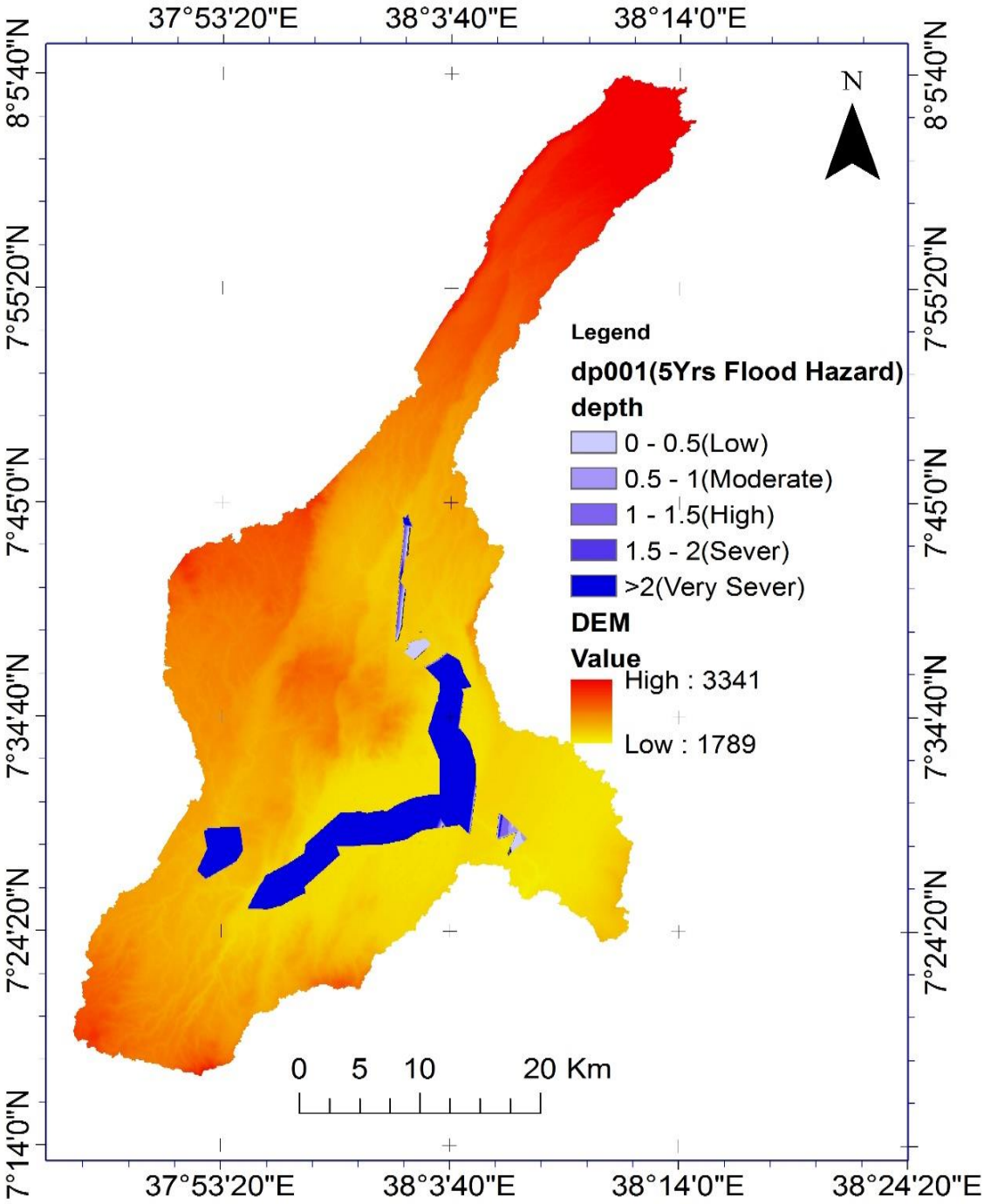

E

Appendix Figure 7 A, B, C, D and E Showing Hazard Maps of Different Return Period

Appendix 8 (A-D)

A

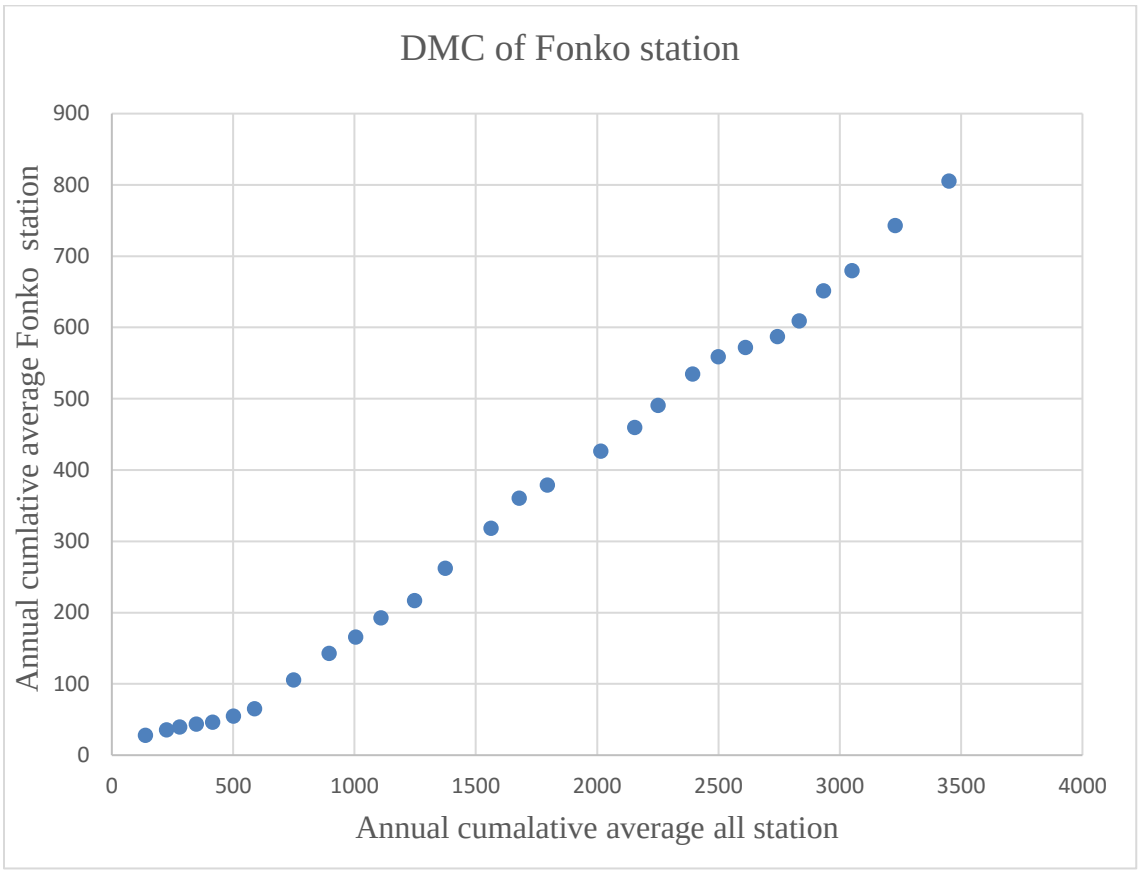

B

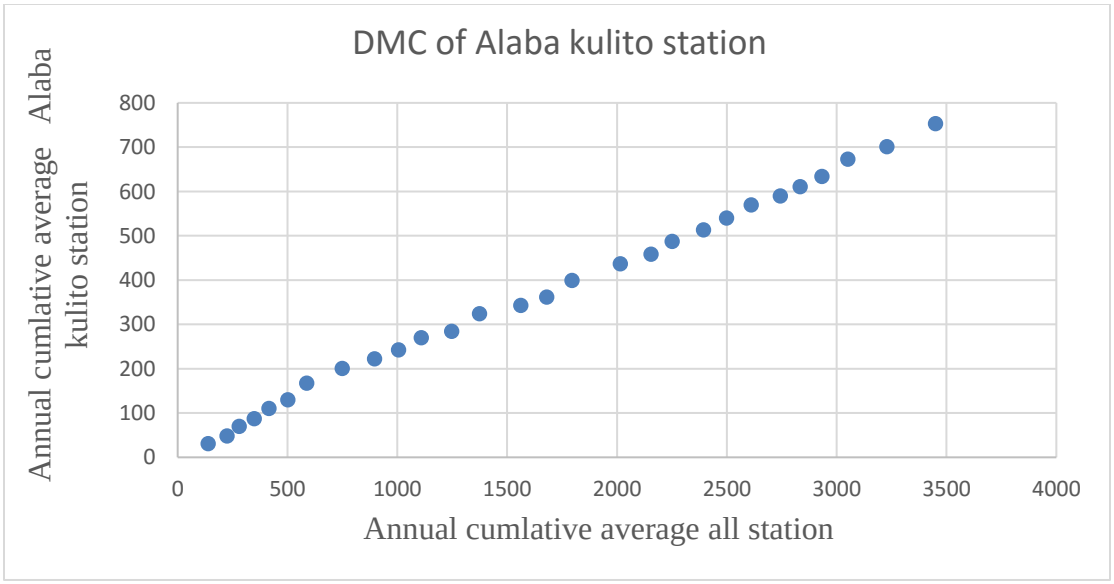

C

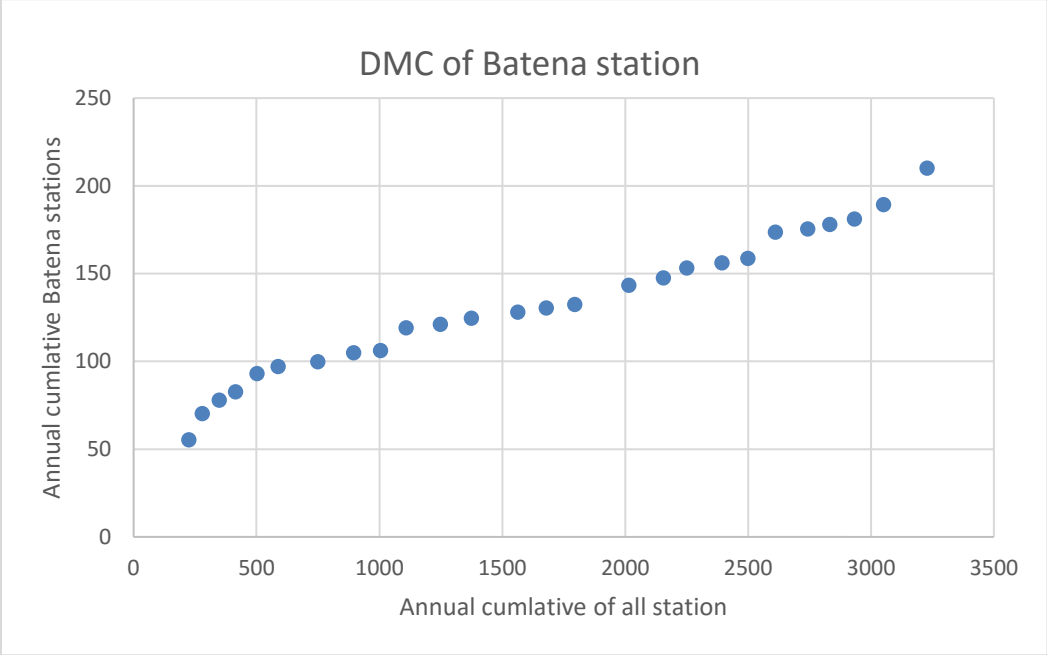
DMC of Batena station
Annual cumlative Batena stations
250
200
150
100
50
0
0
500
1000
1500
2000
2500
3000
3500
Annual cumlative of all station

D

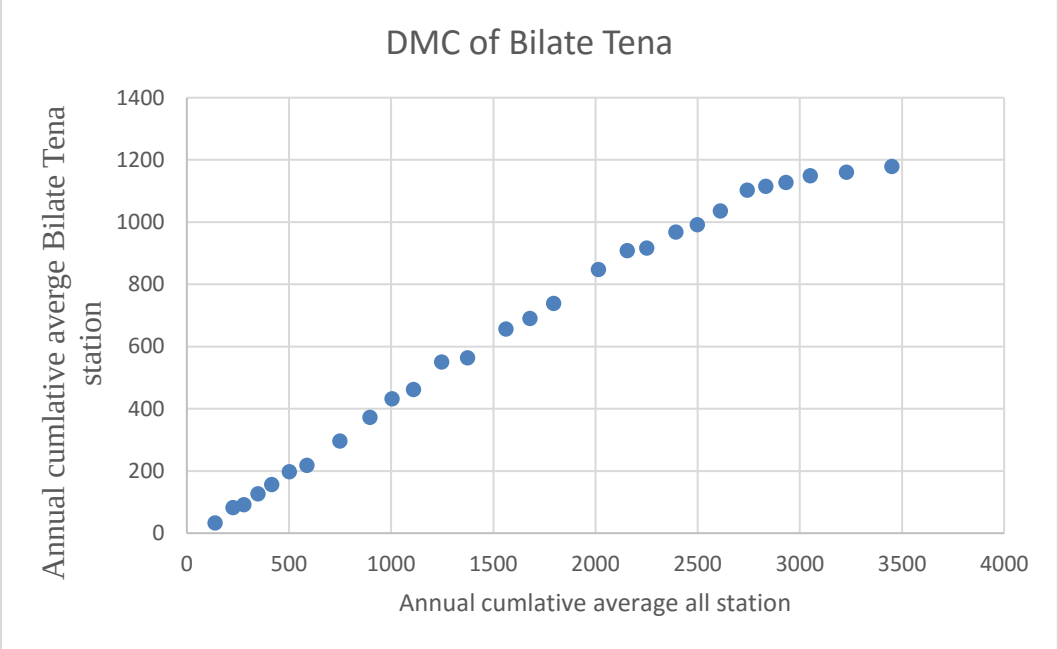
DMC of Bilate Tena
Annual cumlative averge Bilate Tena station
1400
1200
1000
800
600
400
200
0
0
500
1000
1500
2000
2500
3000
3500
4000
Annual cumlative average all station

E

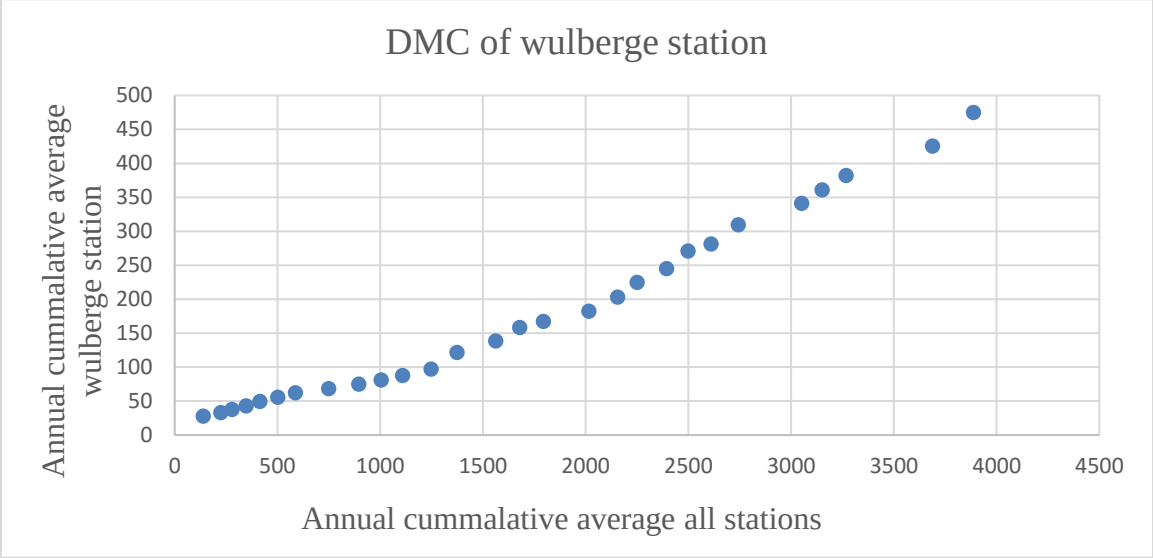

Figure 8 (A-E) Double mass curves for consistency Flood plain Boyo catchment station

Appendix 9(A-C)

A)

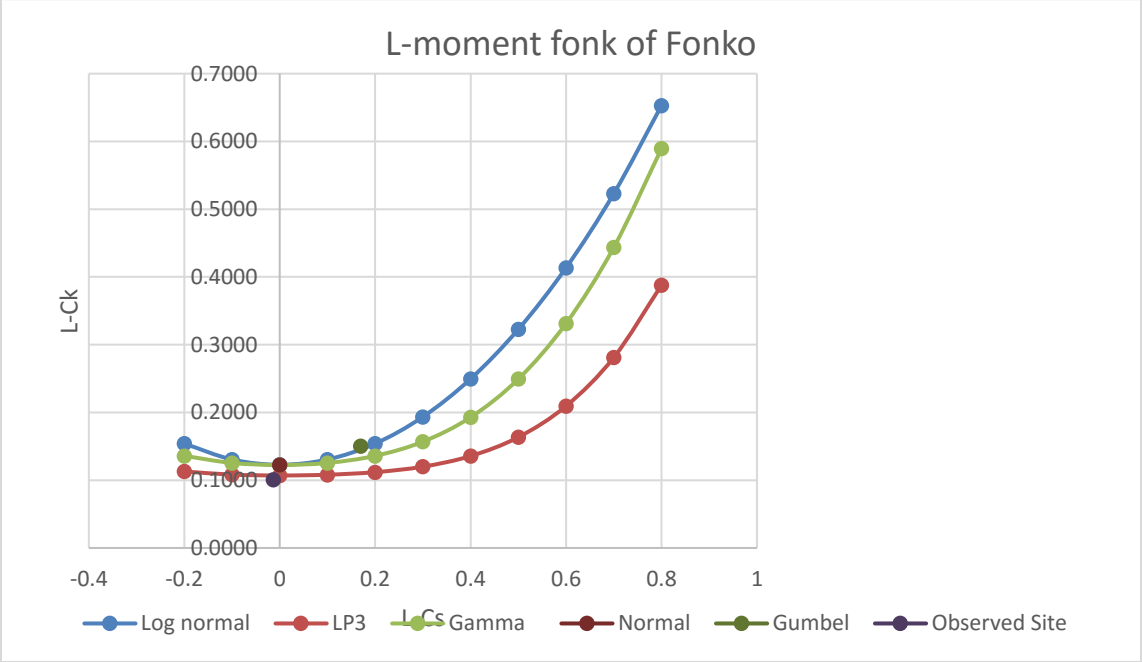

B)

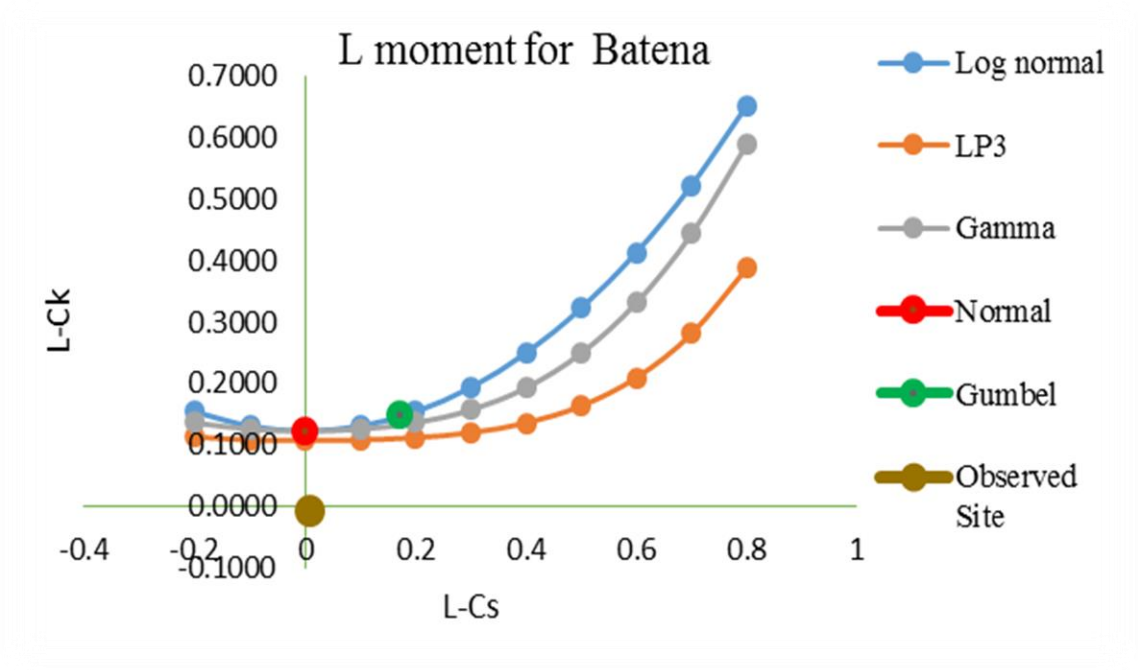

Figure 9 (A-B): L-moment of Wear River flood plain Boyo catchment station

Appendix 10 (A-C**)**

A)

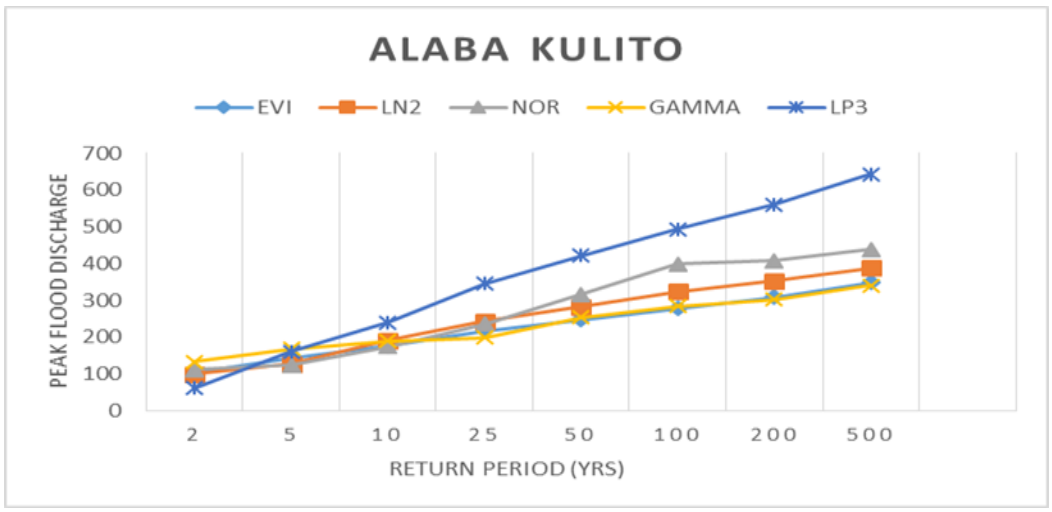

B)

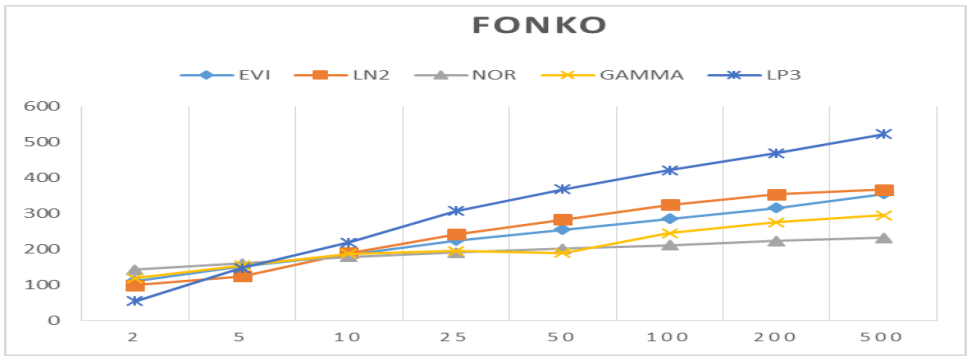
FONKO
EVI
LN2
NOR
GAMMA
LP3
600
500
400
300
200
100
0
2
5
10
25
50
100
200
500

C)

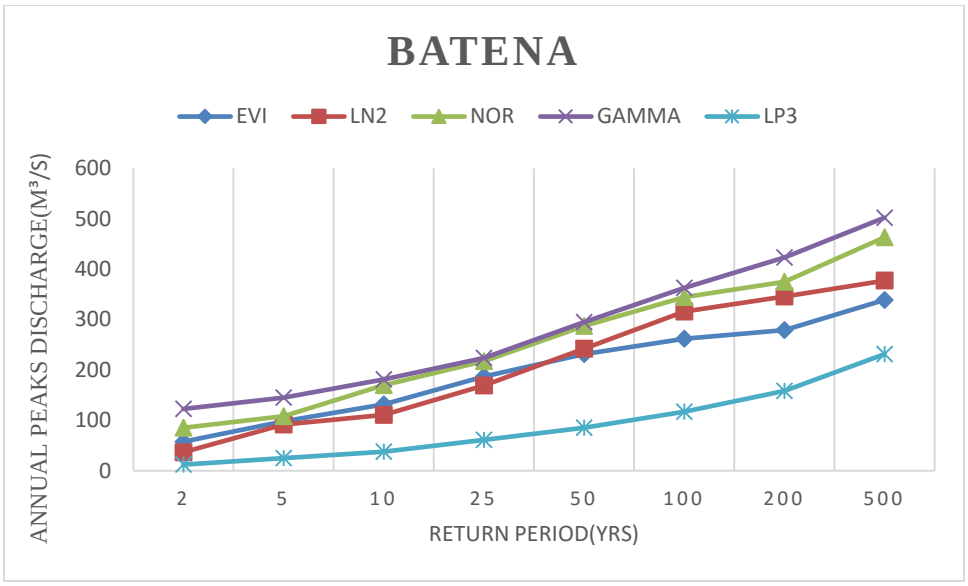
BATENA
EVI
LN2
NOR
GAMMA
LP3
ANNUAL PEAKS DISCHARGE(M³/S)
600
500
400
300
200
100
0
2
5
10
25
50
100
200
500
RETURN PERIOD(YRS)